

Visible Light Photocatalytic Cross-Coupling and Addition

Reaction of Arylalkynes with Perfluoroalkyl Iodides

Yelan Xiao, Yuen-Kiu Chun, Shun-Cheung Cheng, Ruoyang Liu, Man-Kit Tse and

Chi-Chiu Ko*

Department of Chemistry, City University of Hong Kong, Tat Chee Avenue, Kowloon

Tong, Hong Kong, China

Email: vinccko@cityu.edu.hk

Electronic Supplementary Information

Contents

1. Experimental Section
2. GC-FID Methods and Calibration Curves of Products
3. Quenching Study
4. Computational Details
5. NOESY Spectra for the Spectral Assignments of E/Z Isomers
6. Characterization of Radicals Formed in the Photocatalytic Reactions by TEMPO Radical Trap Experiments
7. Cyclic Voltammogram of **2a**
8. Characterization of Products
9. ^1H , ^{19}F and $^{13}\text{C}\{^1\text{H}\}$ NMR Spectra of Products from the Photocatalytic Reactions
10. References

1. Experimental Section

Materials and Reagents

All starting materials and solvents were purchased from commercial suppliers and used without further purification. *fac*-[Ir(ppy)₃] used in this study was prepared according to the related literatures with modifications.¹

Physical Measurements and Instrumentation

¹H NMR spectra were recorded on a Bruker AV600 (600 MHz) and ¹³C{¹H} NMR spectra were recorded on a Bruker AV600 (151 MHz) using tetramethylsilane (Me₄Si) (δ 0 ppm) as internal standard. ¹⁹F NMR spectra were recorded on a Bruker AV600 (565 MHz) using fluorobenzene (δ -113.15 ppm) as external standard. Splitting patterns were reported as s, singlet; d, doublet; t, triplet; q, quartet; m, multiplet. IR spectra were recorded from KBr disc by using a Perkin-Elmer Spectrum 100 FT-IR spectrophotometer. All EI high-resolution mass spectra (HRMS) were recorded on a Thermo Scientific DFS high-resolution magnetic sector mass spectrometer. Conversion was monitored by thin layer chromatography (TLC) using Merck TLC silica gel 60 F254, gas chromatography-flame ionization detector (GC-FID) using Agilent 7890A fitted with a J&W 122-5532: column (30 m, 0.25 mm, 0.25 μ m film) for FID analysis, and gas chromatography-mass spectrometry (GC-MS) using a HP 5973 fitted with a HP-5MS column (30m, 0.25 mm, 0.25 μ m film) for MS analysis. 1,2-Dichlorobenzene was used as the internal standard for GC-FID analysis.

General Procedure for Photocatalytic Cross-Coupling Reaction

To a solution of substituted phenyl acetylene (0.36 mmol, 9 mM), perfluoroalkyl iodide (0.54 mmol, 1.5 mol. equiv., 13.5 mM) and *fac*-[Ir(ppy)₃] (4.7 mg, 7.2 μ mol, 2 mol%)

in dichloromethane (40 mL) were added, a aqueous solution of potassium carbonate (0.72 mmol, 2.0 mol. equiv) in 8 mL of water. It was then transfer to reaction tubes, degassed by bubbling argon and sealed by rubber septa. Thereafter, the solution was irradiated for 40 hours in a merry-go-round photoreactor equipped with white-light LEDs as the excitation source (Figure S1 in Supporting Information). After light irradiation, the organic layer was separated and dried over anhydrous MgSO₄. The crude product was collected after removing the organic solvent under reduced pressure. Analytically pure product can be obtained after purification with column chromatography on silica gel using *n*-pentane as eluent.

General Procedure for Photocatalytic Addition Reaction

The procedure for photocatalyzed addition reaction was similar to photocatalyzed cross-coupling reaction except it was carried out under air. To a solution of substituted phenyl acetylene (0.36 mmol, 9 mM), perfluoroalkyl iodide (0.54 mmol, 1.5 mol. equiv., 13.5 mM) and *fac*-[Ir(ppy)₃] (4.7 mg, 7.2 μmol, 2 mol%) in dichloromethane (40 mL) were added, 8 mL of water. It was then transfer to the reaction tubes and the solution was irradiated for 10 hours in a merry-go-round photoreactor equipped with white-light LEDs as the excitation source (Figure S1 in Supporting Information). After light irradiation, the organic layer was separated and dried over anhydrous MgSO₄. The crude product was collected after removing the organic solvent under reduced pressure. The pure product can be obtained after purification with column chromatography on silica gel using *n*-pentane or *n*-pentane/dichloromethane (v:v = 10:1) as eluent.

Photoreactor Setup and Light Source

The home-made merry-go-round irradiation apparatus, which equipped a holder for eight reaction tubes and four Osram Parathom 13W white-light LEDs fixed at a distance of *ca.* 10 cm from the sample tube, is shown in Figure S1a. The lamp spectrum for Osram Parathom 13W white-light LED is shown in Figure S1b. Photocatalytic reactions were performed in glass tubes equipped with a magnetic stirrer. During irradiation reaction, the reaction tubes sealed by septa are rotating with the temperature controlled at around 25 °C.

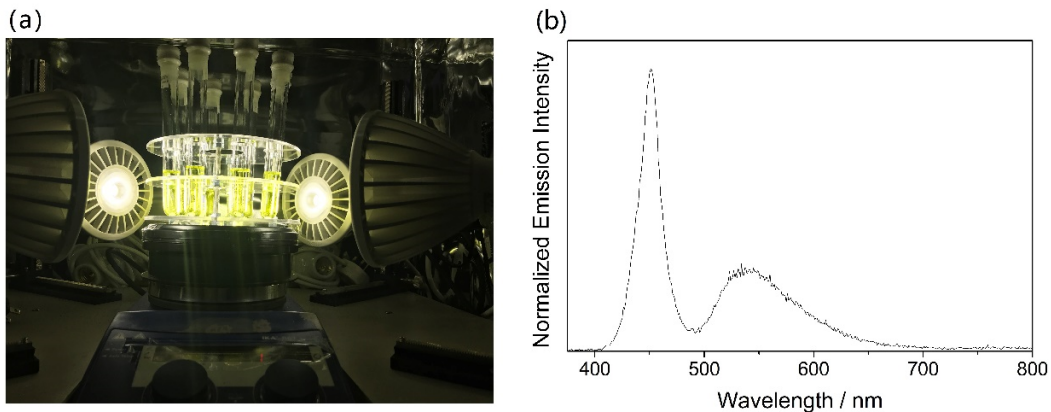


Figure S1. (a) Photo of the home-made merry-go-round irradiation apparatus and (b) lamp spectrum of Osram Parathom 13W white-light LED used in the reactor.

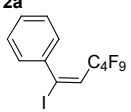
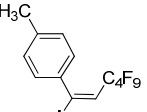
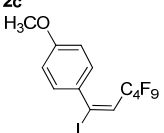
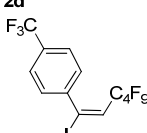
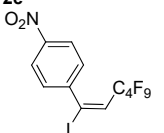
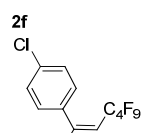
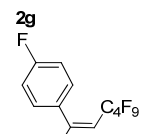
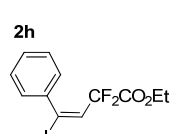
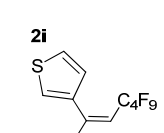
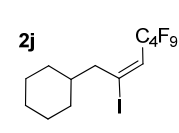
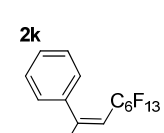
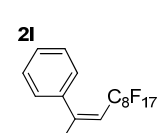
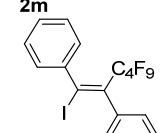
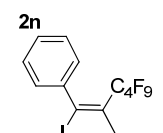
2. GC-FID Methods and Calibration Curves of Products

GC-FID methods: 1 μ L sample solution was injected in a pulse split mode (50:1) into GC-FID system consisting of an Agilent 6890 (Agilent Inc, Palo Alto, CA, USA) gas chromatography, Agilent 7890A autosampler. The retention times for the isolated products are listed in Table S1 (alkyne products) and Table S2 (alkene products). For the products of photocatalyzed addition reaction in Table S2, structure of major isomer (*E*-isomer) is presented.

Table S1. Retention time of the alkyne products in GC-FID

Alkyne	Retention time	Alkyne	Retention time
1a 	$t_R = 5.93$ min	1b 	$t_R = 6.62$ min
1c 	$t_R = 7.43$ min	1d 	$t_R = 5.81$ min
1e 	$t_R = 7.90$ min	1f 	$t_R = 6.90$ min
1g 	$t_R = 6.92$ min	1h 	$t_R = 7.29$ min
1i 	$t_R = 6.55$ min	1j 	$t_R = 7.09$ min
1k 	$t_R = 8.21$ min		

Table S2. Retention time of the alkene products in GC-FID

Alkene	Retention time	Alkene	Retention time
2a 	$t_R(E) = 7.39 \text{ min}$ $t_R(Z) = 7.85 \text{ min}$	2b 	$t_R(E) = 7.84 \text{ min}$ $t_R(Z) = 8.34 \text{ min}$
2c 	$t_R(E) = 8.47 \text{ min}$ $t_R(Z) = 8.97 \text{ min}$	2d 	$t_R(E) = 7.25 \text{ min}$ $t_R(Z) = 7.74 \text{ min}$
2e 	$t_R(E) = 9.08 \text{ min}$ $t_R(Z) = 9.51 \text{ min}$	2f 	$t_R(E) = 8.15 \text{ min}$ $t_R(Z) = 8.62 \text{ min}$
2g 	$t_R(E) = 7.33 \text{ min}$ $t_R(Z) = 7.81 \text{ min}$	2h 	$t_R(E) = 9.18 \text{ min}$ $t_R(Z) = 9.57 \text{ min}$
2i 	$t_R(E) = 7.53 \text{ min}$ $t_R(Z) = 8.07 \text{ min}$	2j 	$t_R(E) = 7.87 \text{ min}$ $t_R(Z) = 8.11 \text{ min}$
2k 	$t_R(E) = 7.82 \text{ min}$ $t_R(Z) = 8.26 \text{ min}$	2l 	$t_R(E) = 8.24 \text{ min}$ $t_R(Z) = 8.65 \text{ min}$
2m 	$t_R(E) = 9.30 \text{ min}$ $t_R(Z) = 9.57 \text{ min}$	2n 	$t_R(E) = 7.83 \text{ min}$ $t_R(Z) = 8.06 \text{ min}$

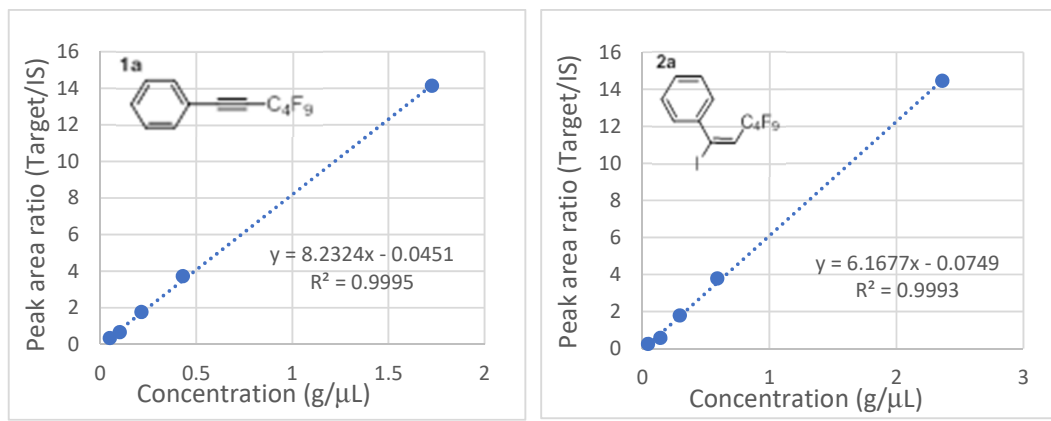


Figure S2. Representative GC calibration curves of the products of **1a** (left) and **2a** (right)
(Target: product; IS: internal standard, 1,2-dichlorobenzene).

3. Quenching Study

Luminescence lifetimes were measured on an Edinburgh Instrument LP920-KS Laser Flash Photolysis Spectrometer using the third harmonic output (355 nm; 6 – 8ns fwhm pulse width) of a Spectra-Physics Quanta-Ray Q-switched LAB-150 pulsed Nd:YAG laser (10 Hz) as the excitation source. Emission quenching experiments were carried out in solutions of a fix concentration of the luminescent complex, *fac*-[Ir(ppy)₃] (1.92×10^{-5} M), with a quencher of different concentrations, which were rigorously degassed on a high-vacuum line in a two-compartment cell with no less than four successive freeze pump-thaw cycles. With the emission lifetimes obtained from these experiments, the bimolecular quenching rate constants were determined using the Stern-Volmer equation:

$$\tau_0/\tau = 1 + k_q\tau_0[Q]$$

Where k_q is bimolecular quenching rate constant;

τ_0 and τ are emission lifetime in the absence and presence of quencher, respectively;

[Q] is quencher concentration in mol dm⁻³

Quantum yield of the bimolecular quenching reactions in the presence of 2 different quenchers (A and B) can be found using the following equations:

$$\Phi_{\text{quenching by A}} = \Phi_0 \frac{k_{q,A}\tau_0[Q_A]}{1+k_{q,A}\tau_0[Q_A]+k_{q,B}\tau_0[Q_B]} \quad (1)$$

and

$$\Phi_{\text{quenching by B}} = \Phi_0 \frac{k_{q,B}\tau_0[Q_B]}{1+k_{q,A}\tau_0[Q_A]+k_{q,B}\tau_0[Q_B]} \quad (2)$$

where Φ_0 and τ_0 are emission quantum yield and emission lifetime of the $\text{Ir}(\text{ppy})_3$ without quenchers (0.46 and 1.54 μs in aerated and degassed dichloromethane, respectively), k_q and $[Q]$ are the bimolecular quenching rate constants and the concentrations of the two quenchers.

Using the quenching rate constants found in the quenching rate studies (k_{q,O_2} is estimated to be $8.34 \times 10^9 \text{ M}^{-1} \text{ s}^{-1}$) and the optimized reaction conditions ($[\text{C}_4\text{F}_9\text{I}] = 13.5 \text{ mM}$, $[\text{O}_2] = 2.32 \text{ mM}$)² in the photocatalytic reactions, the initial quantum yields of the quenching reactions are:

In degassed condition,

$$\begin{aligned} \Phi_{\text{quenching by C}_4\text{F}_9\text{I}} &= 0.46 \left(\frac{(4.16 \times 10^9 \text{ M}^{-1}\text{s}^{-1})(1.54 \text{ } \mu\text{s})(13.5 \text{ mM})}{1 + (4.16 \times 10^9)(1.54 \text{ } \mu\text{s})(13.5 \text{ mM})} \right) \\ &= 0.454 \end{aligned}$$

In aerated condition,

$$\begin{aligned} \Phi_{\text{quenching by C}_4\text{F}_9\text{I}} &= 0.46 \left(\frac{(4.16 \times 10^9 \text{ M}^{-1}\text{s}^{-1})(1.54 \text{ } \mu\text{s})(13.5 \text{ mM})}{1 + (8.34 \times 10^9)(1.54 \text{ } \mu\text{s})(2.32 \text{ mM}) + (4.16 \times 10^9)(1.54 \text{ } \mu\text{s})(13.5 \text{ mM})} \right) \\ &= 0.339 \end{aligned}$$

4. Computational Details

All the calculations were done using GAUSSIAN 09 package, version B.01.³ The structures of the reactant complexes, transition states and product complexes of the *E*- and *Z*- isomers of the alkene **2a** were optimized using density functional theory (DFT). The B3LYP functional⁴ and a split basis set of 6-31+G(d)⁵ (for H, C and F), and LANL2DZ⁶ (for I) were employed. Frequency analysis was done after optimization to ensure the structures are at minimum (for products) and in a first-order saddle point (for transition states) of the potential energy surfaces. The solvent effects were taken account by the polarized continuum model with integral equation formulism (IEF-PCM).^{7]} The Cartesian coordinates of the optimized structures for reactant complexes, transition states and product complexes are summarized in Tables S3 – S8. The computed total electronic energies, zero-point energy corrections, thermal corrections to Gibbs free energies of all the optimized structures are listed in Table S9.

Table S3. Cartesian coordinates of the optimized reactant complex for the formation of *E*-isomer of **2a** (E-RC)

	Coordinates (Angstroms)		
	X	Y	Z
C	-2.571680	2.468578	-1.285645
C	-2.402467	1.938066	0.037630
C	-3.285132	2.337202	1.097904
C	-4.300221	3.232945	0.827243
C	-4.456269	3.738590	-0.477026
C	-3.598519	3.359223	-1.526807
H	-1.896664	2.153249	-2.073702
H	-3.142423	1.922397	2.089635
H	-4.979326	3.543335	1.614152
H	-5.260626	4.439745	-0.679256
H	-3.747042	3.765384	-2.521642
C	-1.422724	1.029430	0.285181
C	-0.591477	0.076429	0.507634
C	0.813967	0.296531	1.020107
C	1.909156	0.013242	-0.063129
C	3.396176	0.127313	0.421411
C	4.468300	0.134979	-0.719575
F	1.048060	-0.515329	2.087734
F	0.960946	1.587131	1.438176
F	1.715375	-1.243164	-0.533796
F	1.717191	0.891366	-1.082070
F	3.669291	-0.924109	1.228610
F	3.566321	1.272906	1.125060
F	5.686492	0.071982	-0.160557
F	4.313152	-0.918386	-1.534467
F	4.390963	1.261187	-1.442330
H	-0.987325	-0.968367	0.335577
I	-2.855686	-2.655154	-0.182105

Table S4. Cartesian coordinates of the optimized transition state in the formation of *E*-isomer of **2a** (E-TS)

	Coordinates (Angstroms)		
	X	Y	Z
C	-2.488595	2.342400	-1.299844
C	-2.362319	1.808690	0.028401
C	-3.196083	2.303964	1.088959
C	-4.114908	3.297278	0.816399
C	-4.226485	3.807165	-0.491266
C	-3.416978	3.334702	-1.542018
H	-1.855280	1.953059	-2.089478
H	-3.091826	1.884489	2.083629
H	-4.753089	3.682354	1.604557
H	-4.956507	4.585269	-0.694757
H	-3.526685	3.748626	-2.538718
C	-1.443226	0.840901	0.287424
C	-0.533699	-0.035843	0.553246
C	0.859412	0.331107	1.014683
C	1.942285	-0.026209	-0.058823
C	3.429401	0.066287	0.420822
C	4.497556	0.021912	-0.721755
F	1.143629	-0.353632	2.158869
F	0.953220	1.661205	1.289369
F	1.717207	-1.296384	-0.478080
F	1.764840	0.812577	-1.112181
F	3.680422	-0.972730	1.250691
F	3.618128	1.223919	1.100288
F	5.715675	-0.063987	-0.166493
F	4.308289	-1.044495	-1.512816
F	4.447474	1.133717	-1.468342
H	-0.796454	-1.102639	0.456856
I	-3.034684	-2.513339	-0.168891

Table S5. Cartesian coordinates of the optimized product complex of the *E*-isomer of **2a**
(E-PC)

	Coordinates (Angstroms)		
	X	Y	Z
C	-1.545121	1.854211	-1.093712
C	-1.985927	1.172369	0.052113
C	-2.671598	1.876649	1.056176
C	-2.884141	3.249827	0.927618
C	-2.433084	3.928894	-0.210647
C	-1.765931	3.228131	-1.220113
H	-1.030176	1.310160	-1.879949
H	-3.026207	1.350162	1.938085
H	-3.403051	3.789116	1.715402
H	-2.603526	4.997421	-0.310156
H	-1.416349	3.748424	-2.107727
C	-1.760080	-0.284174	0.180803
C	-0.656786	-0.943399	0.551898
C	0.639310	-0.326743	1.003714
C	1.789242	-0.480227	-0.049893
C	3.236856	-0.158867	0.450603
C	4.303681	0.022771	-0.679615
F	1.056871	-0.981222	2.144026
F	0.535602	0.993228	1.314899
F	1.788939	-1.764679	-0.498051
F	1.503680	0.334038	-1.100868
F	3.659777	-1.174106	1.241466
F	3.231308	0.985411	1.177633
F	5.519895	0.100815	-0.116937
F	4.289234	-1.019298	-1.525696
F	4.084863	1.148617	-1.372731
H	-0.631053	-2.027483	0.570364
I	-3.481504	-1.502070	-0.322894

Table S6. Cartesian coordinates of the optimized reactant complex for the formation of *Z*-isomer of **2a** (Z-RC)

	Coordinates (Angstroms)		
	X	Y	Z
C	3.449154	0.912991	0.885928
C	2.317883	1.629514	0.296662
C	2.557627	2.569604	-0.788772
C	3.839427	2.868086	-1.145636
C	4.943076	2.267783	-0.456696
C	4.754162	1.317824	0.524838
H	3.281212	0.360291	1.800357
H	1.705234	3.026737	-1.279519
H	4.031530	3.578862	-1.941750
H	5.951747	2.573574	-0.718336
H	5.602631	0.862798	1.024771
C	1.088877	1.450700	0.790188
C	-0.107863	1.222345	1.243826
C	-0.969386	0.126681	0.651554
C	-2.437821	0.596811	0.400175
C	-3.444604	-0.510827	-0.054916
C	-4.842103	0.012534	-0.523979
F	-1.017083	-0.937417	1.514059
F	-0.453856	-0.318136	-0.524388
F	-2.907912	1.136152	1.557218
F	-2.406111	1.573807	-0.543680
F	-3.660206	-1.354474	0.982270
F	-2.916460	-1.211742	-1.086799
F	-5.644820	-1.041684	-0.735290
F	-5.400363	0.796515	0.410959
F	-4.738201	0.704573	-1.666827
H	-0.517326	1.768897	2.092310
I	3.308670	-1.756298	-0.209143

Table S7. Cartesian coordinates of the optimized transition state in the formation of Z-isomer of **2a**
(Z-TS)

	Coordinates (Angstroms)		
	X	Y	Z
C	3.793973	1.109041	0.909480
C	2.613164	1.644801	0.281619
C	2.731655	2.693432	-0.699900
C	3.979093	3.184693	-1.017050
C	5.122001	2.664453	-0.372938
C	5.028665	1.641900	0.584635
H	3.688510	0.322297	1.644387
H	1.834065	3.076005	-1.173502
H	4.085120	3.972369	-1.755558
H	6.098919	3.067198	-0.624836
H	5.925696	1.261895	1.061904
C	1.378785	1.202535	0.626194
C	0.167417	0.993185	1.037803
C	-0.812553	-0.016524	0.474750
C	-2.245857	0.606603	0.366863
C	-3.394883	-0.378976	-0.029495
C	-4.757992	0.303603	-0.384920
F	-0.888193	-1.100218	1.302020
F	-0.441982	-0.444606	-0.754173
F	-2.562800	1.146782	1.574120
F	-2.190713	1.610100	-0.547081
F	-3.622898	-1.217088	1.008878
F	-3.021535	-1.107729	-1.107729
F	-5.684974	-0.651956	-0.548487
F	-5.156025	1.124141	0.599462
F	-4.662198	1.004087	-1.523248
H	-0.188981	1.587590	1.882234
I	2.849391	-2.083990	-0.221335

Table S8. Cartesian coordinates of the optimized product complex of the Z-isomer of **2a** (Z-PC)

Coordinates (Angstroms)			
	X	Y	Z
C	4.087550	0.879725	0.876377
C	2.970541	1.058700	0.040715
C	2.910018	2.201454	-0.779357
C	3.937503	3.147305	-0.753012
C	5.036648	2.967707	0.091840
C	5.106553	1.831990	0.907140
H	4.153031	0.001454	1.511368
H	2.068308	2.335696	-1.452254
H	3.880744	4.018471	-1.399845
H	5.836843	3.702465	0.110516
H	5.956628	1.686014	1.567723
C	1.843236	0.099167	0.023673
C	0.566131	0.508909	0.088656
C	-0.677757	-0.326222	0.000715
C	-1.966407	0.553986	0.078675
C	-3.327259	-0.212034	0.183641
C	-4.599831	0.667201	-0.056385
F	-0.760296	-1.253233	1.014507
F	-0.739353	-1.031903	-1.176049
F	-1.871566	1.359664	1.171315
F	-1.997504	1.347849	-1.026889
F	-3.434053	-0.739229	1.427076
F	-3.367727	-1.219625	-0.721260
F	-5.687256	-0.062870	0.237046
F	-4.589703	1.755481	0.729396
F	-4.683002	1.055964	-1.336444
H	0.398825	1.573588	0.225717
I	2.387890	-1.971583	-0.144293

Table S9. Calculated total electronic energies (E), zero-point energy (ZPE) corrections,^a thermal corrections to Gibbs free energies,^a and number of imaginary frequencies of all the optimized structures in the formation of *E*- and *Z*- isomers of **2a**.

	E / Hartree	ZPE corr./ Hartree	Thermal corrections to Gibbs free energies / Hartree	No. of imaginary frequencies
E-RC	-1370.81195804	0.161199	0.10541	0
E-TS	-1370.81031021	0.16135	0.105017	1 (-97.5cm ⁻¹)
E-PC	-1370.86309239	0.163591	0.109421	0
Z-RC	-1370.81033565	0.162285	0.104222	0
Z-TS	-1370.80431756	0.161965	0.106895	1 (-99.0cm ⁻¹)
Z-PC	-1370.86208062	0.163507	0.109454	0

^aComputed at 298.15K.

5. NOESY Spectra for the Spectral Assignments of *E/Z* Isomers

With 1D and 2D ^1H NOESY NMR spectroscopy, signals corresponding to *E/Z*-isomers can be distinguished. For example, in the ^1H NMR spectrum of **2a** (Figure S3), the alkenyl proton signals ($\text{H}-\text{C}=\text{C}$) of the major and minor isomers are observed at ~ 6.6 and ~ 6.5 ppm, respectively; whereas 2-phenyl proton signals of the major and minor species are observed at ~ 7.3 and ~ 7.5 ppm, respectively. The 1D ^1H - ^1H NOESY experiments have been conducted on these two sets of protons to observe their spatial correlation. For signals corresponding to the minor species, a NOE signal of the phenyl proton at ~ 7.5 ppm is observed when the alkenyl proton at 6.5 ppm is selectively excited (Figure S5). In contrast, no NOE signal of the phenyl proton (major form) is observed when the alkenyl proton of the major form at 6.6 ppm is selectively excited (Figure S4). The observation of the NOE signal of phenyl proton in the minor form upon selective excitation of alkenyl proton suggests that these two protons are located within the NOE correlation range (4-5 Å).⁸ This result confirms that the minor species is *Z*-isomer. It can be further supported by 2D ^1H - ^1H NOESY experiment, in which the NOE correlated cross peaks between the alkenyl and phenyl protons of the minor form are observed in the 2D NOESY spectrum (Figure S6). With NOESY experiments together with the reported NMR signals of the *E/Z* isomers,⁹ signals corresponding to the *E*- or *Z*-isomers of the major and minor isomers of the alkenes formed in the reaction are similarly assigned.

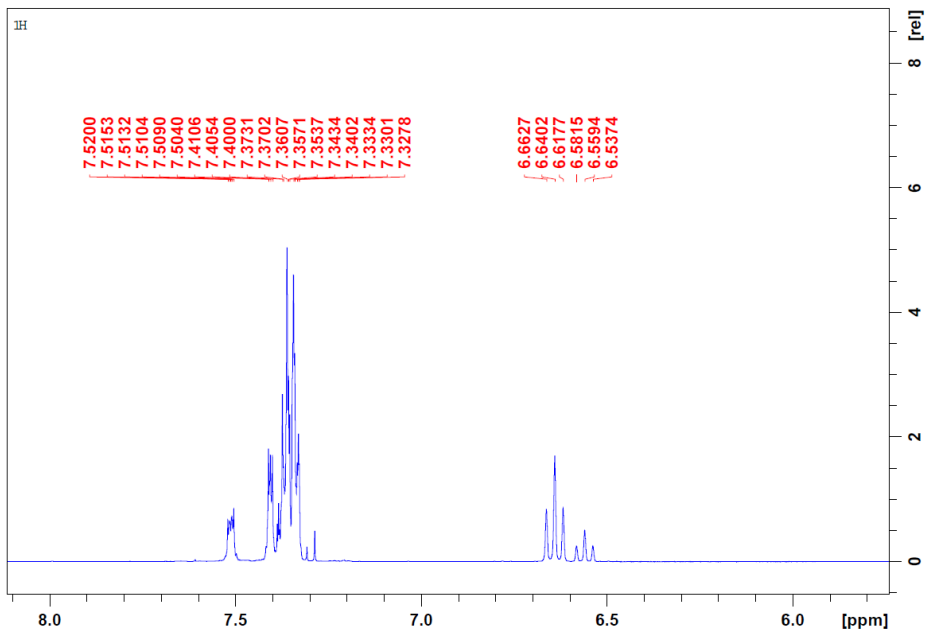


Figure S3. ¹H NMR spectrum of **2a** as a mixture of *E/Z* species

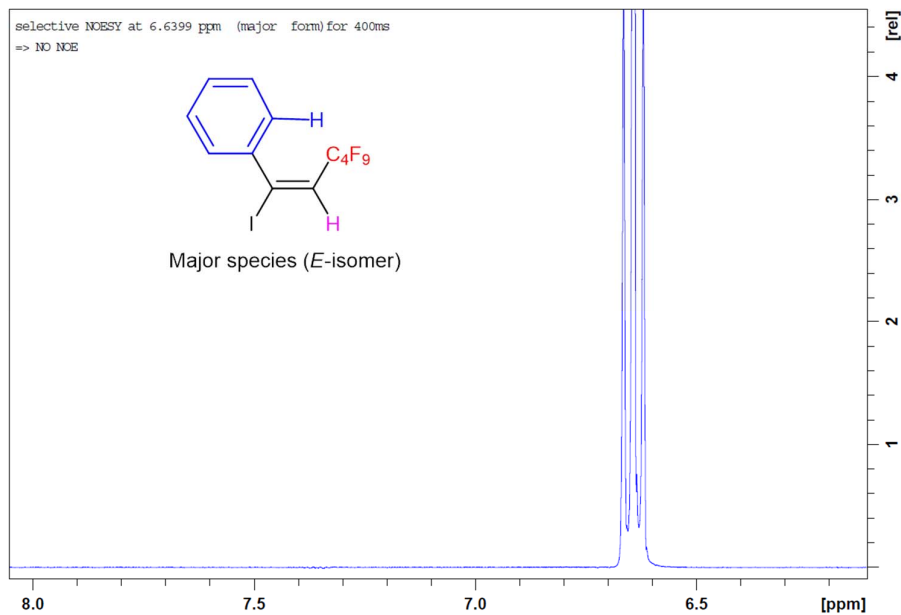


Figure S4. Selective 1D ¹H-¹H NOESY spectrum of **2a** between selective excited proton of C=C group and proton of aryl group in major species

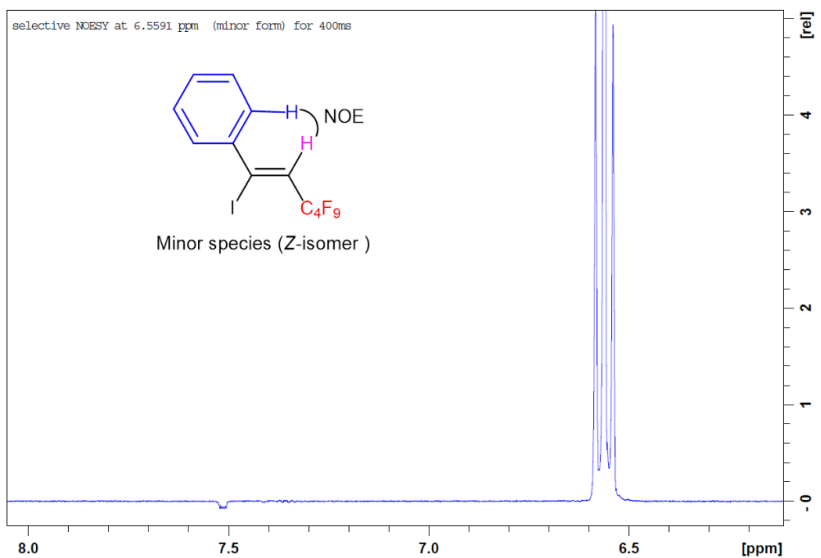


Figure S5. Selective 1D ^1H - ^1H NOESY spectrum of **2a** between selective excited proton of C=C group and proton of aryl group in minor species

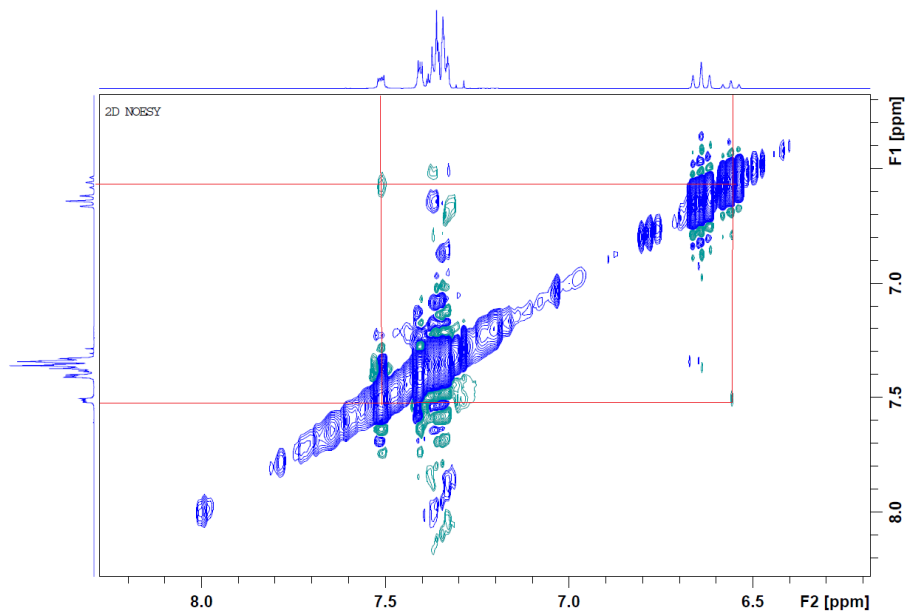


Figure S6. 2D ^1H - ^1H NOESY spectrum of **2a** as a mixture of *E/Z* species (CDCl_3 , 298K, 600 MHz, 400ms mixing time), showing the NOE signals between proton of C=C group and proton of aryl group.

6. Characterization of Radicals Formed in the Photocatalytic Reactions by TEMPO Radical Trap Experiments

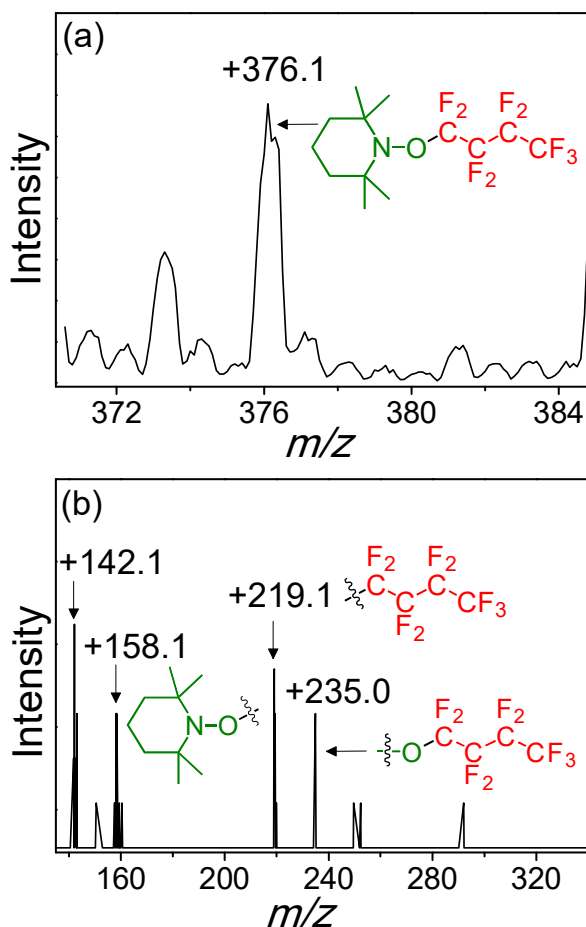


Figure S7. ESI-mass spectrum of (a) the reaction intermediate trapped by TEMPO radical from the photoreaction of phenylacetylene (0.045 mmol), $\text{C}_4\text{F}_9\text{I}$ (0.0675 mmol, 1.5 mol equiv), *fac*- $[\text{Ir}(\text{ppy})_3]$ (0.6 mg, 0.9 μmol , 2 mol%) and TEMPO radical (0.09 mmol, 2.0 mol equiv) in solvent mixture of $\text{CH}_2\text{Cl}_2:\text{H}_2\text{O}$ (v/v: 5:1, 5 mL) under air (photocatalytic reaction condition for addition reaction). (b) MS/MS mass spectrum for ion detected at $m/z +376.1$.

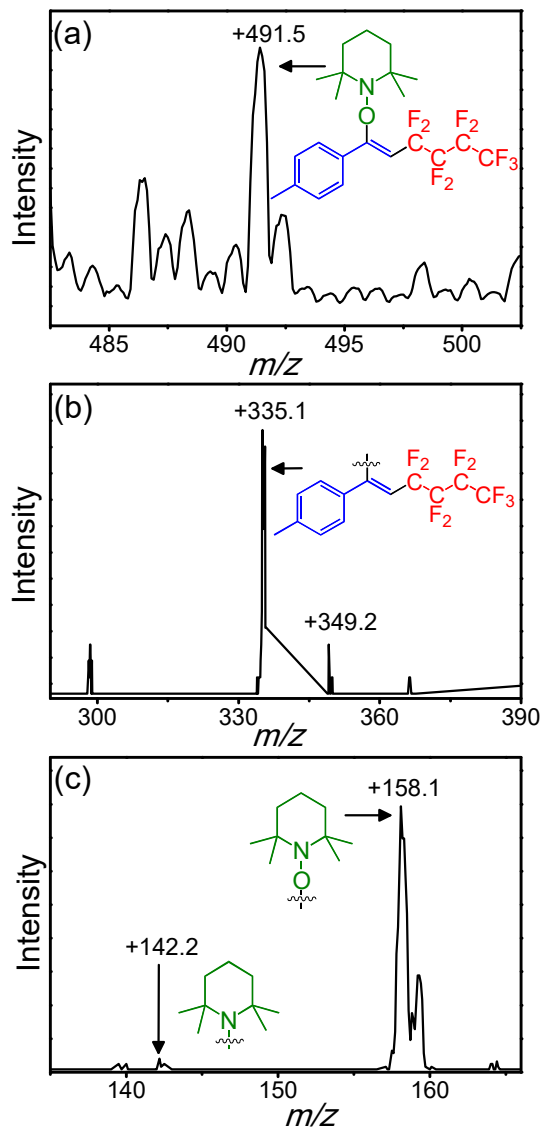


Figure S8. (a) ESI-mass spectrum of the reaction intermediate trapped by TEMPO radical from the photocatalytic reaction of addition product **2b** (0.045 mmol), *fac*-[Ir(ppy)₃] (0.6 mg, 0.9 μ mol, 2 mol%) and TEMPO radical (0.09 mmol, 2.0 mol equiv) in solvent mixture of CH₂Cl₂:H₂O (v/v: 5:1, 5 mL) under argon (photocatalytic reaction condition for cross-coupling). (b) and (c) MS/MS mass spectra for ion detected at m/z +491.5.

7. Cyclic Voltammogram of **2a**

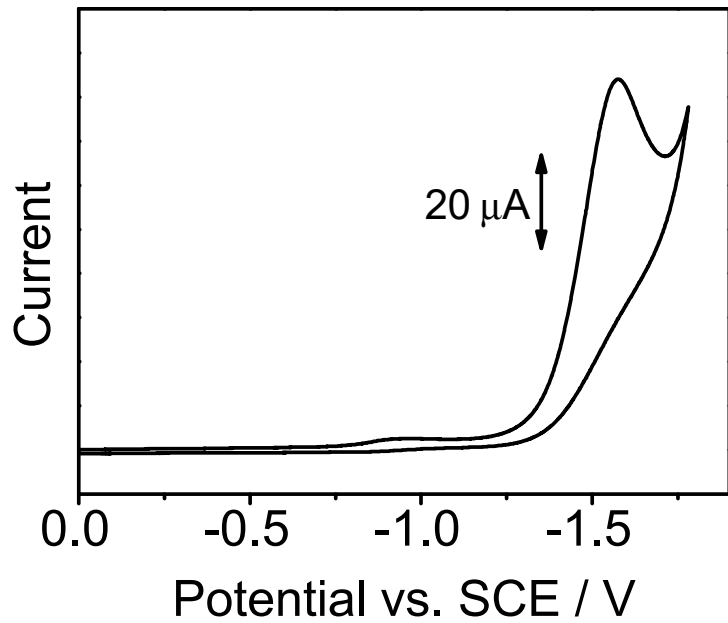
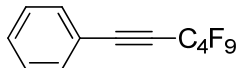


Figure S9. Cyclic voltammogram of **2a** (reductive scan) in MeCN (0.1 mol dm⁻³ $^n\text{Bu}_4\text{NPF}_6$). Working electrode, glassy carbon; scan rate, 100 mVs⁻¹.

8. Characterization of Products

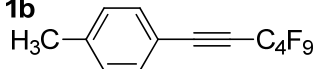
Characterization of Photocatalytic Cross-Coupling Products

1a



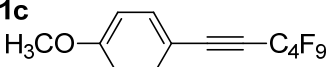
1-Phenyl-2-perfluorobutyl acetylene (1a)¹⁰: colorless oil. Yield: 67 mg, 57%. ¹H NMR (600 MHz, CDCl₃): δ 7.56 (dd, *J* = 7.9, 0.9 Hz, 2H), 7.49 (m, 1H), 7.40 (m, 2H). ¹⁹F NMR (565 MHz, CDCl₃): δ -81.17 (t, *J* = 9.6 Hz, 3F), -97.52 (s, 2F), -123.53 (m, 2F), -125.53 (dd, *J* = 13.6, 5.5 Hz, 2F). ¹³C{¹H} NMR (151 MHz, CDCl₃) δ 132.54 (s), 131.12 (m), 128.72 (s), 118.53 (m), 92.38 (m), 74.68 (m). IR (KBr disc): 2923, 2853, 2255 (C≡C), 1636, 1463, 1351, 1235, 1204, 1136 cm⁻¹. HRMS (EI) *m/z* calculated for C₁₂H₅F₉: 320.0247, found 320.0237.

1b



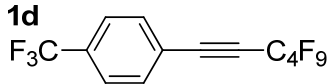
1-(4-Methylphenyl)-2-perfluorobutyl acetylene (1b)¹⁰: colorless oil. Yield: 68 mg, 56%. ¹H NMR (600 MHz, CDCl₃): δ 7.44 (d, *J* = 8.0 Hz, 2H), 7.19 (d, *J* = 8.0 Hz, 2H), 2.39 (s, 3H). ¹⁹F NMR (565 MHz, CDCl₃): δ -81.27 (t, *J* = 9.5 Hz, 3F), -97.24 (s, 2F), -123.57 (d, *J* = 2.6 Hz, 2F), -125.61 (d, *J* = 8.5 Hz, 2F). ¹³C{¹H} NMR (151 MHz, CDCl₃) δ 141.87 (s), 132.50 (t, *J* = 2.3 Hz), 129.52 (s), 115.50 (m), 92.91 (m), 74.21 (m), 21.72 (s). IR (KBr disc): 2927, 2857, 2246 (C≡C), 1607, 1509, 1458, 1353, 1316, 1307, 1239, 1206, 1134 cm⁻¹. HRMS (EI) *m/z* calculated for C₁₃H₇F₉: 334.0404, found 334.0404.

1c

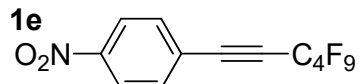


1-(4-Methoxyphenyl)-2-perfluorobutyl acetylene (1c)^{10,11}: colorless oil. Yield: 64 mg, 51%. ¹H NMR (600 MHz, CDCl₃): δ 7.49 (m, 2H), 6.90 (m, 2H), 3.84 (s, 3H). ¹⁹F NMR

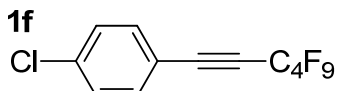
(565 MHz, CDCl₃): δ -81.17 (t, *J* = 8.7 Hz, 3F), -96.86 (s, 2F), -123.49 (s, 2F), -125.53 (s, 2F). ¹³C{¹H} NMR (151 MHz, CDCl₃) δ 161.88 (m), 134.33 (s), 114.45 (s), 110.39 (m), 93.06 (m), 73.78 (m), 55.46 (s). IR (KBr disc): 2969, 2941, 2847, 2243 (C≡C), 1607, 1573, 1514, 1469, 1354, 1297, 1241, 1136 cm⁻¹. HRMS (EI) *m/z* calculated for C₁₃H₇F₉O: 350.0353, found 350.0342.



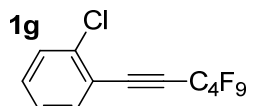
1-(4-Trifluoromethylphenyl)-2-perfluorobutyl acetylene (1d): colorless oil. Yield: 81 mg, 58%. ¹H NMR (600 MHz, CDCl₃): δ 7.68 (m, 4H). ¹⁹F NMR (565 MHz, CDCl₃): δ -63.44 (s, 3F), -81.11 (t, *J* = 9.4 Hz, 3F), -98.30 (s, 2F), -123.43 (dt, *J* = 9.5, 7.1 Hz, 2F), -125.53 (m, 2F). ¹³C{¹H} NMR (151 MHz, CDCl₃) δ 132.89 (m), 125.77 (m), 122.39 (m), 90.30 (m), 76.42 (m). IR (KBr disc): 2920, 2851, 2256 (C≡C), 1619, 1407, 1355, 1326, 1241, 1178, 1136 cm⁻¹. HRMS (EI) *m/z* calculated for C₁₃H₄F₁₂: 388.0121, found 388.0126.



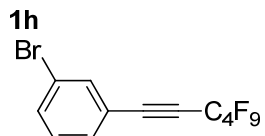
1-(4-Nitrophenyl)-2-perfluorobutyl acetylene (1e): pale yellow powder. Yield: 42 mg, 32%. ¹H NMR (600 MHz, CDCl₃): δ 8.29 (m, 2H), 7.76 (d, *J* = 8.8 Hz, 2H). ¹⁹F NMR (565 MHz, CDCl₃): δ -81.09 (t, *J* = 9.7 Hz, 3F), -98.70 (d, *J* = 6.3 Hz, 2F), -123.37 (dd, *J* = 9.6, 4.0 Hz, 2F), -125.53 (t, *J* = 8.9 Hz, 2F). ¹³C{¹H} NMR (151 MHz, CDCl₃) δ 149.02 (m), 133.62 (s), 124.94 (m), 123.95 (s), 89.30 (m), 78.28 (m). IR (KBr disc): 3116, 2251 (C≡C), 1605, 1535, 1489, 1352, 1283, 1235, 1200, 1132 cm⁻¹. HRMS (EI) *m/z* calculated for C₁₂H₄F₉NO₂: 365.0098, found 365.0088.



1-(4-Chlorophenyl)-2-perfluorobutyl acetylene (1f)¹¹: colorless oil. Yield: 75 mg, 59%. ¹H NMR (600 MHz, CDCl₃): δ 7.48 (d, *J* = 8.5 Hz, 2H), 7.37 (m, 2H). ¹⁹F NMR (565 MHz, CDCl₃): δ -81.35 (t, *J* = 8.7 Hz, 3F), -97.97 (s, 2F), -123.59 (m, 2F), -125.67 (d, *J* = 8.2 Hz, 2F). ¹³C{¹H} NMR (151 MHz, CDCl₃) δ 137.94 (m), 133.88 (d, *J* = 1.8 Hz), 129.37 (s), 117.17 (m), 91.11 (m), 75.49 (m). IR (KBr disc): 2925, 2250 (C≡C), 1595, 1491, 1384, 1353, 1287, 1239, 1207, 1136 cm⁻¹. HRMS (EI) *m/z* calculated for C₁₂H₄F₉Cl: 353.9857, found 353.9847.



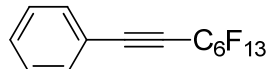
1-(2-Chlorophenyl)-2-perfluorobutyl acetylene (1g): colorless oil. Yield: 80 mg, 63%. ¹H NMR (600 MHz, CDCl₃): δ 7.57 (d, *J* = 7.7 Hz, 1H), 7.46 (d, *J* = 8.0 Hz, 1H), 7.41 (m, 1H), 7.29 (td, *J* = 7.7, 0.9 Hz, 1H). ¹⁹F NMR (565 MHz, CDCl₃): δ -81.21 (t, *J* = 9.3 Hz, 3F), -98.08 (s, 2F), -123.38 (m, 2F), -125.45 (dd, *J* = 17.1, 10.6 Hz, 2F). ¹³C{¹H} NMR (151 MHz, CDCl₃) δ 137.25 (m), 134.30 (m), 132.22 (s), 129.87 (s), 126.83 (s), 119.01 (m), 88.83 (m), 79.23 (m). IR (KBr disc): 2924, 2252(C≡C), 1476, 1435, 1353, 1293, 1239, 1153, 1136 cm⁻¹. HRMS (EI) *m/z* calculated for C₁₂H₄F₉Cl: 353.9857, found 353.9848.



1-(3-Bromophenyl)-2-perfluorobutyl acetylene (1h): colorless oil. Yield: 109 mg, 76%. ¹H NMR (600 MHz, CDCl₃): δ 7.70 (s, 1H), 7.61 (d, *J* = 8.1 Hz, 1H), 7.49 (d, *J* = 7.7 Hz, 1H), 7.26 (dd, *J* = 13.5, 5.6 Hz, 1H). ¹⁹F NMR (565 MHz, CDCl₃): δ -81.22 (t, *J*

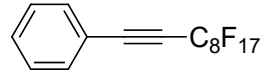
$= 9.1$ Hz, 3F), -98.08 (d, $J = 4.7$ Hz, 2F), -123.51 (dq, $J = 9.9, 5.9$ Hz, 2F), -125.61 (m, 2F). $^{13}\text{C}\{\text{H}\}$ NMR (151 MHz, CDCl_3) δ 135.24 (s), 134.49 (s), 131.14 (s), 130.25 (s), 122.65 (s), 120.52 (m), 90.52 (m), 75.62 (m). IR (KBr disc): 2919, 2850, 2253 ($\text{C}\equiv\text{C}$), 1475, 1458, 1353, 1239, 1207, 1135 cm^{-1} . HRMS (EI) m/z calculated for $\text{C}_{12}\text{H}_4\text{F}_9\text{Br}$: 397.9352, found 397.9343.

1i

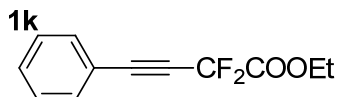


1-Phenyl-2-perfluorohexyl acetylene (1i)¹¹: colorless oil. Yield: 94 mg, 62%. ^1H NMR (600 MHz, CDCl_3): δ 7.53 (m, 2H), 7.45 (dd, $J = 10.8, 4.3$ Hz, 1H), 7.37 (m, 2H). ^{19}F NMR (565 MHz, CDCl_3): δ -81.34 (t, $J = 9.8$ Hz, 3F), -97.46 (s, 2F), -121.56 (s, 2F), -122.79 (s, 2F), -123.10 (d, $J = 5.6$ Hz, 2F), -126.49 (dd, $J = 13.8, 9.2$ Hz, 2F). $^{13}\text{C}\{\text{H}\}$ NMR (151 MHz, CDCl_3) δ 132.75 (d, $J = 2.0$ Hz), 131.32 (s), 128.93 (s), 92.51 (m), 74.92 (m). IR (KBr disc): 2926, 2246 ($\text{C}\equiv\text{C}$), 1637, 1493, 1447, 1384, 1316, 1242, 1204, 1148 cm^{-1} . HRMS (EI) m/z calculated for $\text{C}_{14}\text{H}_5\text{F}_{13}$: 420.0183, found 420.0168.

1j



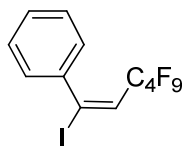
1-Phenyl-2-perfluoroctyl acetylene (1j)¹⁰: white solid. Yield: 60 mg, 32%. ^1H NMR (600 MHz, CDCl_3): δ 7.52 (d, $J = 7.2$ Hz, 2H), 7.44 (t, $J = 7.6$ Hz, 1H), 7.35 (t, $J = 7.7$ Hz, 2H). ^{19}F NMR (565 MHz, CDCl_3): δ -81.61 (m, 3F), -97.63 (s, 2F), -121.48 (s, 2F), -122.30 (dd, $J = 35.2, 11.7$ Hz, 4F), -122.87 (s, 2F), -123.21 (s, 2F), -126.71 (dd, $J = 15.7, 11.4$ Hz, 2F). $^{13}\text{C}\{\text{H}\}$ NMR (151 MHz, CDCl_3) δ 132.84 (d, $J = 2.3$ Hz), 131.38 (s), 129.01 (s), 119.08 (m), 92.43 (m), 75.07 (m). IR (KBr disc): 2927, 2247 ($\text{C}\equiv\text{C}$), 1637, 1493, 1447, 1384, 1312, 1245, 1214, 1150 cm^{-1} . HRMS (EI) m/z calculated for $\text{C}_{16}\text{H}_5\text{F}_{17}$: 520.0119, found 520.0106.



1-Phenyl-2-ethoxydifluoromethylcarbonyl acetylene (1k)¹⁰: colorless oil. Yield: 58 mg, 71%. ¹H NMR (600 MHz, CDCl₃): δ 7.52 (dd, *J* = 10.5, 9.4 Hz, 2H), 7.43 (t, *J* = 7.5 Hz, 1H), 7.36 (dd, *J* = 10.6, 4.6 Hz, 2H), 4.40 (q, *J* = 7.1 Hz, 2H), 1.38 (m, 3H). ¹⁹F NMR (565 MHz, CDCl₃): δ -90.00 (d, *J* = 24.5 Hz, 2F). ¹³C{¹H} NMR (151 MHz, CDCl₃) δ 161.59 (t), 132.40 (d, *J* = 2.1 Hz), 130.62 (s), 128.64 (s), 119.36 (s), 106.63 (m), 105.03 (s), 103.41 (m), 89.72 (s), 78.44 (t), 63.89 (s), 13.89 (s). IR (KBr disc): 2988, 2928, 2243 (C≡C), 1775 (C=O), 1490, 1445, 1384, 1305, 1274, 1144, 1079 cm⁻¹. HRMS (EI) *m/z* calculated for C₁₂H₁₀F₂O₂: 224.0648, found 224.0640.

Characterization of Photocatalytic Addition Products

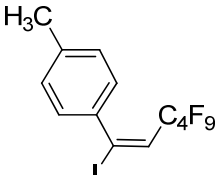
2a



(E/Z)-1-phenyl-1-iodo-2-perfluorobutyl ethene (2a) (*E/Z*=85:15)^{9c}: pale yellow oil.

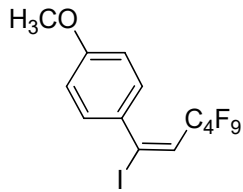
Yield: 113 mg, 70%. ¹H NMR (600 MHz, CDCl₃): *E*-isomer (major): δ 7.28 (m, 5H), 6.61 (t, *J* = 13.5 Hz, 1H). ¹⁹F NMR (565 MHz, CDCl₃): δ -81.33 (t, *J* = 9.0 Hz, 3F), -105.54 (t, *J* = 12.1 Hz, 2F), -123.97 (m, 2F), -126.06 (s, 2F). ¹³C{¹H} NMR (151 MHz, CDCl₃) δ 141.54 (s), 130.33 (s), 129.42 (s), 128.68 (s), 128.38 (s), 128.14 (s), 127.01 (d, *J* = 1.7 Hz), 112.97 (m). IR (KBr disc): 2918, 2848, 1649, 1638, 1489, 1445, 1351, 1233, 1134 cm⁻¹. HRMS (EI) *m/z* calculated for C₁₂H₆F₉I: 447.9371, found 447.9371.

2b



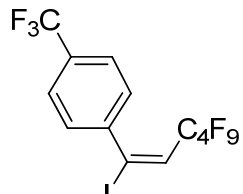
(E/Z)-1-(4-methylphenyl)-1-iodo-2-perfluorobutyl ethene (2b) (*E/Z*=84:16)¹²: pale yellow oil. Yield: 132 mg, 80%. ¹H NMR (600 MHz, CDCl₃): *E*-isomer (major): δ 7.19 (d, *J* = 8.1 Hz, 2H), 7.13 (d, *J* = 7.9 Hz, 2H), 6.56 (t, *J* = 13.5 Hz, 1H), 2.35 (s, 3H). ¹⁹F NMR (565 MHz, CDCl₃): δ -81.10 (t, *J* = 9.1 Hz, 3F), -105.34 (t, *J* = 12.1 Hz, 2F), -123.86 (m, 2F), -125.86 (m, 2F). ¹³C{¹H} NMR (151 MHz, CDCl₃) δ 139.49 (m), 138.47 (m), 129.17 (m), 128.68 (m), 128.17 (m), 126.92 (m), 126.49 (m), 113.41 (m), 21.28 (m). IR (KBr disc): 3072, 2927, 2861, 1641, 1601, 1524, 1489, 1349, 1232, 1132 cm⁻¹. HRMS (EI) *m/z* calculated for C₁₃H₈F₉I: 461.9527, found 461.9511.

2c

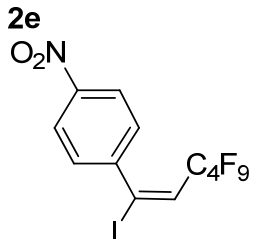


(E/Z)-1-(4-methoxyphenyl)-1-iodo-2-perfluorobutyl ethene (2c) (*E/Z*=83:17)¹²: pale yellow oil. Yield: 105 mg, 61%. ¹H NMR (600 MHz, CDCl₃): *E*-isomer (major): δ 7.26 (t, *J* = 5.8 Hz, 2H), 6.83 (m, 2H), 6.55 (t, *J* = 13.5 Hz, 1H), 3.79 (s, 3H). ¹⁹F NMR (565 MHz, CDCl₃): δ -81.18 (t, *J* = 49.1, 10.1 Hz, 3F), -105.15 (t, *J* = 12.1 Hz, 2F), -123.90 (m, 2F), -125.95 (m, 2F). ¹³C{¹H} NMR (151 MHz, CDCl₃) δ 160.39 (s), 133.74 (s), 128.90 (d, *J* = 2.0 Hz), 126.40 (m), 113.45 (s), 55.32 (s). IR (KBr disc): 2961, 2933, 2843, 1636, 1605, 1575, 1508, 1468, 1444, 1353, 1296, 1235, 1177, 1134 cm⁻¹. HRMS (EI) *m/z* calculated for C₁₃H₈F₉OI: 477.9476, found 477.9454.

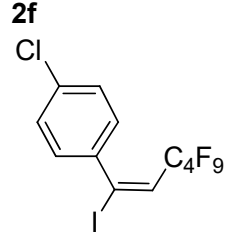
2d



(E/Z)-1-(4-trifluorophenyl)-1-iodo-2-perfluorobutyl ethene (2d) (*E/Z*=90:10): pale yellow oil. Yield: 118 mg, 64%. ¹H NMR (600 MHz, CDCl₃): *E*-isomer (major): δ 7.60 (d, *J* = 8.2 Hz, 2H), 7.40 (d, *J* = 8.2 Hz, 2H), 6.66 (t, *J* = 13.4 Hz, 1H). ¹⁹F NMR (565 MHz, CDCl₃): δ -63.30 (s, 3F), -81.42 (t, *J* = 9.2 Hz, 3F), -105.86 (t, *J* = 12.1 Hz, 2F), -124.05 (m, 2F), -126.11 (m, 2F). ¹³C{¹H} NMR (151 MHz, CDCl₃) δ 144.92 (s), 131.53 (m), 128.68 (m), 128.39 (s), 127.37 (s), 125.33 (q, *J* = 4.0 Hz), 110.02 (m). IR (KBr disc): 3073, 2924, 1638, 1601, 1507, 1354, 1236, 1134 cm⁻¹. HRMS (EI) *m/z* calculated for C₁₃H₅F₁₂I: 515.9244, found 515.9247.

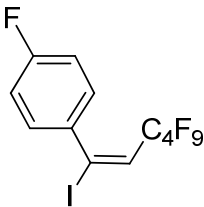


(*E/Z*)-1-(4-nitrophenyl)-1-iodo-2-perfluorobutyl ethene (2e) (*E/Z*=76:24): pale yellow oil. Yield: 51 mg, 29%. ^1H NMR (600 MHz, CDCl_3): *E*-isomer (major): δ 8.23 (m, 2H), 7.46 (d, $J = 8.7$ Hz, 2H), 6.70 (t, $J = 13.4$ Hz, 1H). ^{19}F NMR (565 MHz, CDCl_3): δ -81.29 (t, $J = 10.1$ Hz, 3F), -105.87 (t, $J = 12.2$ Hz, 2F), -123.88 (m, 2F), -126.04 (m, 2F). $^{13}\text{C}\{\text{H}\}$ NMR (151 MHz, CDCl_3) δ 148.12 (s), 147.50 (s), 129.26 (m), 128.86 (m), 127.97 (s), 123.91 (s), 123.57 (s), 108.49 (m). IR (KBr disc): 3072, 2928, 2861, 1640, 1601, 1524, 1349, 1232, 1132 cm^{-1} . HRMS (EI) m/z calculated for $\text{C}_{12}\text{H}_5\text{F}_9\text{INO}_2$: 492.9221, found 492.9211.



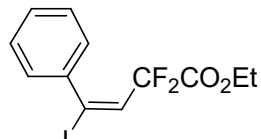
(*E/Z*)-1-(4-chlorophenyl)-1-iodo-2-perfluorobutyl ethene (2f) (*E/Z*=86:14)^{14a}: pale yellow oil. Yield: 96 mg, 55%. ^1H NMR (600 MHz, CDCl_3): *E*-isomer (major): δ 7.30 (m, 2H), 7.22 (d, $J = 8.5$ Hz, 2H), 6.60 (t, $J = 13.4$ Hz, 1H). ^{19}F NMR (565 MHz, CDCl_3): δ -81.32 (t, $J = 9.2$ Hz, 3F), -105.57 (t, $J = 12.1$ Hz, 2F), -123.94 (m, 2F), -126.02 (m, 2F). $^{13}\text{C}\{\text{H}\}$ NMR (151 MHz, CDCl_3) δ 139.86 (s), 135.55 (s), 129.60 (s), 128.44 (d, $J = 16.5$ Hz), 127.79 (t, $J = 22.2$ Hz), 111.09 (m). IR (KBr disc): 3072, 2929, 1639, 1592, 1488, 1399, 1353, 1235, 1135 cm^{-1} . HRMS (EI) m/z calculated for $\text{C}_{12}\text{H}_5\text{F}_9\text{ICl}$: 481.8980, found 481.8963.

2g



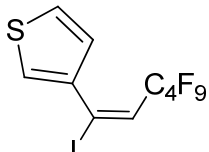
(E/Z)-1-(4-fluorophenyl)-1-iodo-2-perfluorobutyl ethene (2g) (*E/Z*=85:15): pale yellow oil. Yield: 102 mg, 61%. ^1H NMR (600 MHz, CDCl_3): *E*-isomer (major): δ 7.29 (ddd, $J = 6.9, 5.0, 2.5$ Hz, 2H), 7.01 (ddd, $J = 9.7, 5.9, 2.5$ Hz, 2H), 6.60 (t, $J = 13.4$ Hz, 1H). ^{19}F NMR (565 MHz, CDCl_3): δ -81.32 (m, 3F), -105.53 (t, $J = 12.2$ Hz, 2F), -110.99 (s, 1F), -123.97 (dt, $J = 18.2, 6.8$ Hz, 2F), -126.04 (m, 2F). $^{13}\text{C}\{\text{H}\}$ NMR (151 MHz, CDCl_3) δ 163.87 (s), 162.21 (s), 137.48 (d, $J = 3.3$ Hz), 130.28 (m), 129.13 (d, $J = 8.7$ Hz), 127.68 (s), 115.40 (s), 115.25 (s). IR (KBr disc): 3073, 2927, 1637, 1601, 1507, 1354, 1236, 1161, 1134, 1113 cm^{-1} . HRMS (EI) m/z calculated for $\text{C}_{12}\text{H}_5\text{F}_{10}\text{I}$: 465.9276, found 465.9271.

2h



(E/Z)-1-phenyl-1-iodo-2-ethoxydifluoromethylcarbonyl ethene (2h) (*E/Z*=86:14)¹³: pale yellow oil. Yield: 42 mg, 33%. ^1H NMR (600 MHz, CDCl_3): *E*-isomer (major): δ 7.27 (m, 5H), 6.71 (m, 1H), 3.93 (q, $J = 7.2$ Hz, 2H), 1.15 (t, $J = 7.2$ Hz, 3H). ^{19}F NMR (565 MHz, CDCl_3): δ -93.76 (d, $J = 18.4$ Hz, 2F). $^{13}\text{C}\{\text{H}\}$ NMR (151 MHz, CDCl_3) δ 162.43 (t), 140.64 (s), 132.99 (t, $J = 28.5$ Hz), 129.40 (s), 128.01 (s), 127.77 (d, $J = 1.7$ Hz), 112.49 (m), 110.84 (s), 109.17 (m), 108.74 (t), 63.07 (s), 13.62 (s). IR (KBr disc): 3058, 2985, 2938, 1773, 1631, 1595, 1473, 1395, 1302, 1191, 1164, 1105, 1070 cm^{-1} . HRMS (EI) m/z calculated for $\text{C}_{12}\text{H}_{11}\text{F}_2\text{O}_2\text{I}$: 351.9772, found 351.9761.

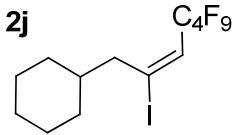
2i



(E/Z)-1-(thiophen-3-yl)-1-iodo-2-perfluorobutyl ethene (2i) (*E/Z*=88:12): yellow oil.

Yield: 144 mg, 88%. ^1H NMR (600 MHz, CDCl_3): *E*-isomer (major): δ 7.37 (d, $J = 2.2$ Hz, 1H), 7.28 (m, 1H), 7.10 (d, $J = 5.0$ Hz, 1H), 6.57 (t, $J = 13.5$ Hz, 1H). ^{19}F NMR (565 MHz, CDCl_3): δ -81.23 (t, $J = 10.2$ Hz, 3F), -105.18 (t, $J = 12.2$ Hz, 2F), -123.97 (s, 2F), -125.94 (m, 2F). $^{13}\text{C}\{\text{H}\}$ NMR (151 MHz, CDCl_3) δ 140.56 (m), 128.89 (s), 127.93 (s), 127.16 (m), 126.92 (s), 126.17 (s), 125.50 (s), 125.19 (m), 121.51 (m), 106.49 (m). IR (KBr disc): 3097, 2988, 2928, 1618, 1517, 1415, 1354, 1235, 1133, 1109 cm^{-1} . HRMS (EI) m/z calculated for $\text{C}_{10}\text{H}_4\text{F}_9\text{IS}$: 453.8935, found 453.8940.

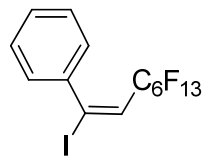
2j



(E/Z)-3-cyclohexyl-2-iodo-1-perfluorobutyl-1-propene (2j) (*E/Z*=73:27): colorless oil.

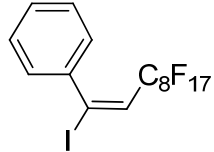
Yield: 81 mg, 48%. ^1H NMR (600 MHz, CDCl_3): *E*-isomer (major): δ 6.39 (t, $J = 14.5$ Hz, 1H), 2.48 (d, $J = 6.4$ Hz, 2H), 1.72 (m, 6H), 1.28 (m, 2H), 1.16 (m, 1H), 0.97 (m, 2H). ^{19}F NMR (565 MHz, CDCl_3): δ -81.20 (tt, $J = 9.4, 2.3$ Hz, 3F), -104.59 (m, 2F), -124.12 (m, 2F), -125.93 (m, 2F). $^{13}\text{C}\{\text{H}\}$ NMR (151 MHz, CDCl_3) δ 127.44 (t, $J = 23.2$ Hz), 122.58 (t, $J = 5.9$ Hz), 47.59 (s), 38.70 (s), 32.17 (s), 26.27 (d, $J = 8.5$ Hz). IR (KBr disc): 2931, 2855, 1635, 1454, 1354, 1236, 1173, 1134, 1112 cm^{-1} . HRMS (EI) m/z calculated for $\text{C}_{13}\text{H}_{14}\text{F}_9\text{I}$: 467.9997, found 467.9983.

2k

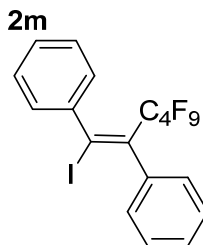


(E/Z)-1-phenyl-1-iodo-2-perfluorohexyl ethene (2k) ($E/Z=86:14$)¹⁴: white solid. Yield: 159 mg, 81%. ^1H NMR (600 MHz, CDCl_3): *E*-isomer (major): δ 7.27 (m, 5H), 6.60 (t, $J = 13.4$ Hz, 1H). ^{19}F NMR (565 MHz, CDCl_3): δ -81.43 (t, $J = 8.6$ Hz, 3F), -105.44 (t, $J = 13.1$ Hz, 2F), -122.00 (s, 2F), -123.16 (m, 4F), -126.62 (m, 2F). $^{13}\text{C}\{\text{H}\}$ NMR (151 MHz, CDCl_3) δ 141.67 (s), 130.37 (s), 129.47 (s), 128.76 (m), 128.19 (s), 127.34 (t, $J = 22.2$ Hz), 127.08 (d, $J = 1.9$ Hz), 112.75 (t, $J = 6.2$ Hz). IR (KBr disc): 3080, 3029, 2928, 1647, 1490, 1444, 1366, 1248, 1194, 1141, 1116, 1062 cm^{-1} . HRMS (EI) *m/z* calculated for $\text{C}_{14}\text{H}_6\text{F}_{13}\text{I}$: 547.9307, found 547.9302.

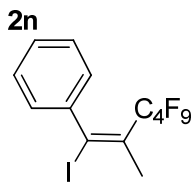
2l



(E/Z)-1-phenyl-1-iodo-2-perfluoroctyl ethene (2l) ($E/Z=87:13$)^{9c,14a}: white powdery solid. Yield: 167 mg, mmol, 71%. ^1H NMR (600 MHz, CDCl_3): *E*-isomer (major): δ 7.28 (m, 5H), 6.60 (t, $J = 13.4$ Hz, 1H). ^{19}F NMR (565 MHz, CDCl_3): δ -81.56 (t, $J = 10.2$ Hz, 3F), -105.52 (t, $J = 13.2$ Hz, 2F), -121.86 (s, 2F), -122.33 (d, $J = 18.4$ Hz, 4F), -123.18 (s, 4F), -126.70 (m, 2F). $^{13}\text{C}\{\text{H}\}$ NMR (151 MHz, CDCl_3) δ 141.71 (s), 130.37 (s), 129.47 (s), 128.74 (m), 128.47 (s), 128.20 (s), 127.40 (t, $J = 22.2$ Hz), 127.10 (s), 112.65 (t, $J = 6.1$ Hz). IR (KBr disc): 3068, 3029, 2929, 1650, 1488, 1442, 1373, 1329, 1253, 1216, 1146, 1114, 1072 cm^{-1} . HRMS (EI) *m/z* calculated for $\text{C}_{16}\text{H}_6\text{F}_{17}\text{I}$: 647.9243, found 647.9224.

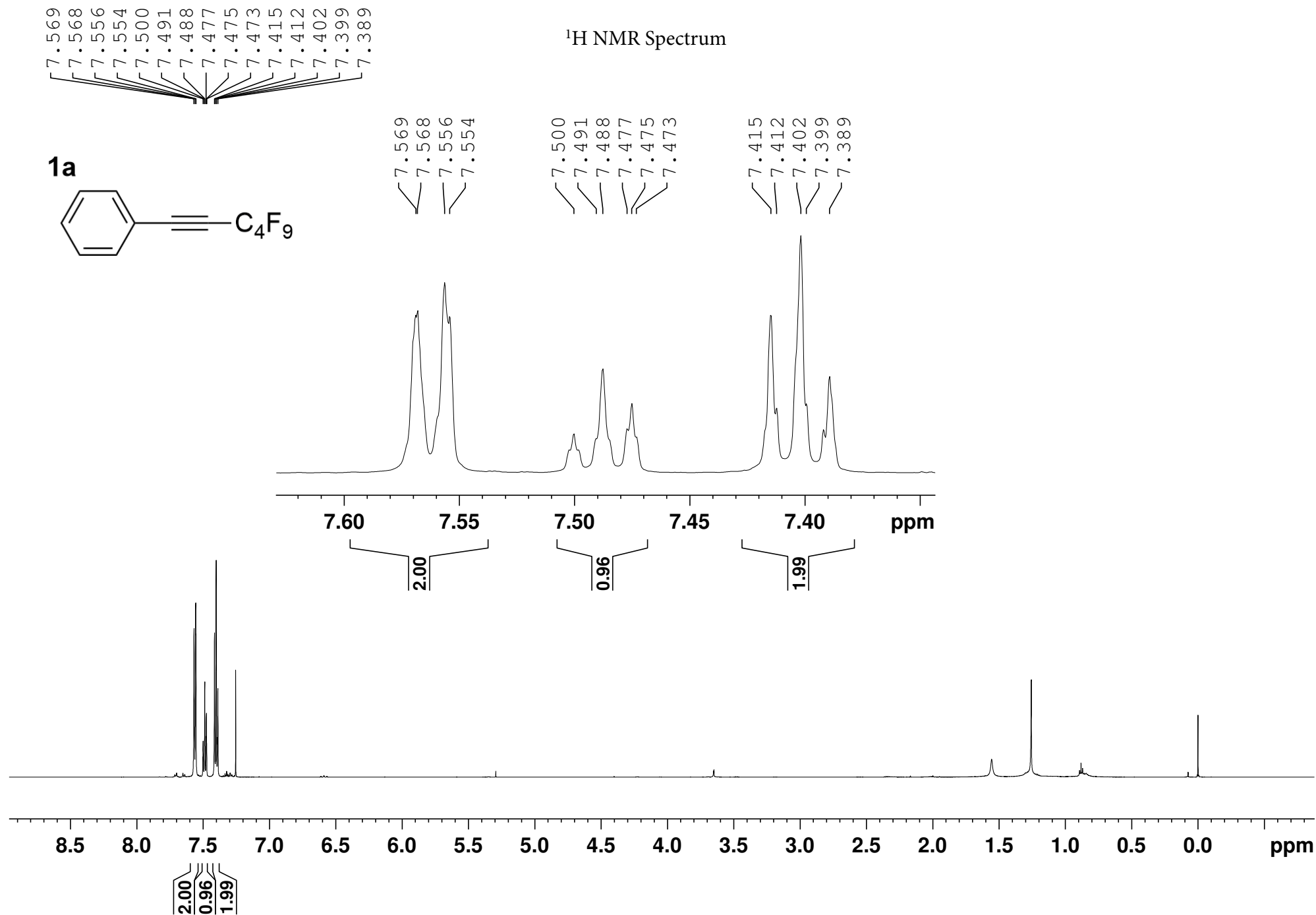


(E/Z)-1,2-diphenyl-1-iodo-2-perfluorobuty ethene (2m) (*E/Z*=91:9): white powdery solid. Yield: 50 mg, 27%. ^1H NMR (600 MHz, CDCl_3): *E*-isomer (major): δ 7.54 (m, 5H), 7.35 (m, 5H). ^{19}F NMR (565 MHz, CDCl_3): δ -81.03 (t, J = 9.2 Hz, 3F), -100.55 (t, J = 14.8 Hz, 2F), -118.21 (d, J = 7.4 Hz, 2F), -126.16 (m, 2F). $^{13}\text{C}\{\text{H}\}$ NMR (151 MHz, CDCl_3) δ 131.61 (s), 128.35 (s), 128.26 (s), 123.28 (s), 89.37 (s). IR (KBr disc): 3064, 2918, 2852, 1598, 1493, 1442, 1236, 1136, 1070, 916 cm^{-1} . HRMS (EI) m/z calculated for $\text{C}_{18}\text{H}_{10}\text{F}_9\text{I}$: 523.9684, found 523.9681.

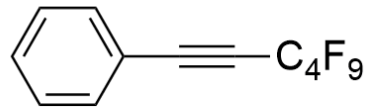


(E/Z)-1-phenyl-1-iodo-2-perfluorobutyl-1-propene (2n) (*E/Z*=87:13)^{9d}: white powdery solid. Yield: 61 mg, 36%. ^1H NMR (600 MHz, CDCl_3): *E*-isomer (major): δ 7.28 (dd, J = 10.4, 4.6 Hz, 2H), 7.21 (m, 1H), 7.17 (d, J = 7.5 Hz, 2H), 2.28 (s, 3H). ^{19}F NMR (565 MHz, CDCl_3): δ -81.10 (m, 3F), -103.47 (t, J = 14.3 Hz, 2F), -120.57 (dd, J = 17.7, 9.3 Hz, 2F), -126.31 (pd, J = 9.3, 7.1 Hz, 2F). $^{13}\text{C}\{\text{H}\}$ NMR (151 MHz, CDCl_3) δ 144.29 (s), 130.15 (t, J = 20.4 Hz), 128.83 (s), 128.33 (s), 127.76 (s), 126.91 (s), 114.90 (t, J = 4.6 Hz), 26.65 (m). IR (KBr disc): 3081, 3031, 2924, 1635, 1444, 1351, 1254, 1197, 1172, 1138, 1138, 1126, 1104 cm^{-1} . HRMS (EI) m/z calculated for $\text{C}_{13}\text{H}_8\text{F}_9\text{I}$: 461.9527, found 461.9530.

9. ^1H , ^{19}F and $^{13}\text{C}\{^1\text{H}\}$ NMR Spectra of Products from the Photocatalytic Reactions



1a



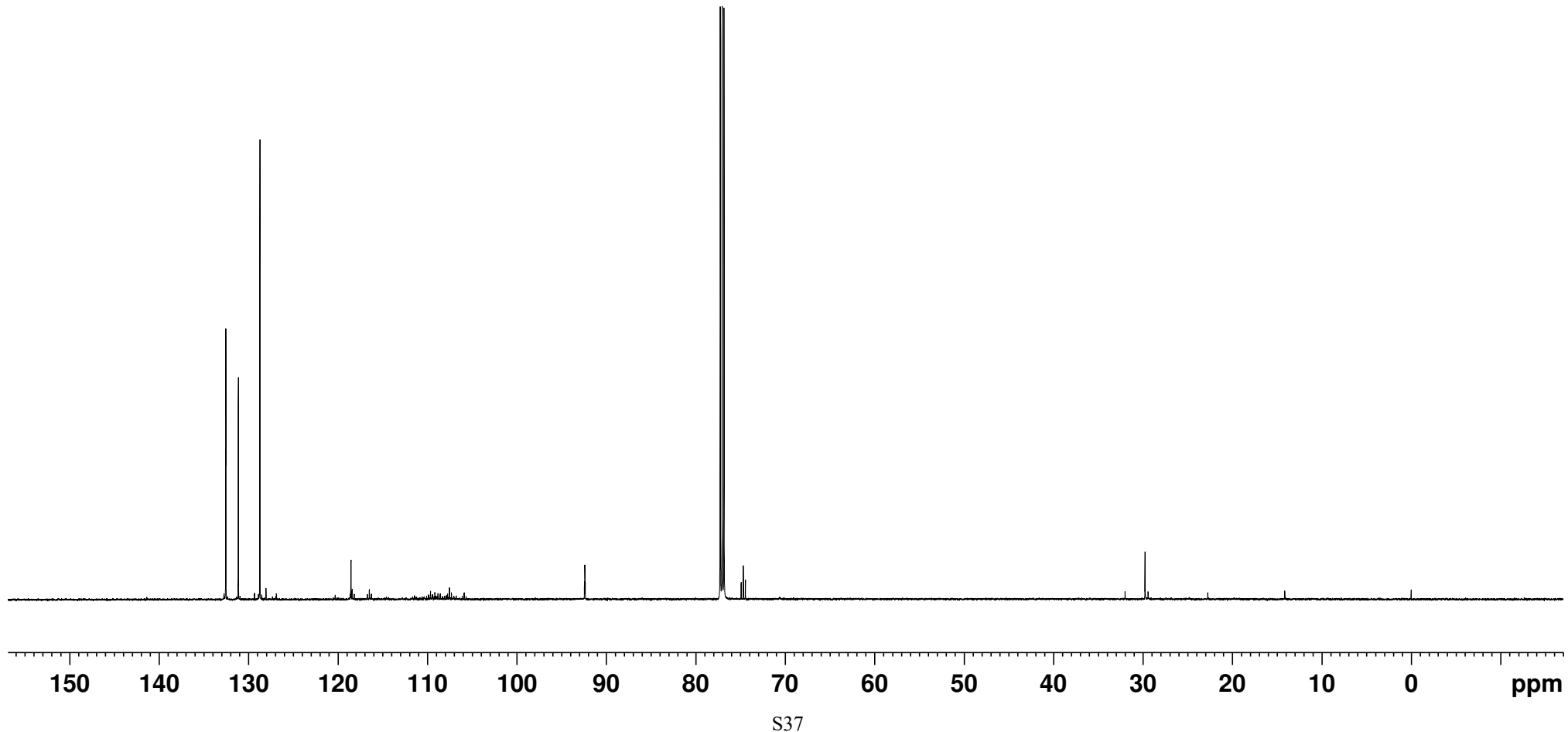
132.54
131.14
128.72

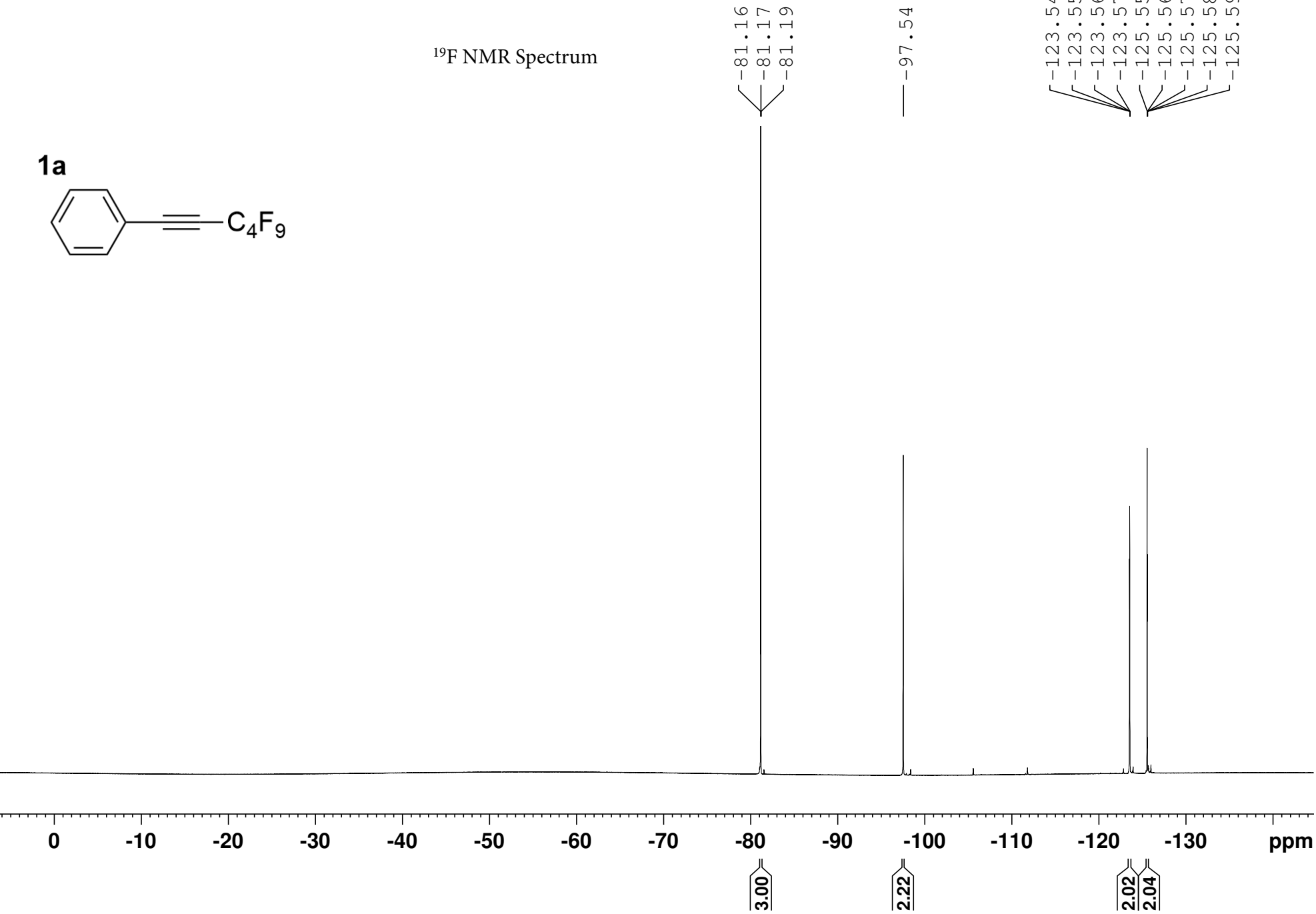
118.56
118.54
118.52

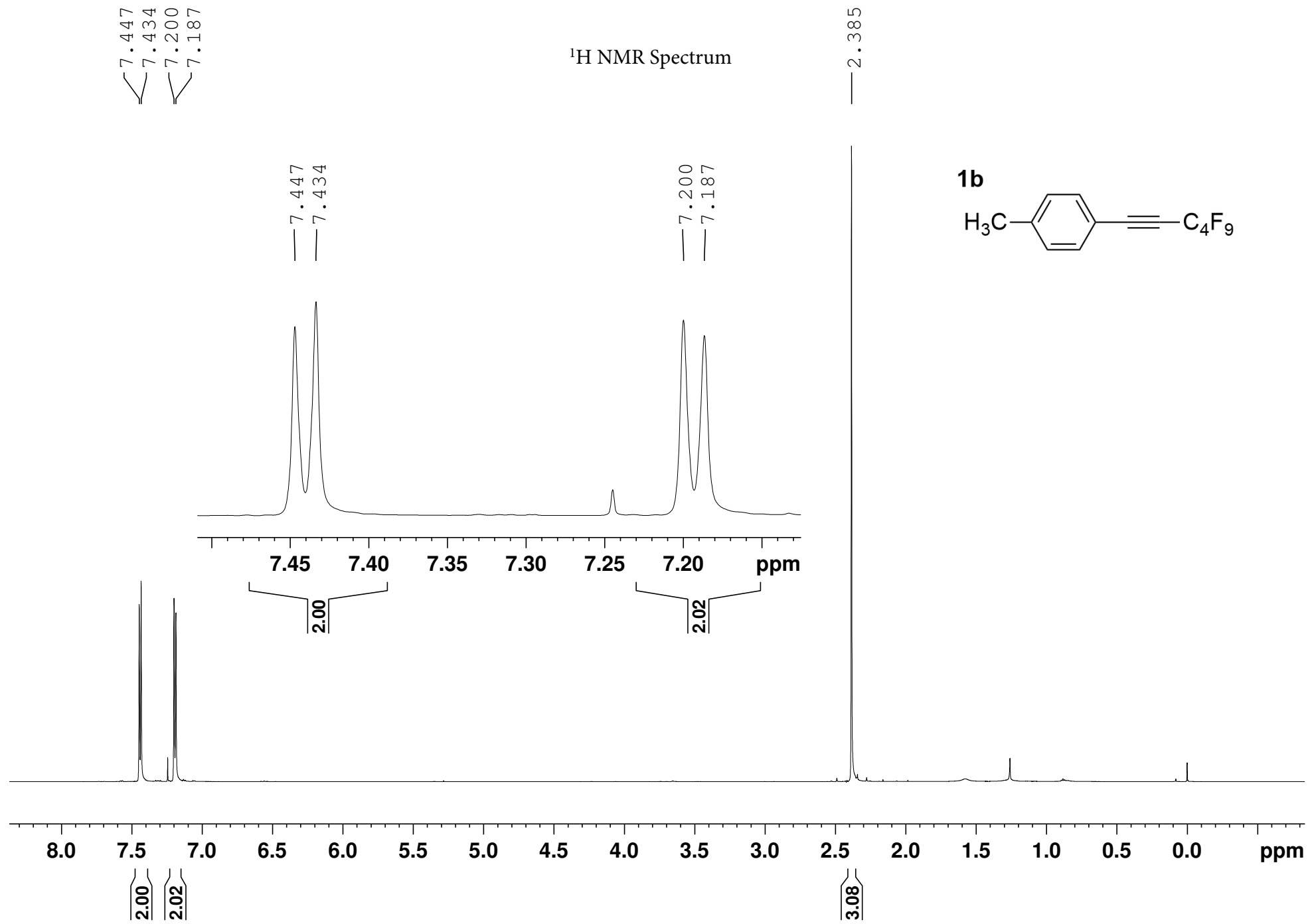
92.43
92.39
92.35

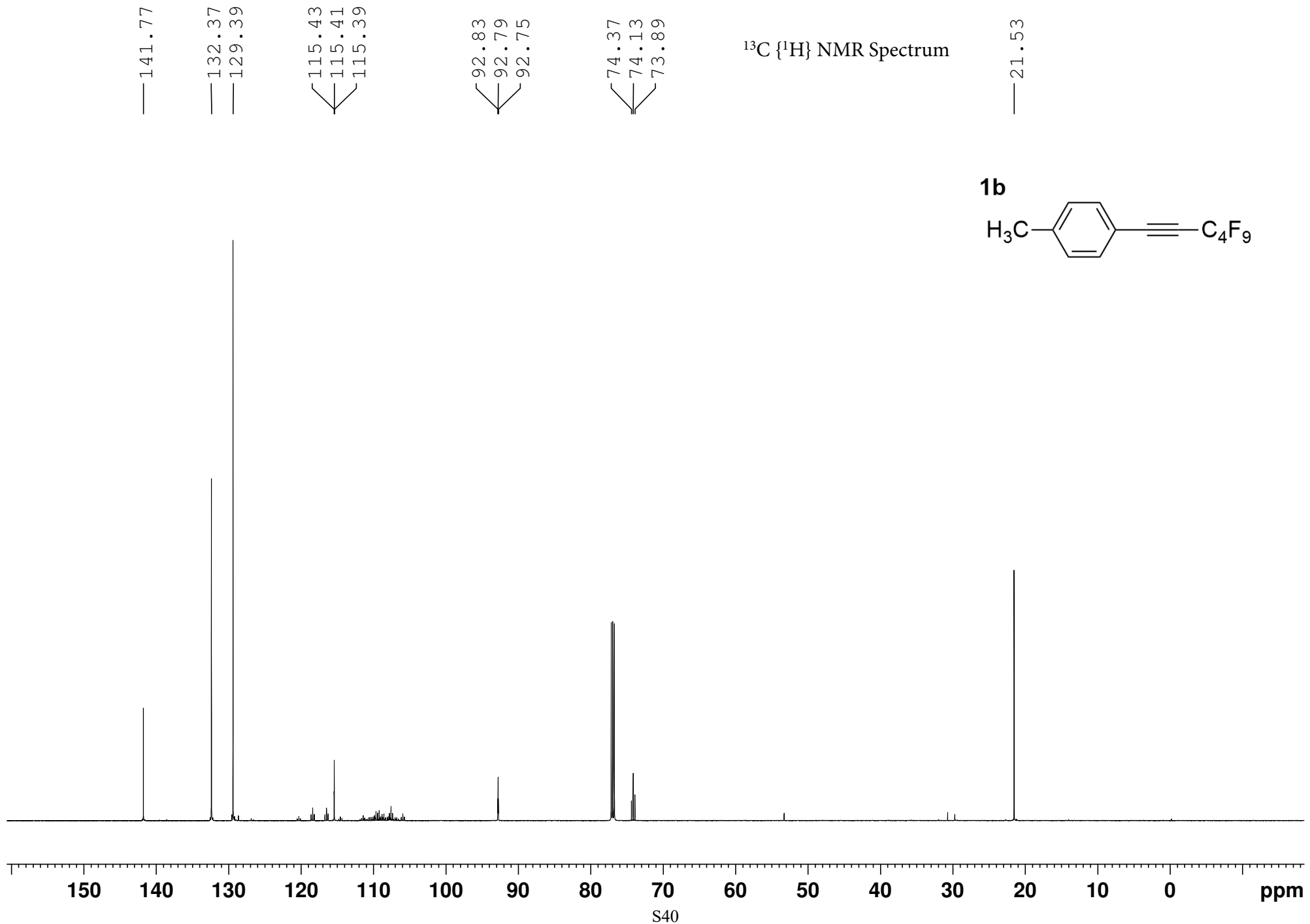
74.91
74.67
74.43

$^{13}\text{C} \{^1\text{H}\}$ NMR Spectrum









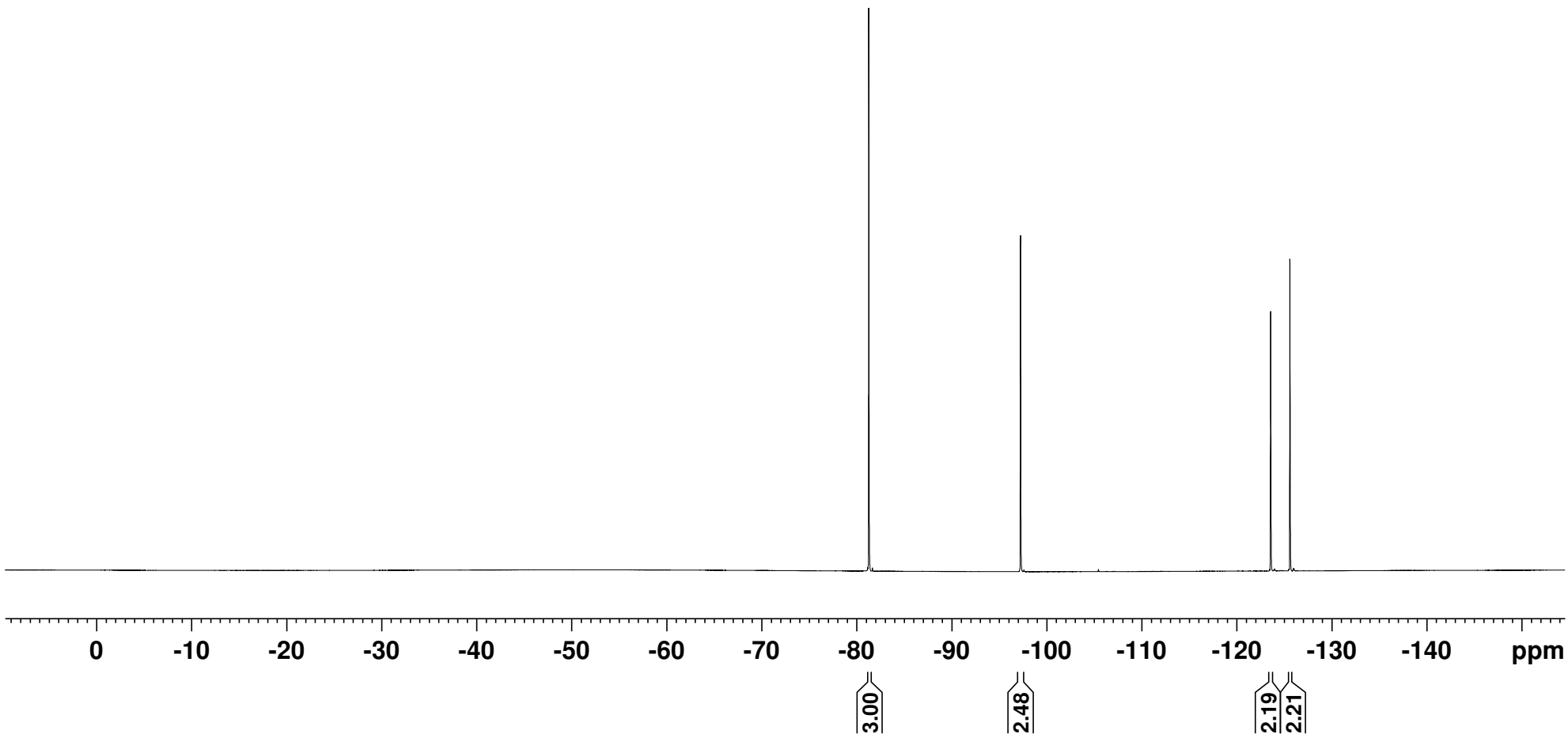
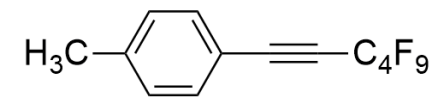
¹⁹F NMR Spectrum

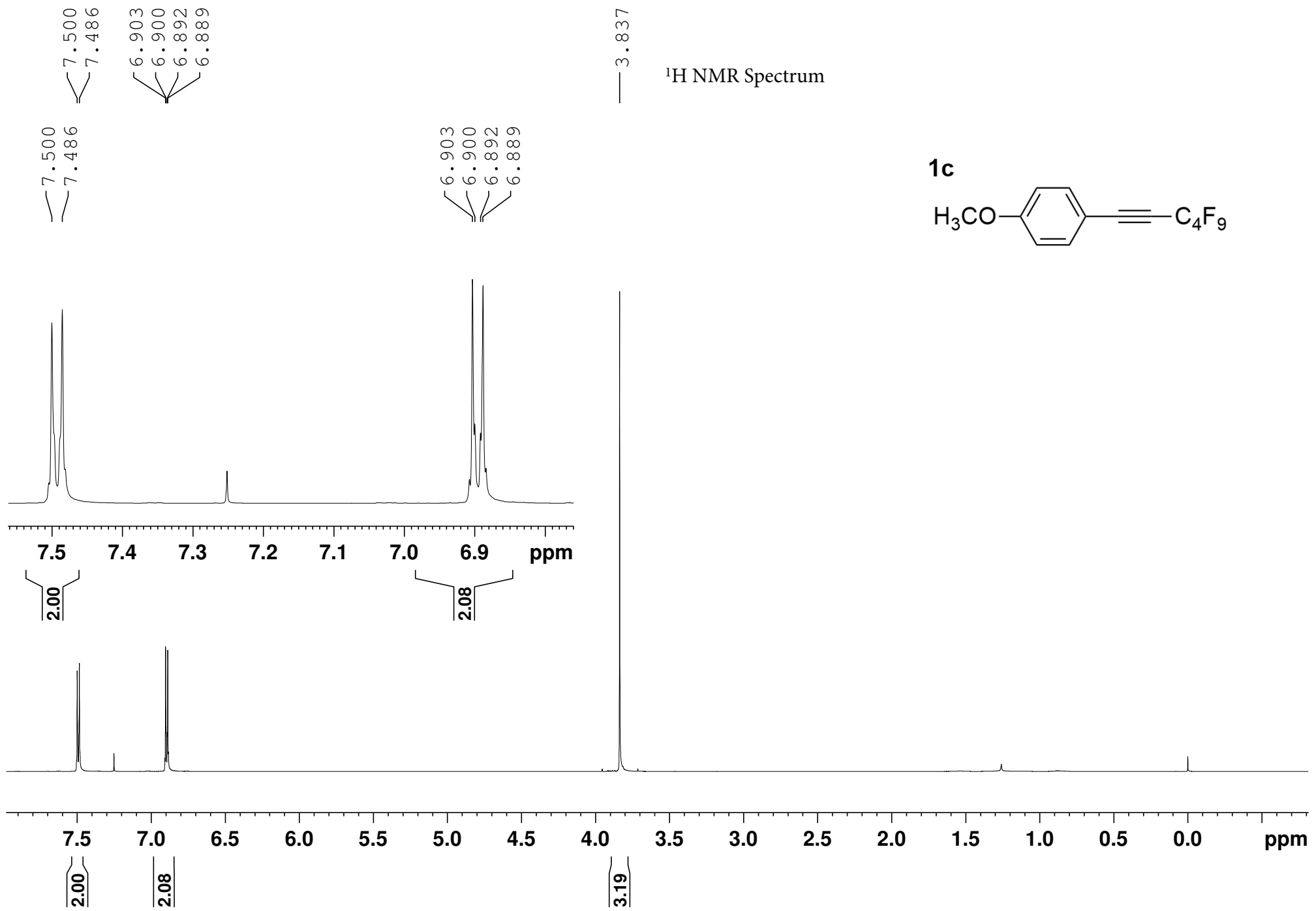
[-81.26
-81.27
-81.29]

-97.24

[-123.57
-123.58
-125.60
-125.61]

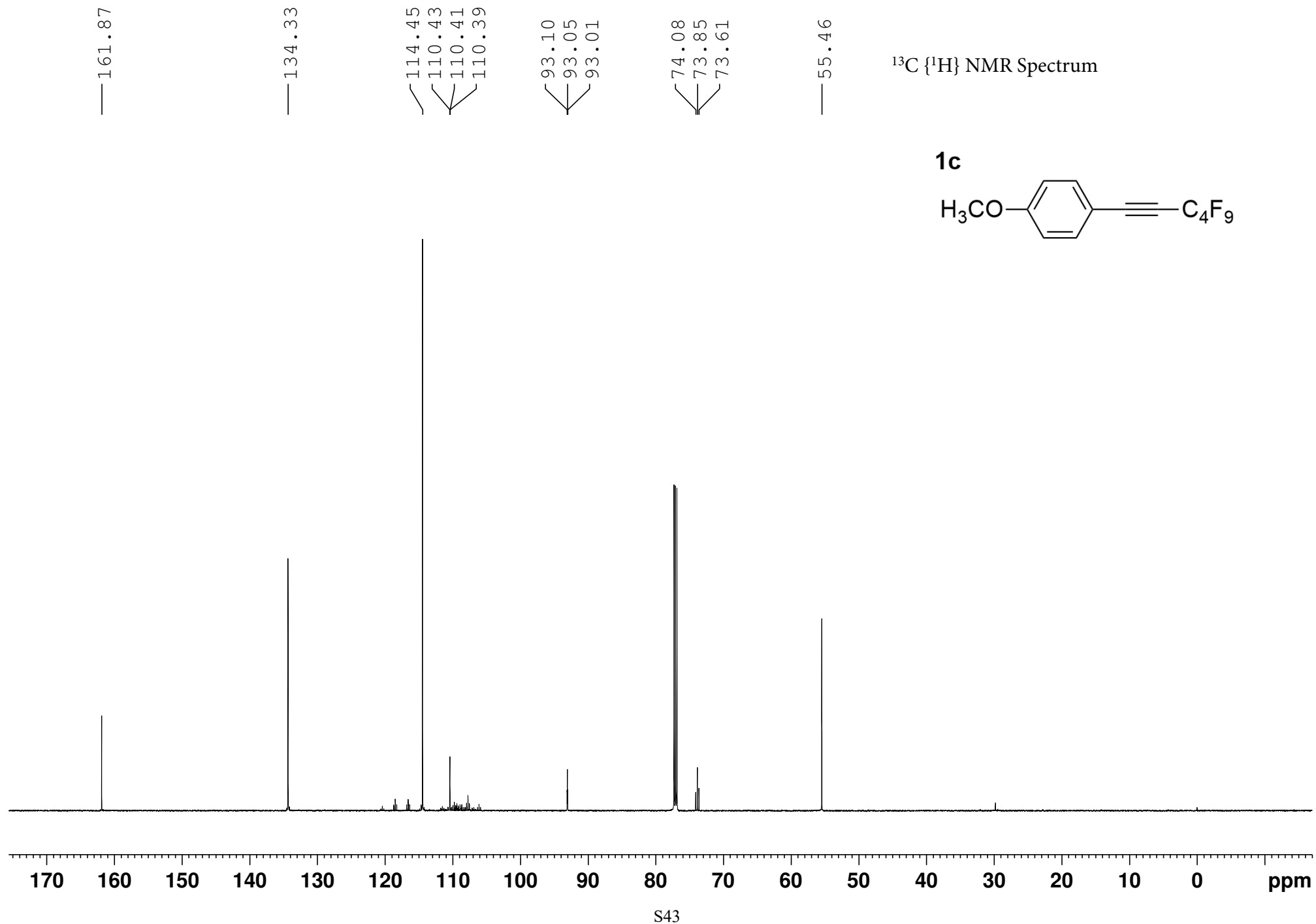
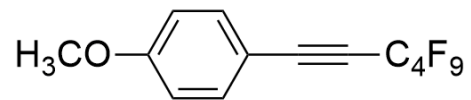
1b

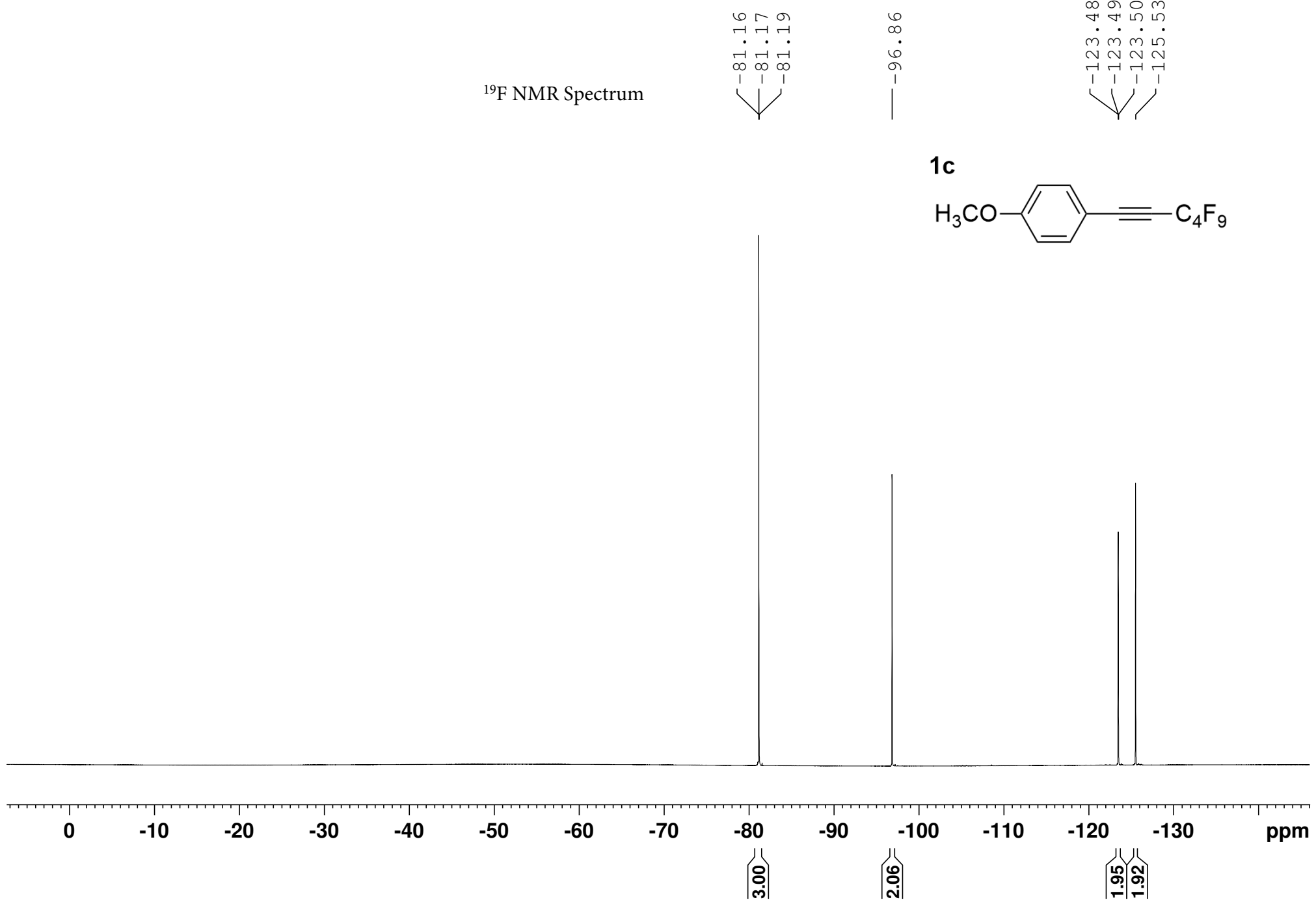


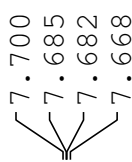


¹³C {¹H} NMR Spectrum

1c

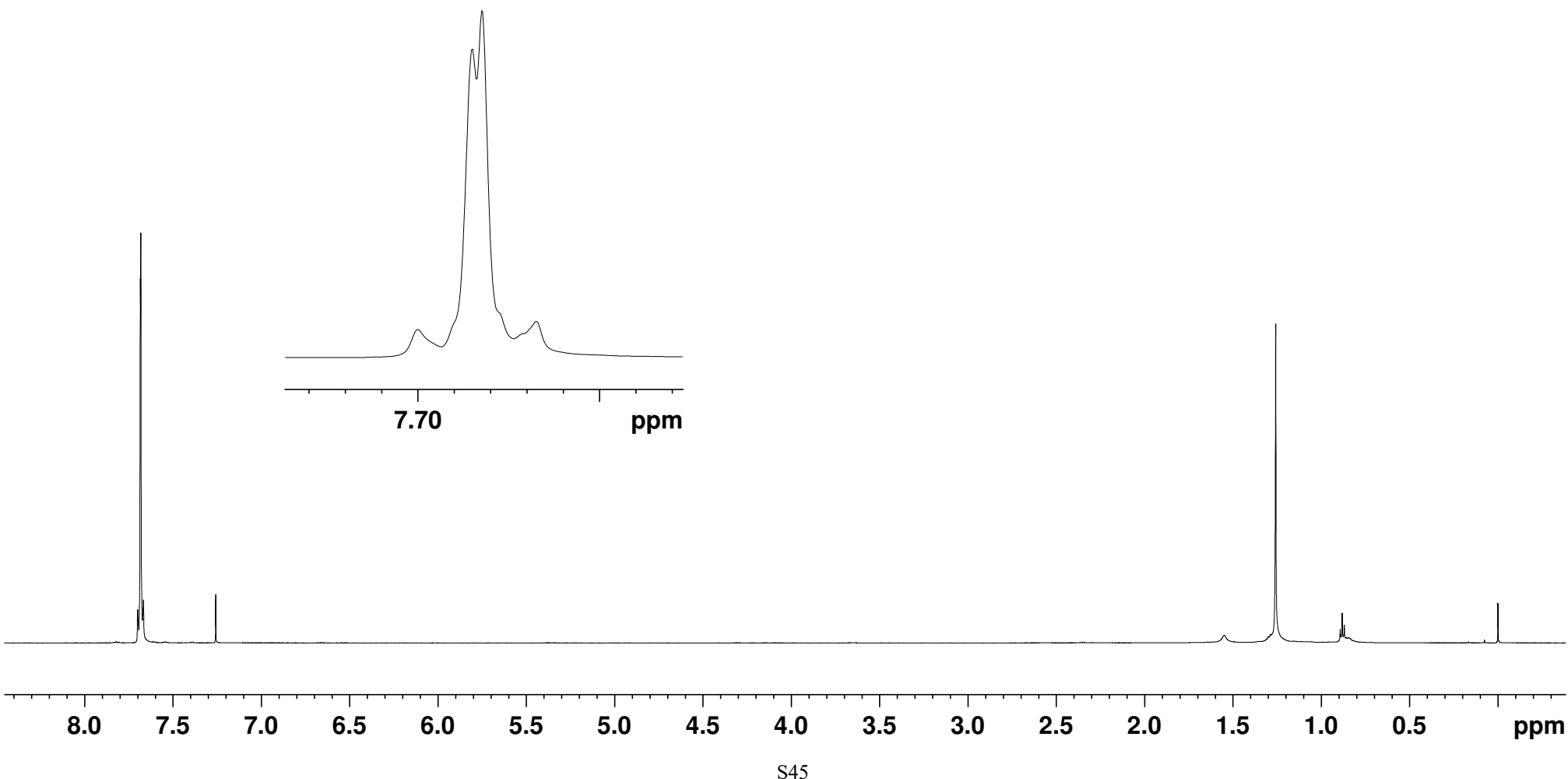
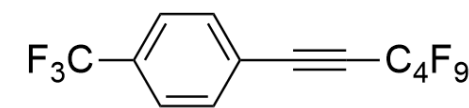


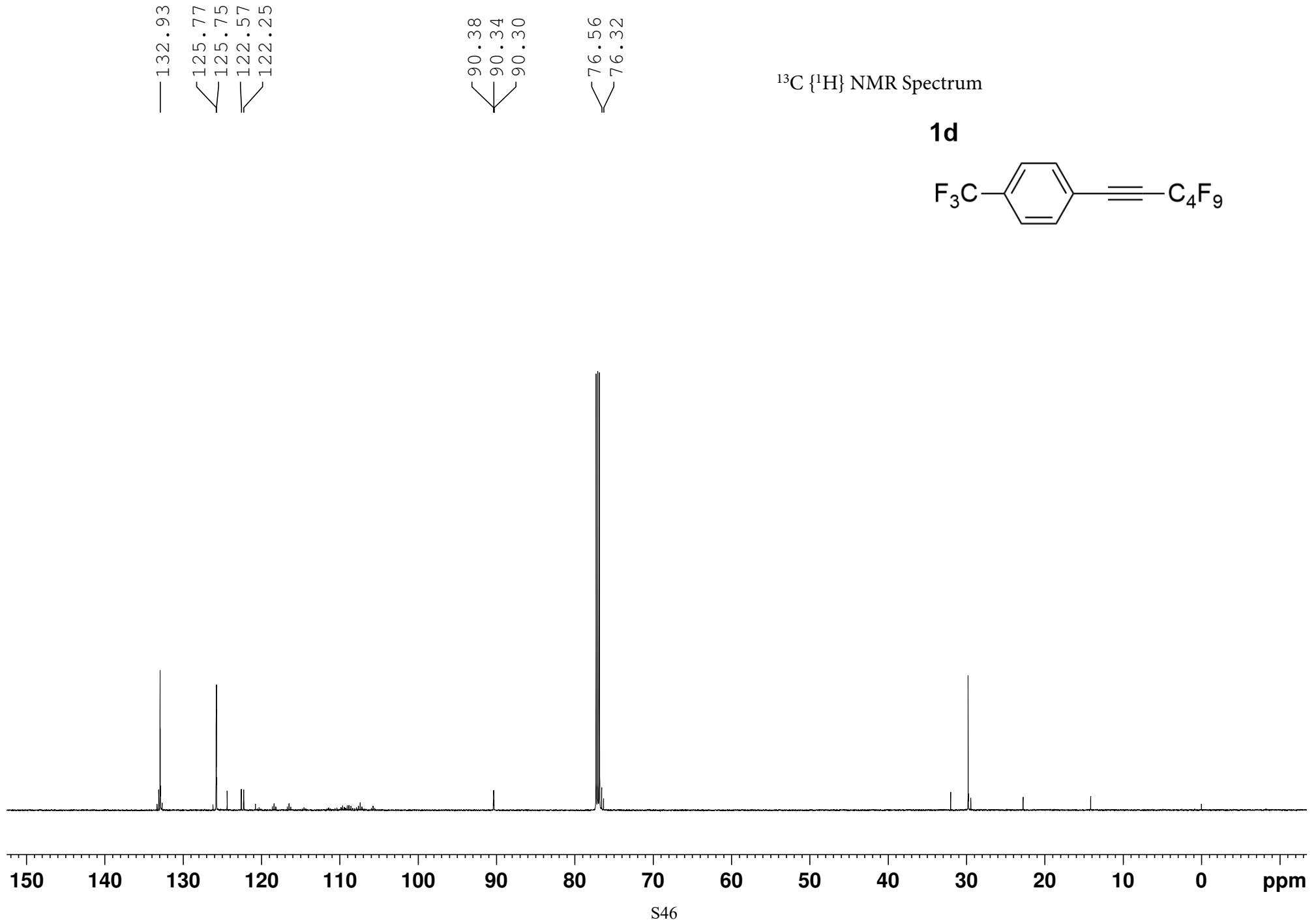




^1H NMR Spectrum

1d





¹⁹F NMR Spectrum

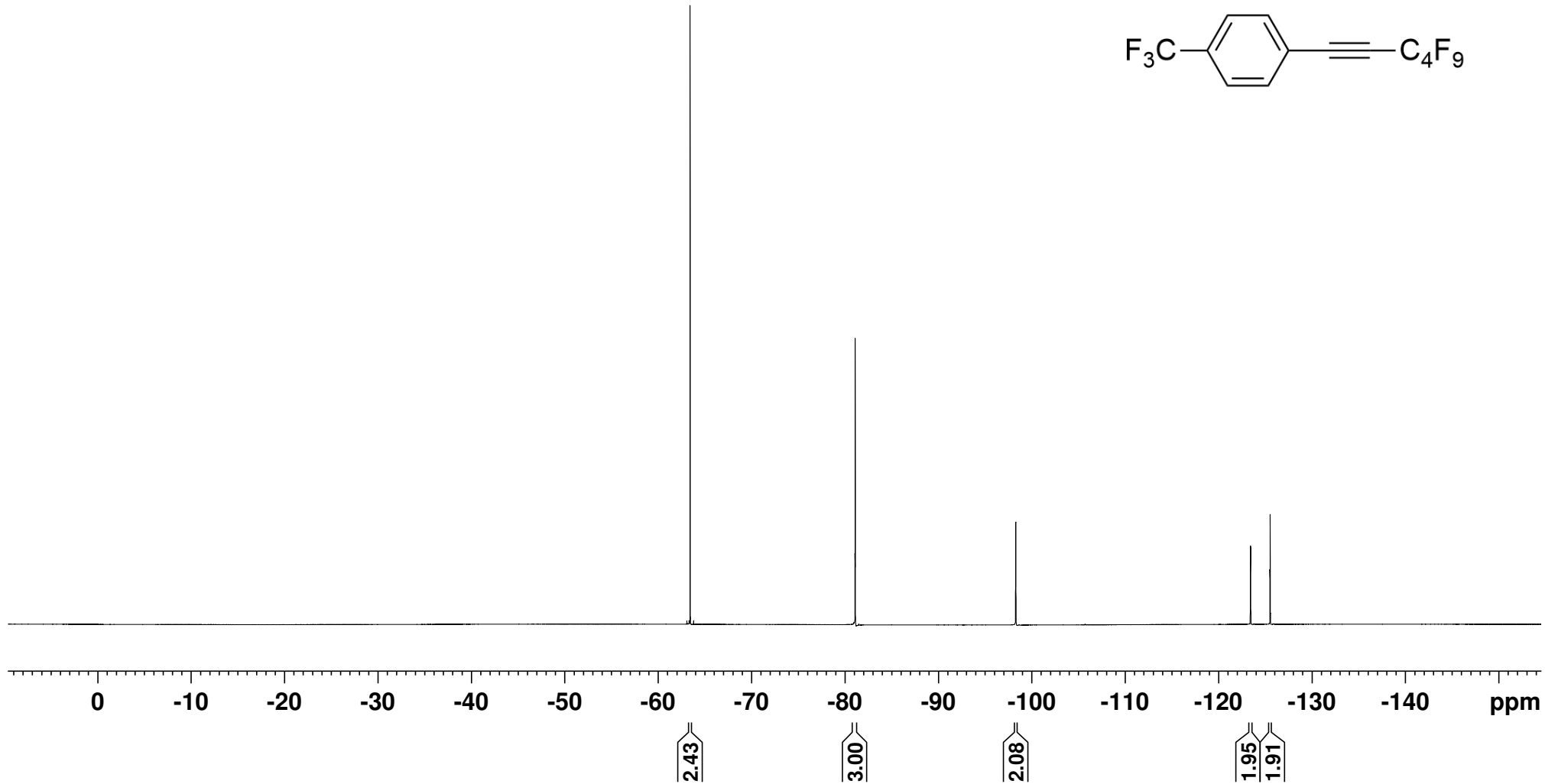
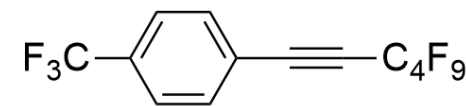
— -63.43

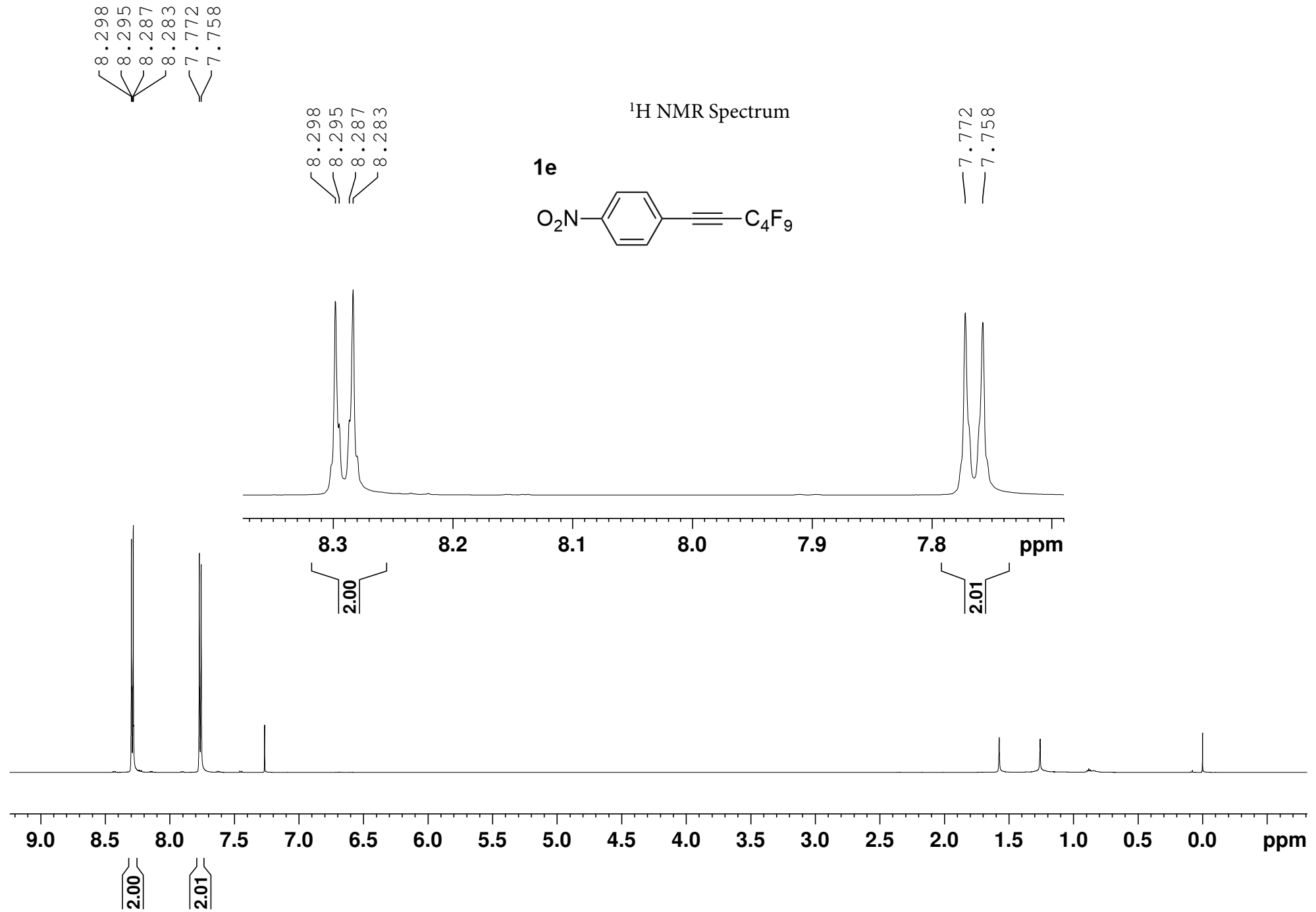
— -81.09
— -81.11
— -81.13

— -98.30

— -123.42
— -123.43
— -123.45
— -125.52
— -125.53

1d





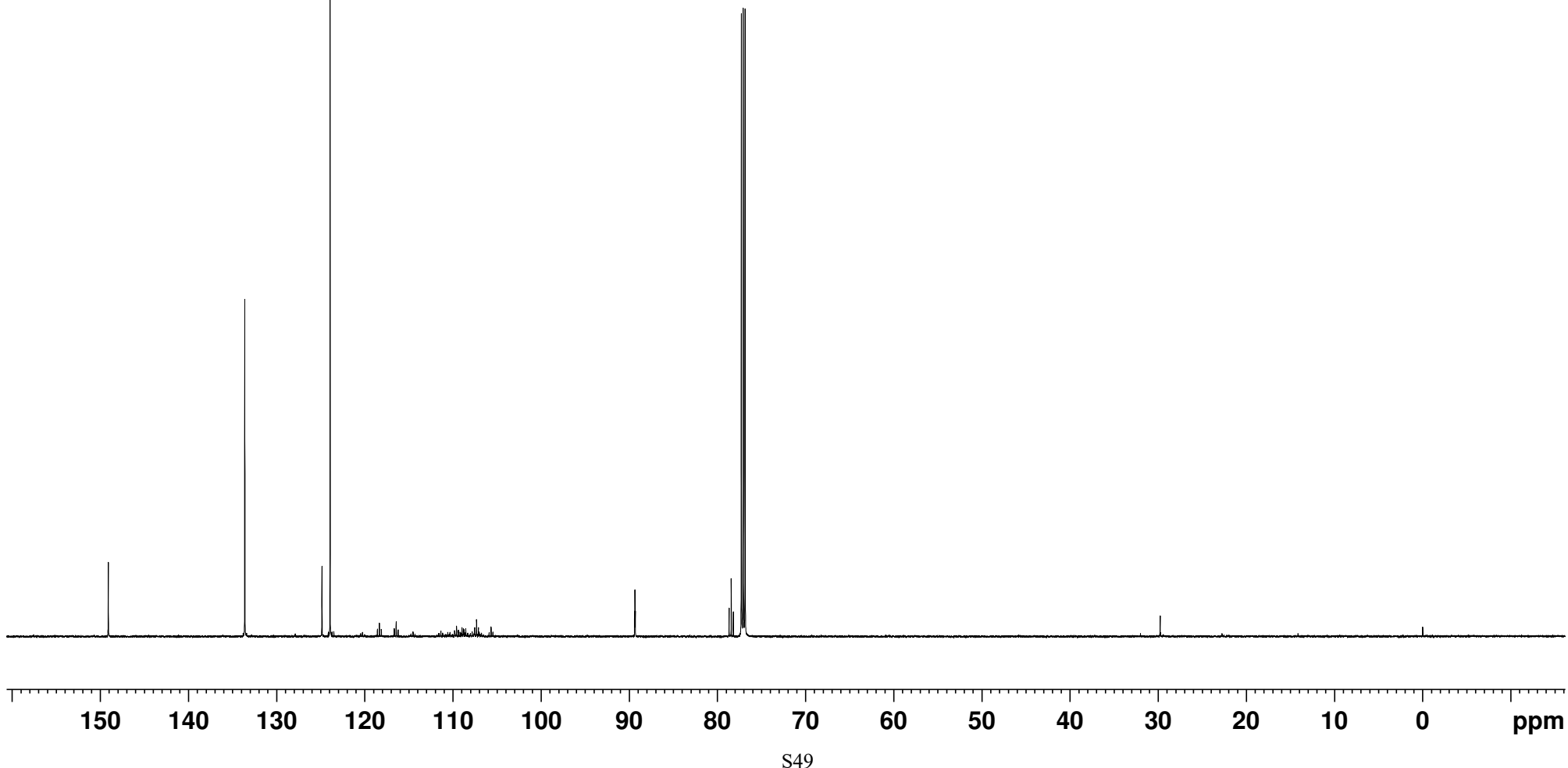
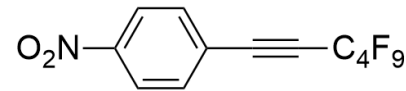
— 149.10

— 133.62
— 124.88
— 124.86
— 124.84
— 123.95

— 89.40
— 89.36
— 89.32
— 78.68
— 78.44
— 78.20

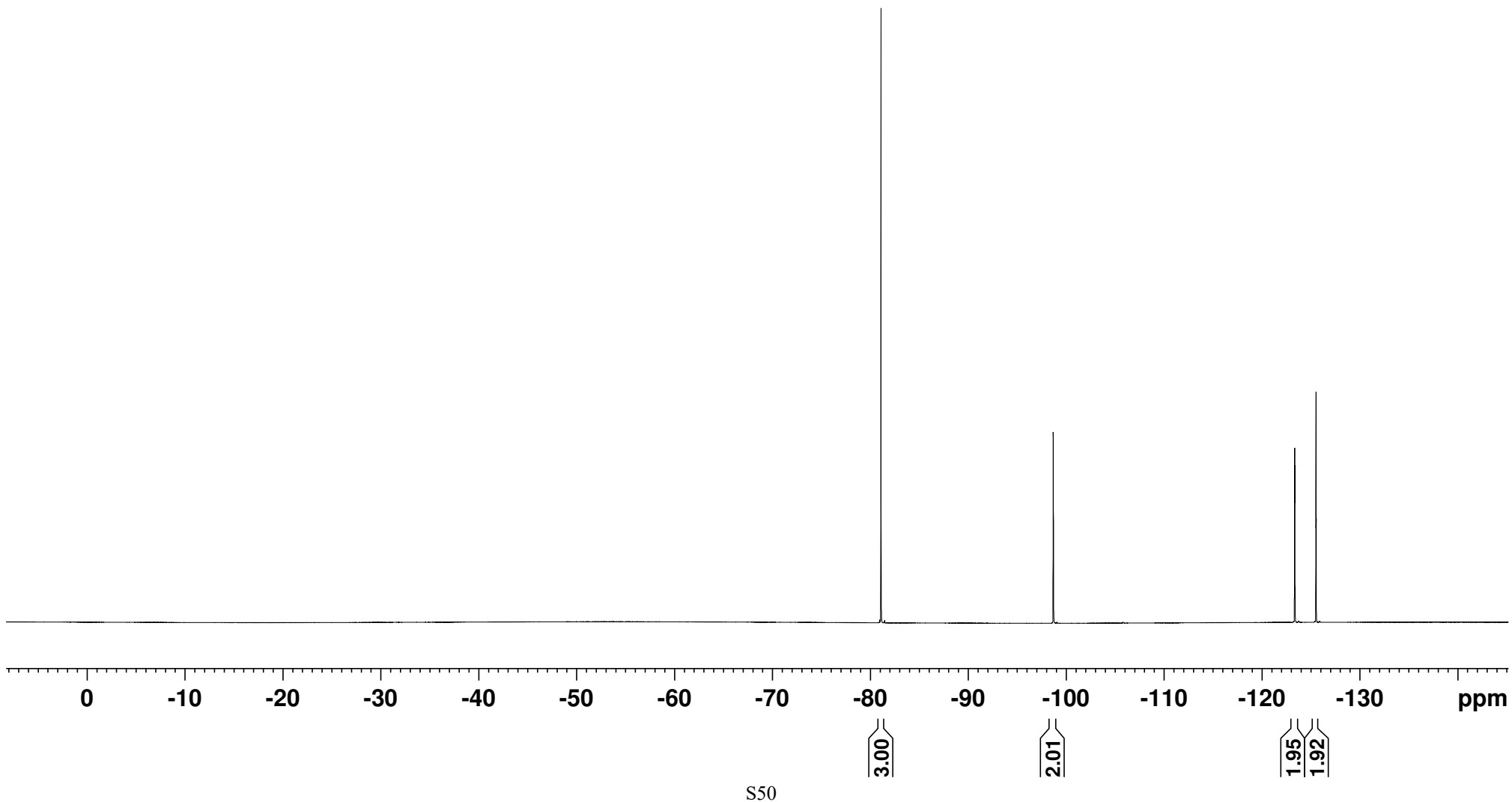
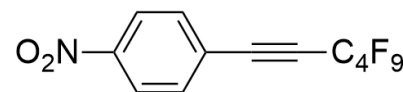
$^{13}\text{C} \{^1\text{H}\}$ NMR Spectrum

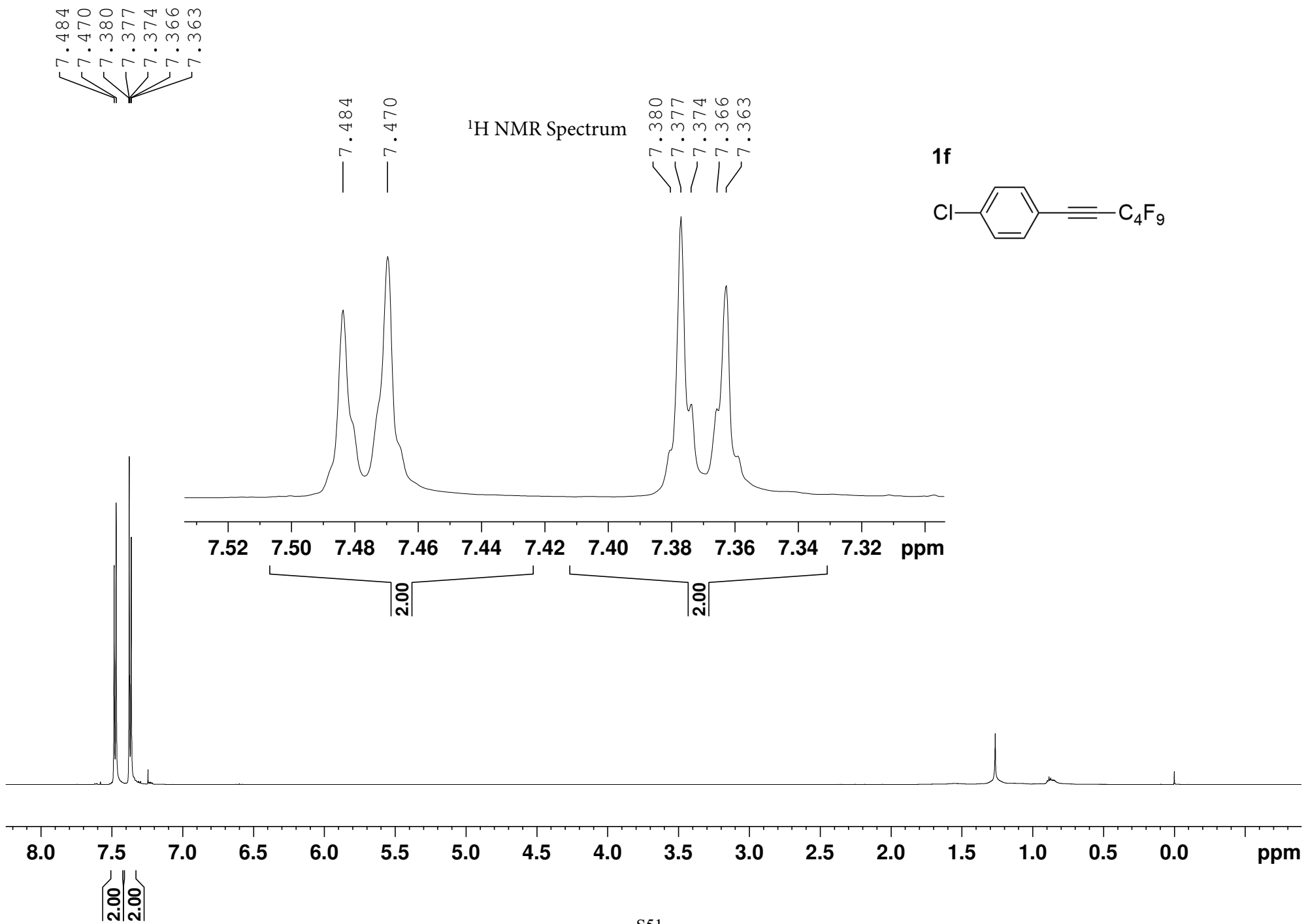
1e



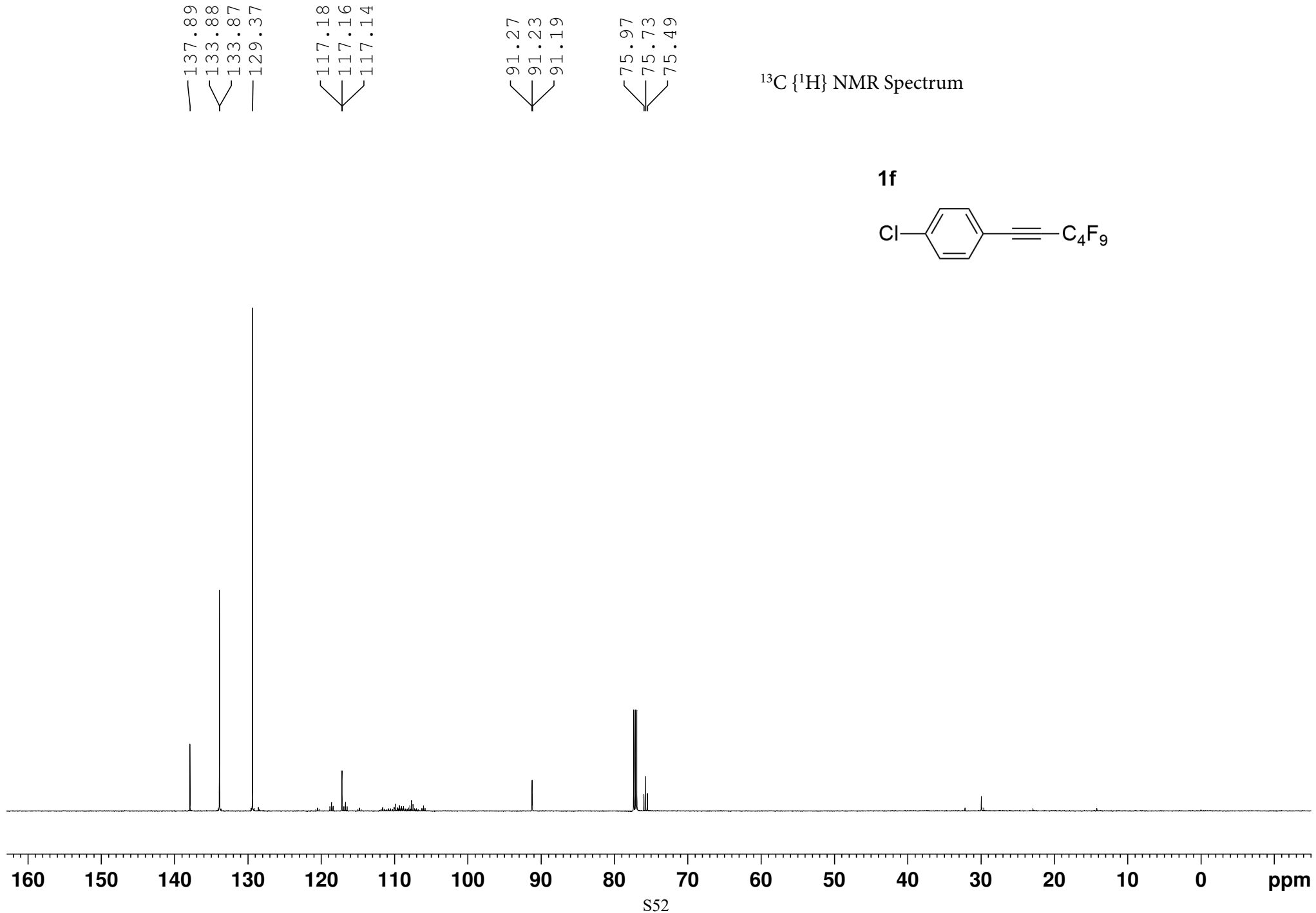
¹⁹F NMR Spectrum

1e

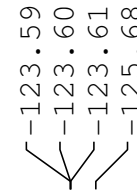
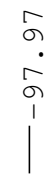
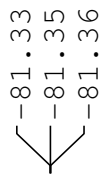




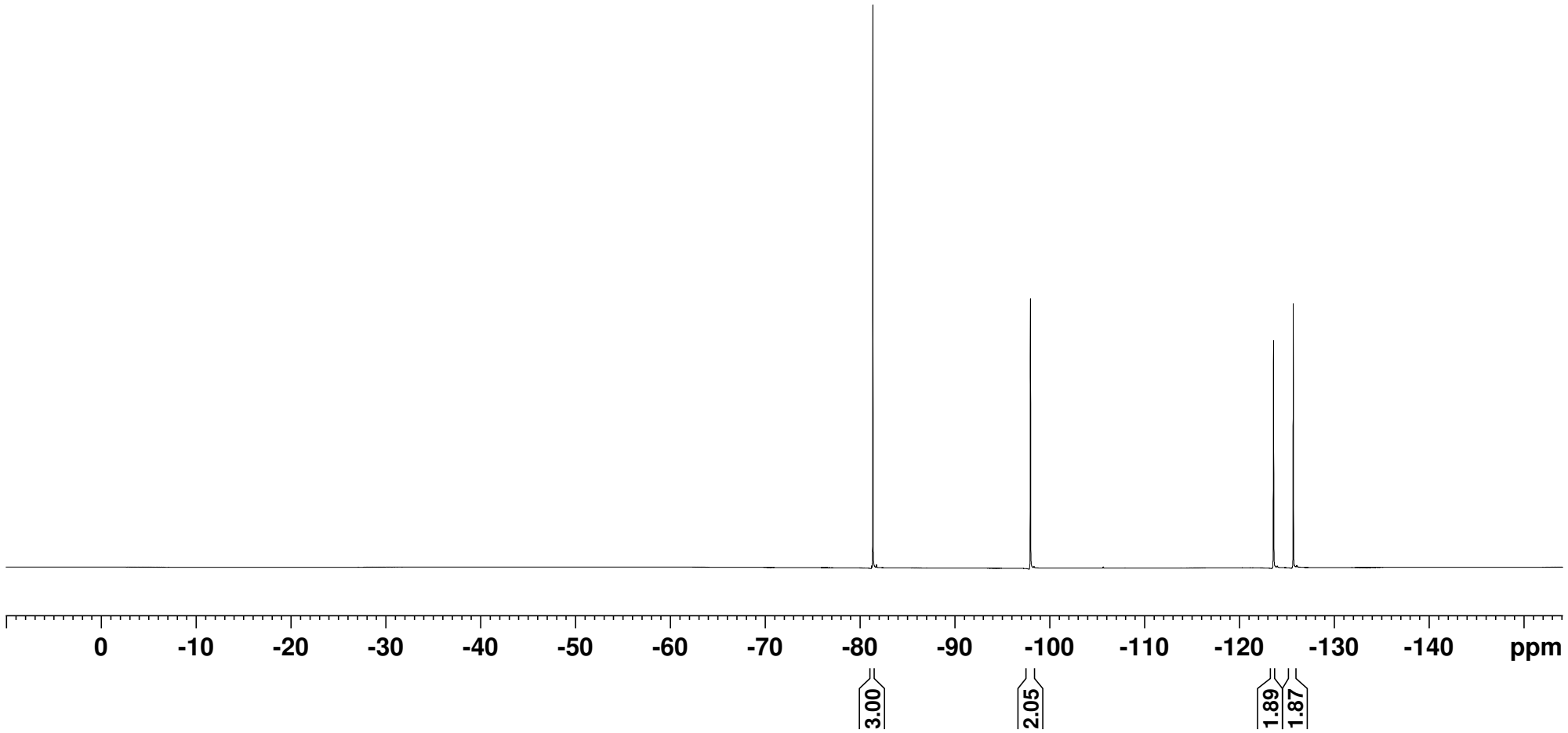
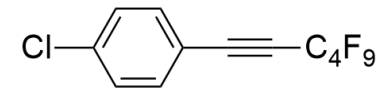
$^{13}\text{C} \{^1\text{H}\}$ NMR Spectrum

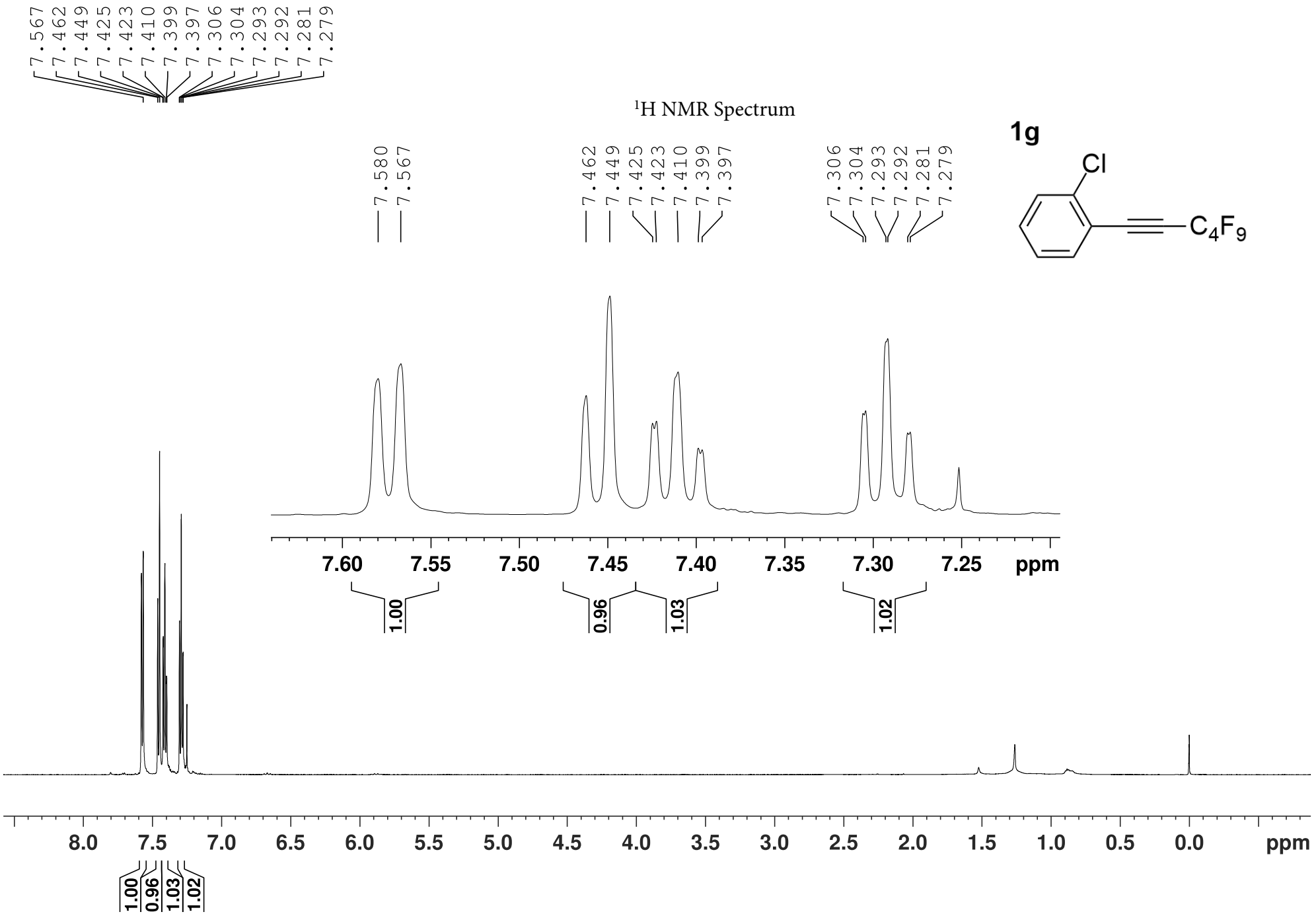


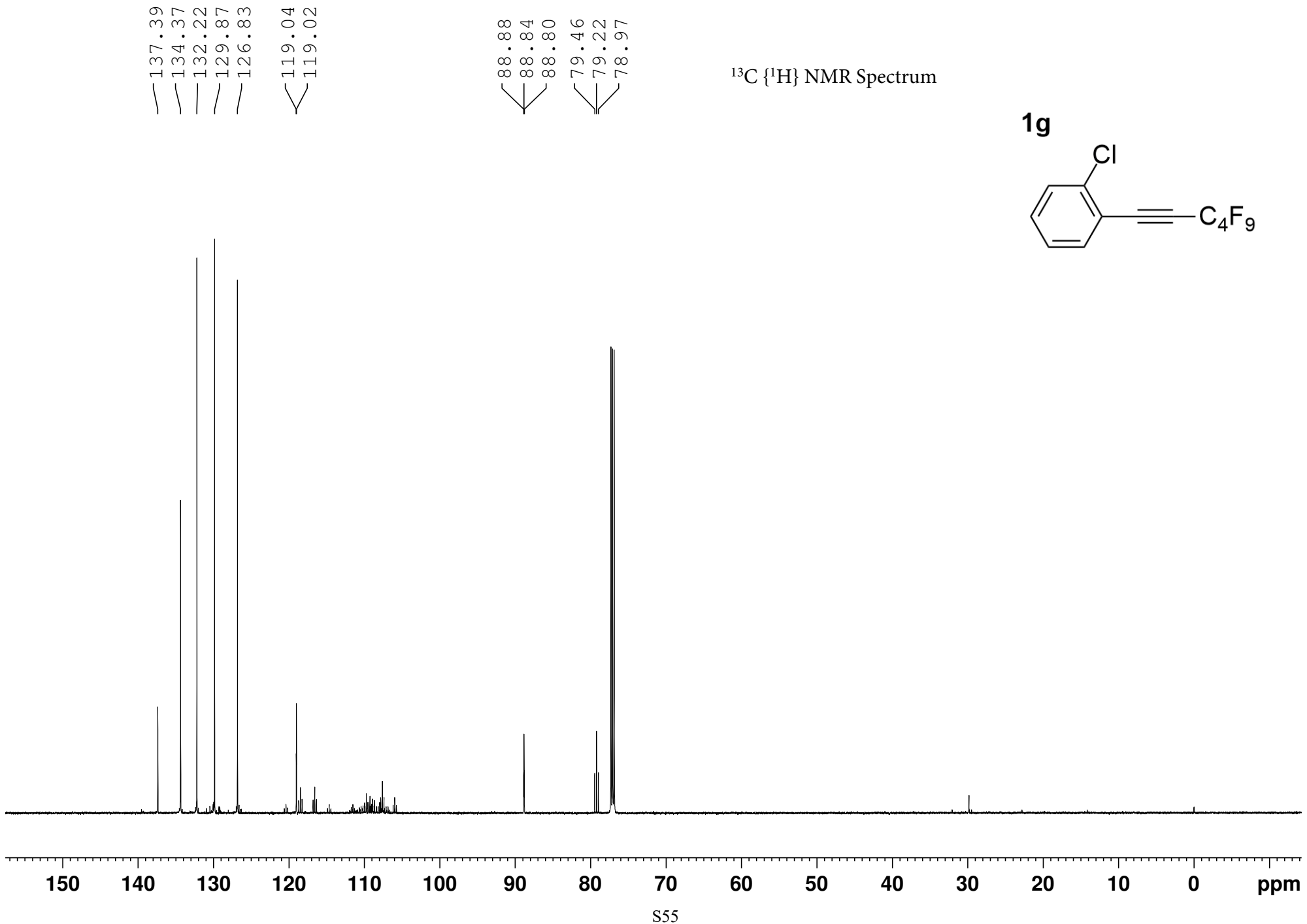
¹⁹F NMR Spectrum



1f







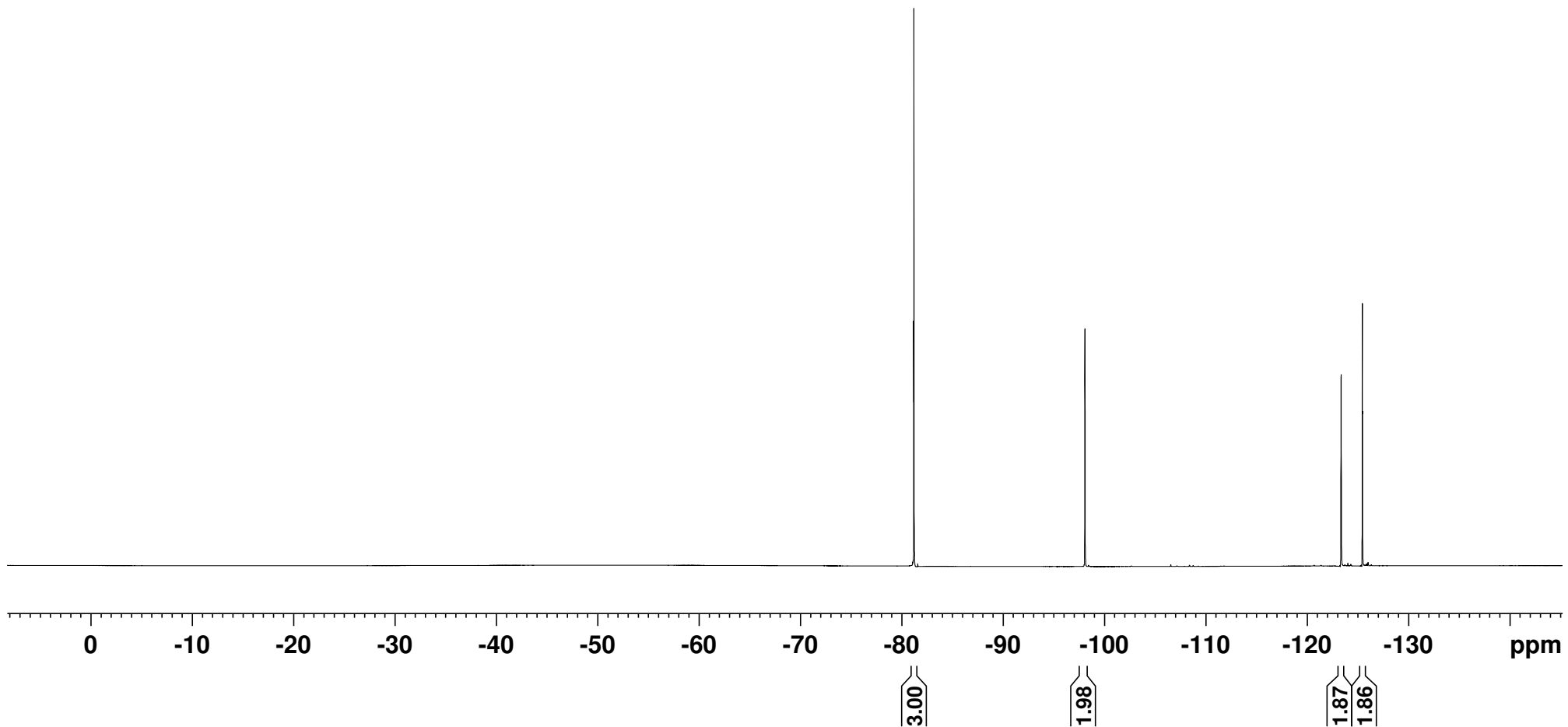
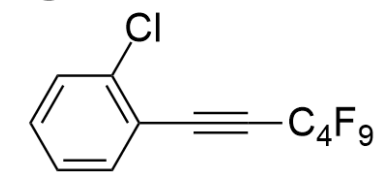
¹⁹F NMR Spectrum

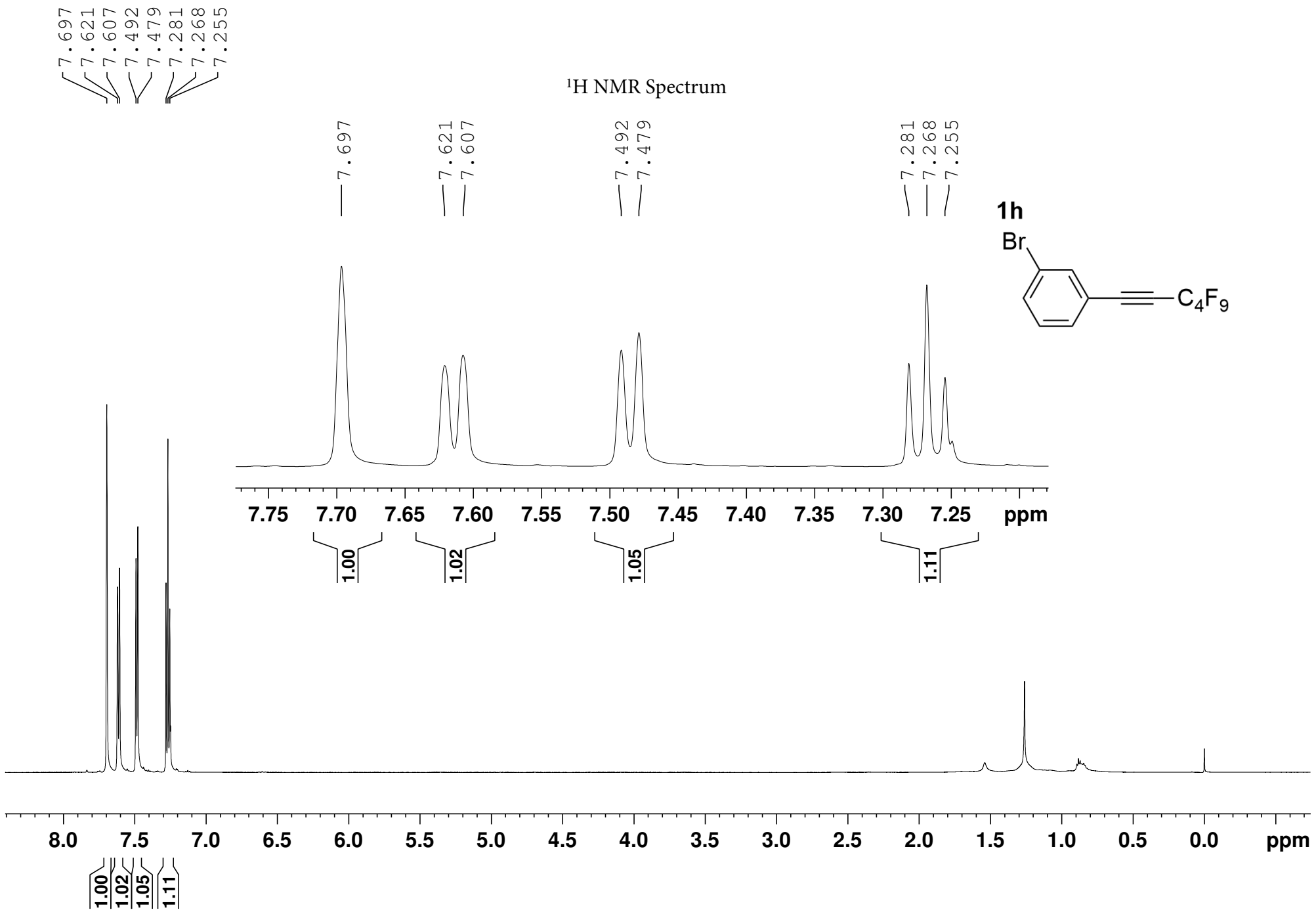
[-81.19
-81.21
-81.22]

-98.08

[-123.36
-123.37
-125.46]

1g



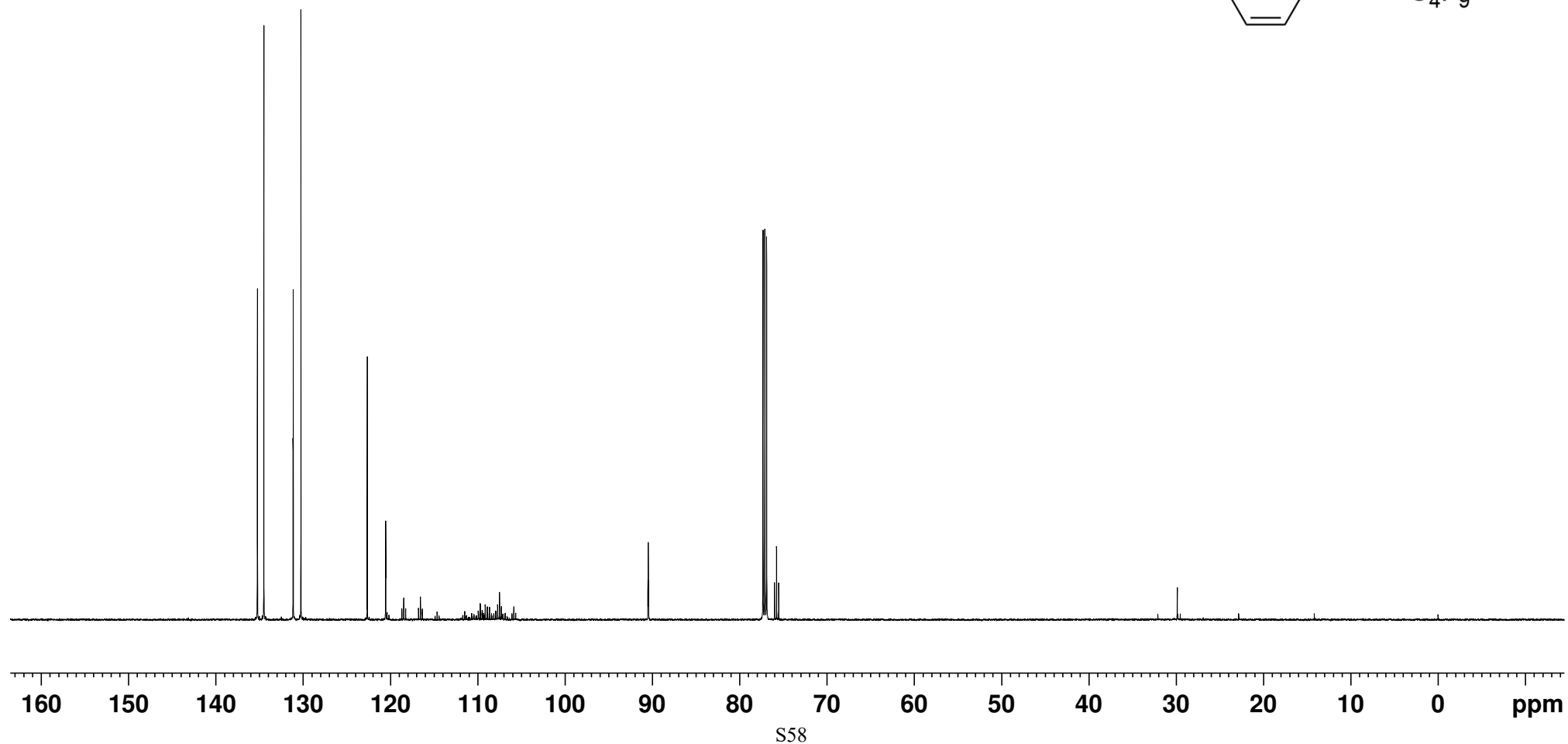
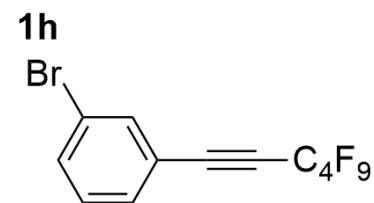


135.23
135.22
134.49
131.15
131.14
131.12
130.25
122.65
120.54

90.50
90.46
90.42

76.00
75.76
75.52

$^{13}\text{C} \{^1\text{H}\}$ NMR Spectrum



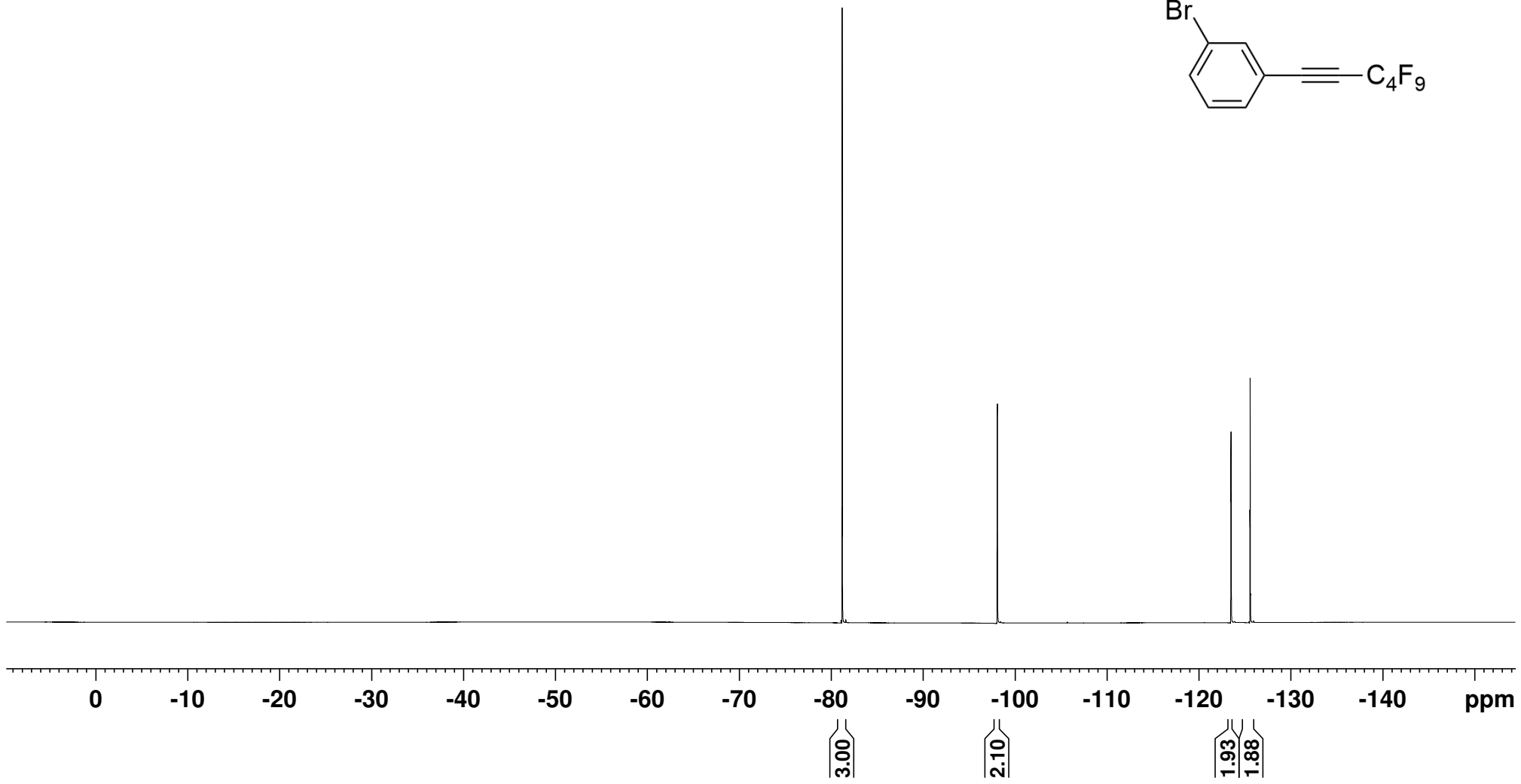
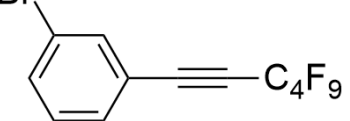
¹⁹F NMR Spectrum

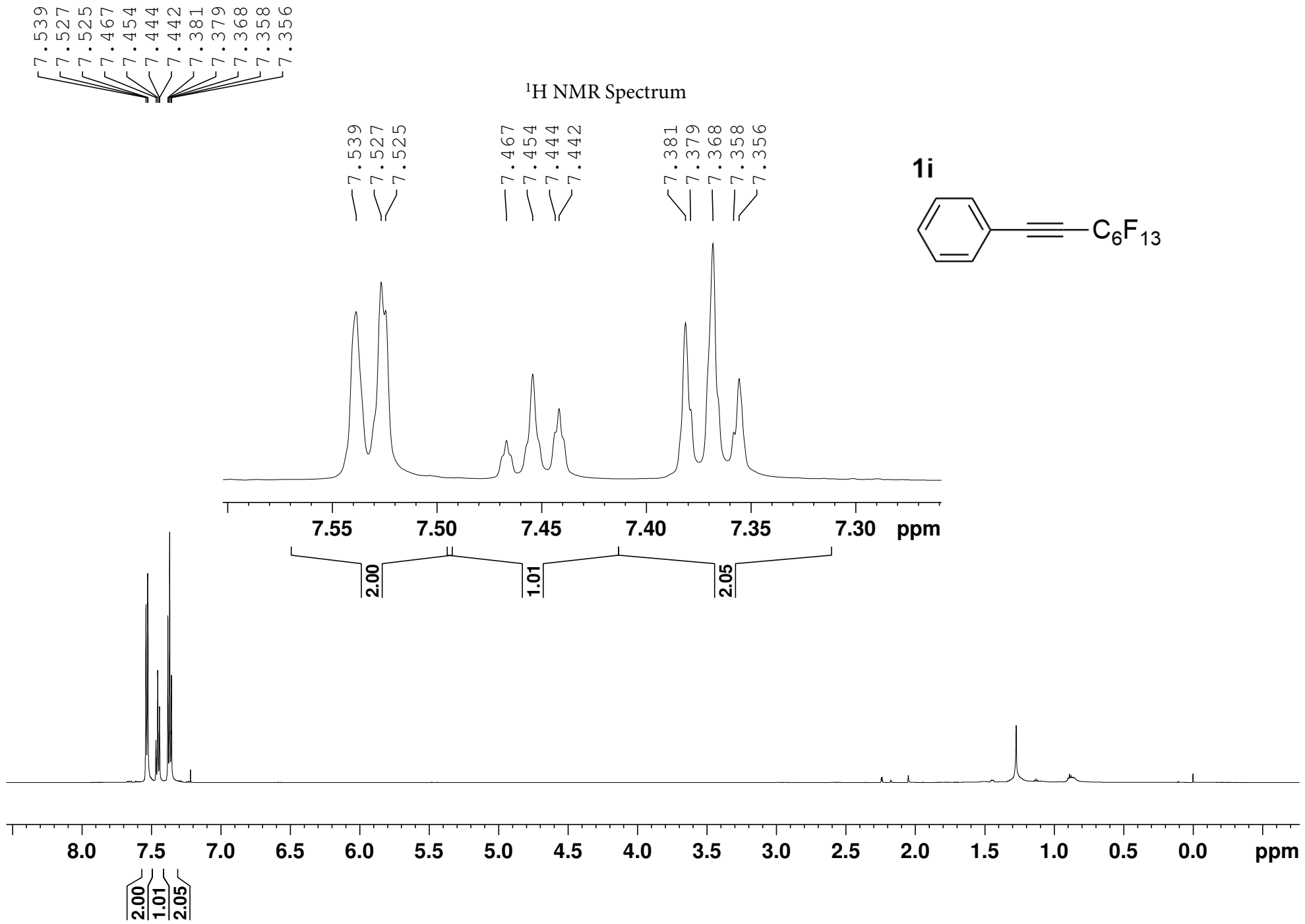
-81.20
-81.22
-81.23

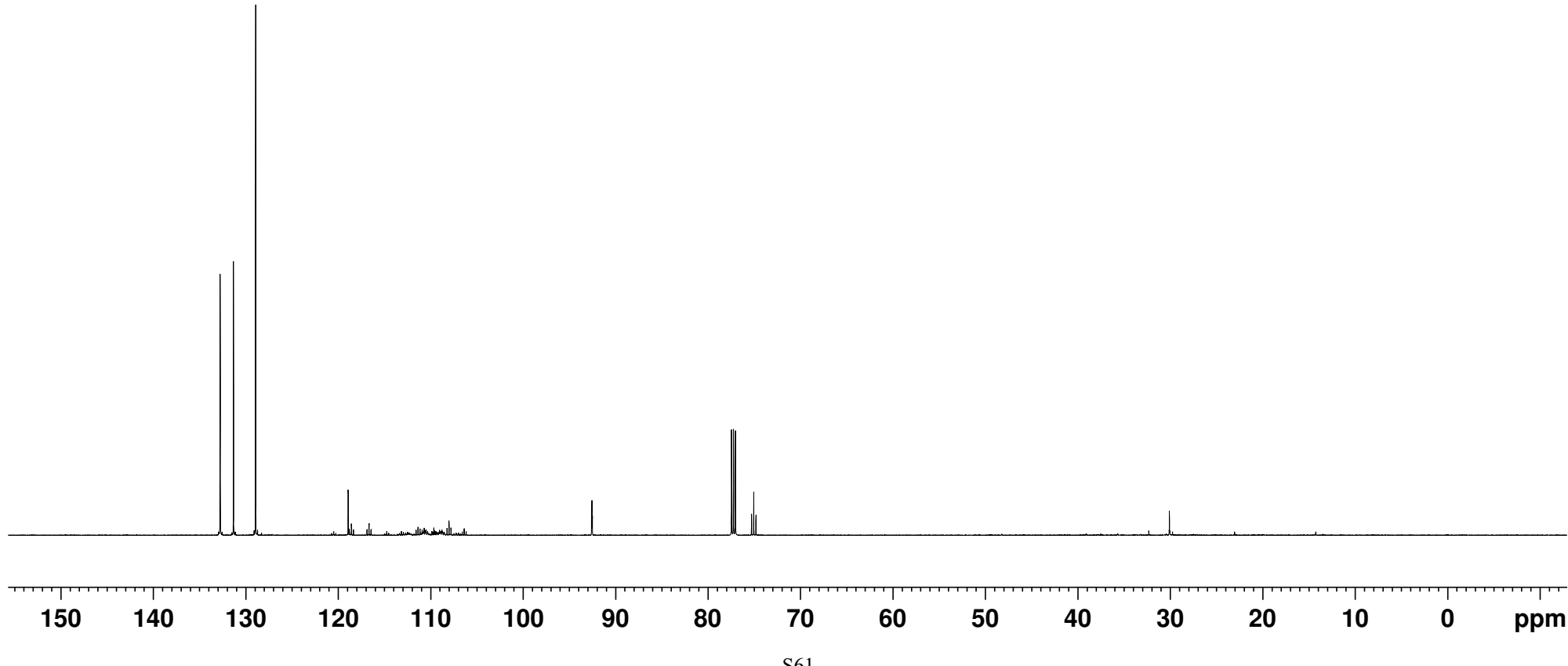
-98.09

-123.50
-123.51
-123.52
-123.52
-125.59

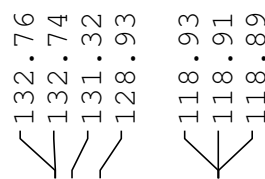
1h



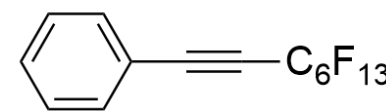




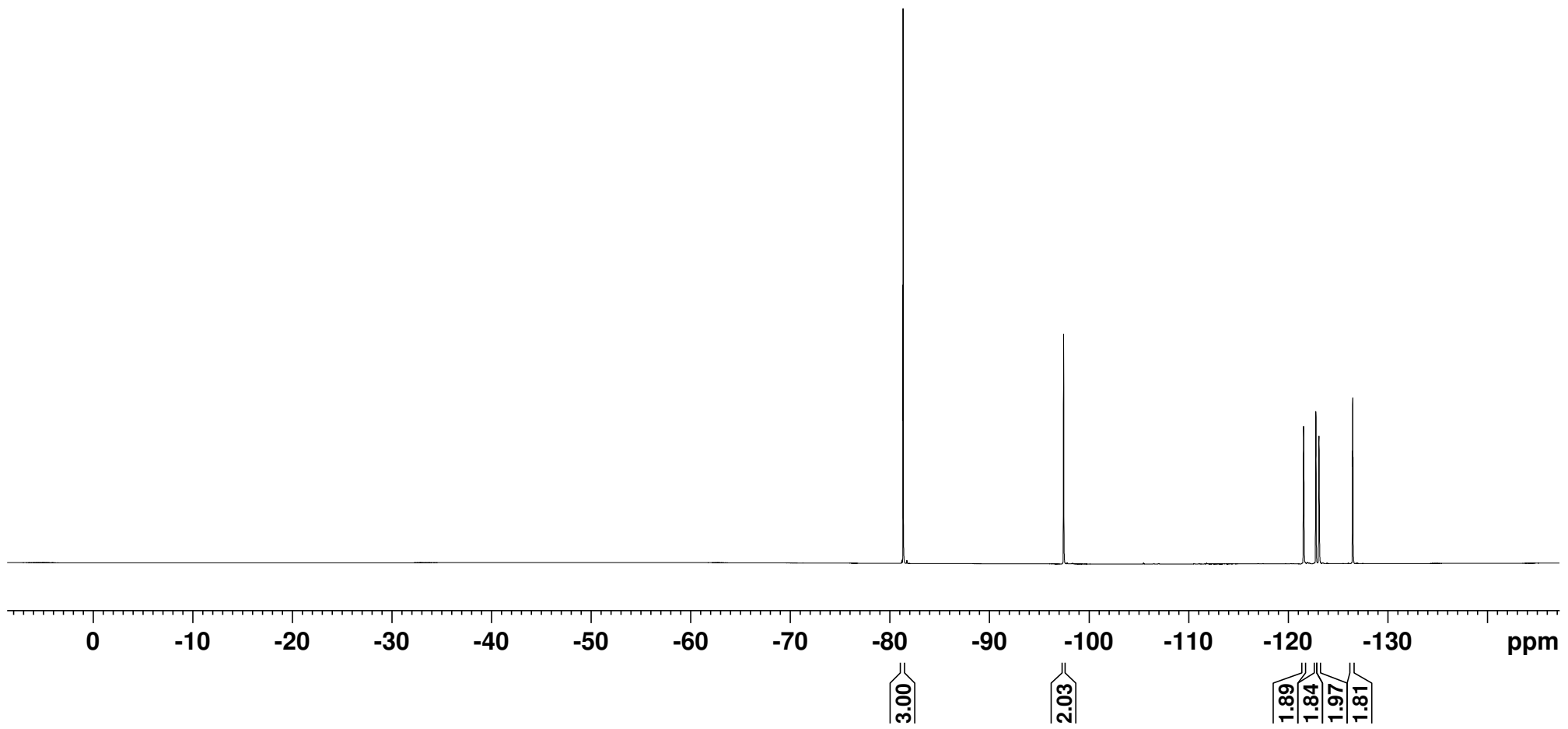
$^{13}\text{C}\{^1\text{H}\}$ NMR Spectrum



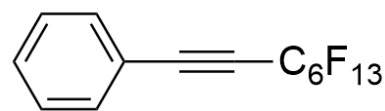
1i

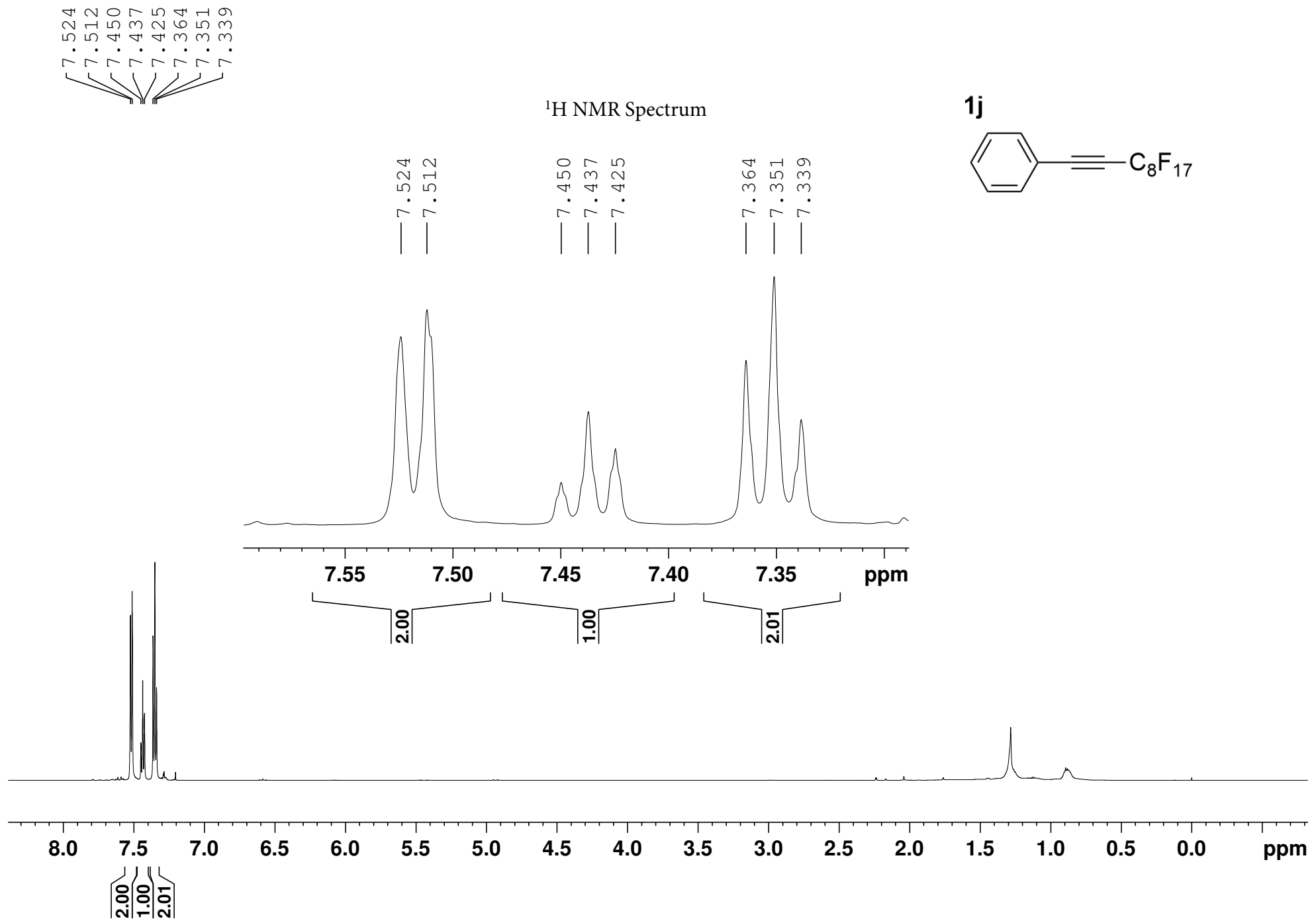


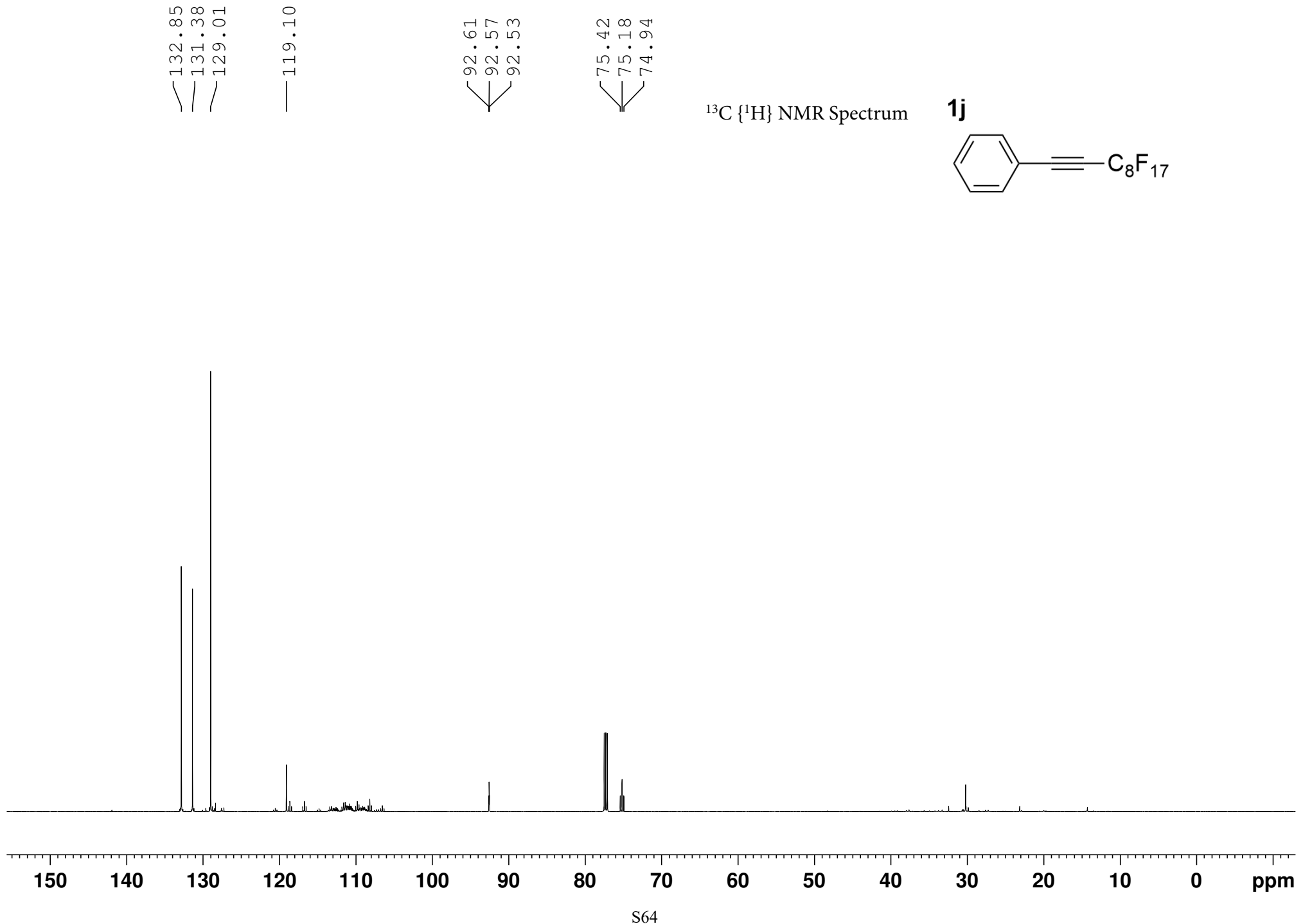
¹⁹F NMR Spectrum



1i

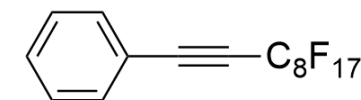


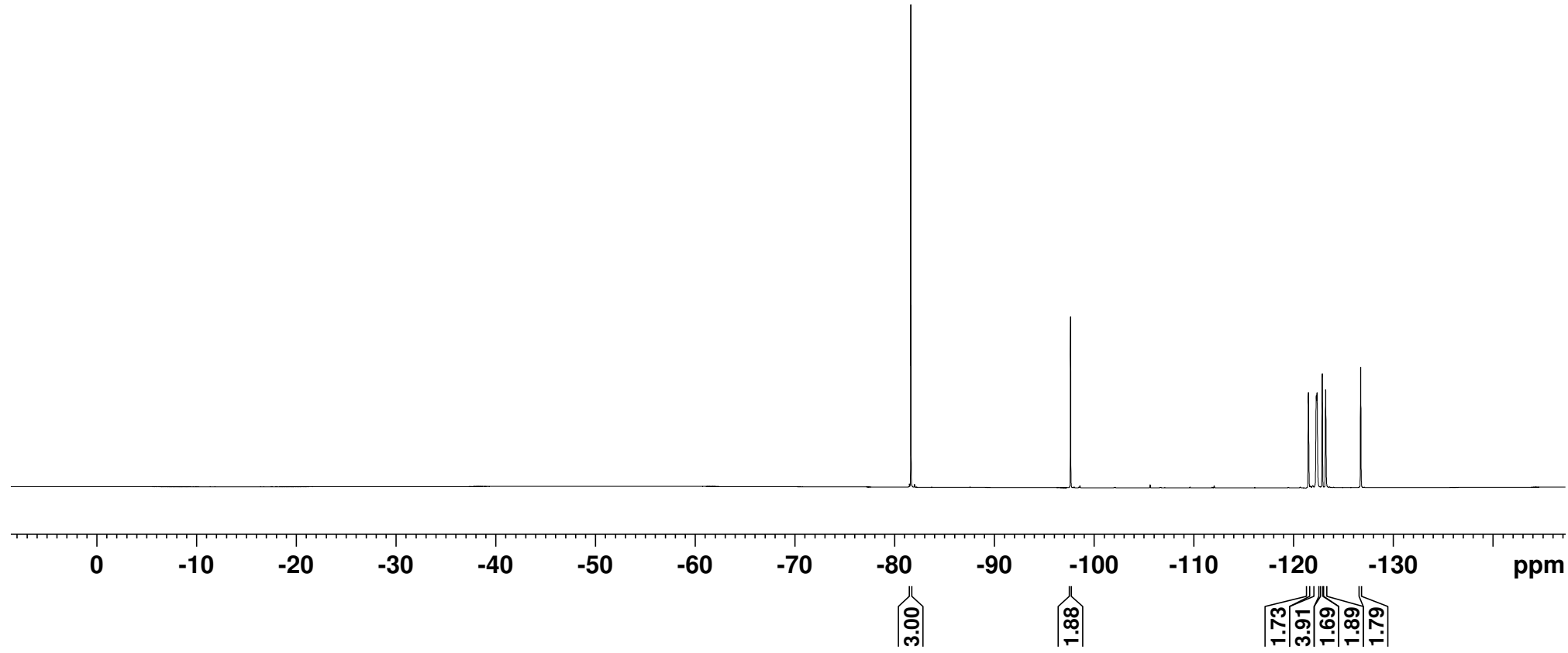




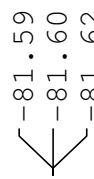
$^{13}\text{C}\{^1\text{H}\}$ NMR Spectrum

1j

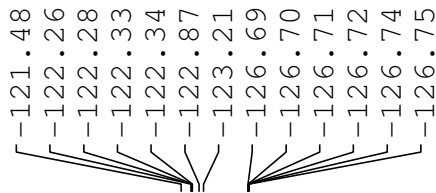




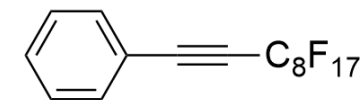
¹⁹F NMR Spectrum

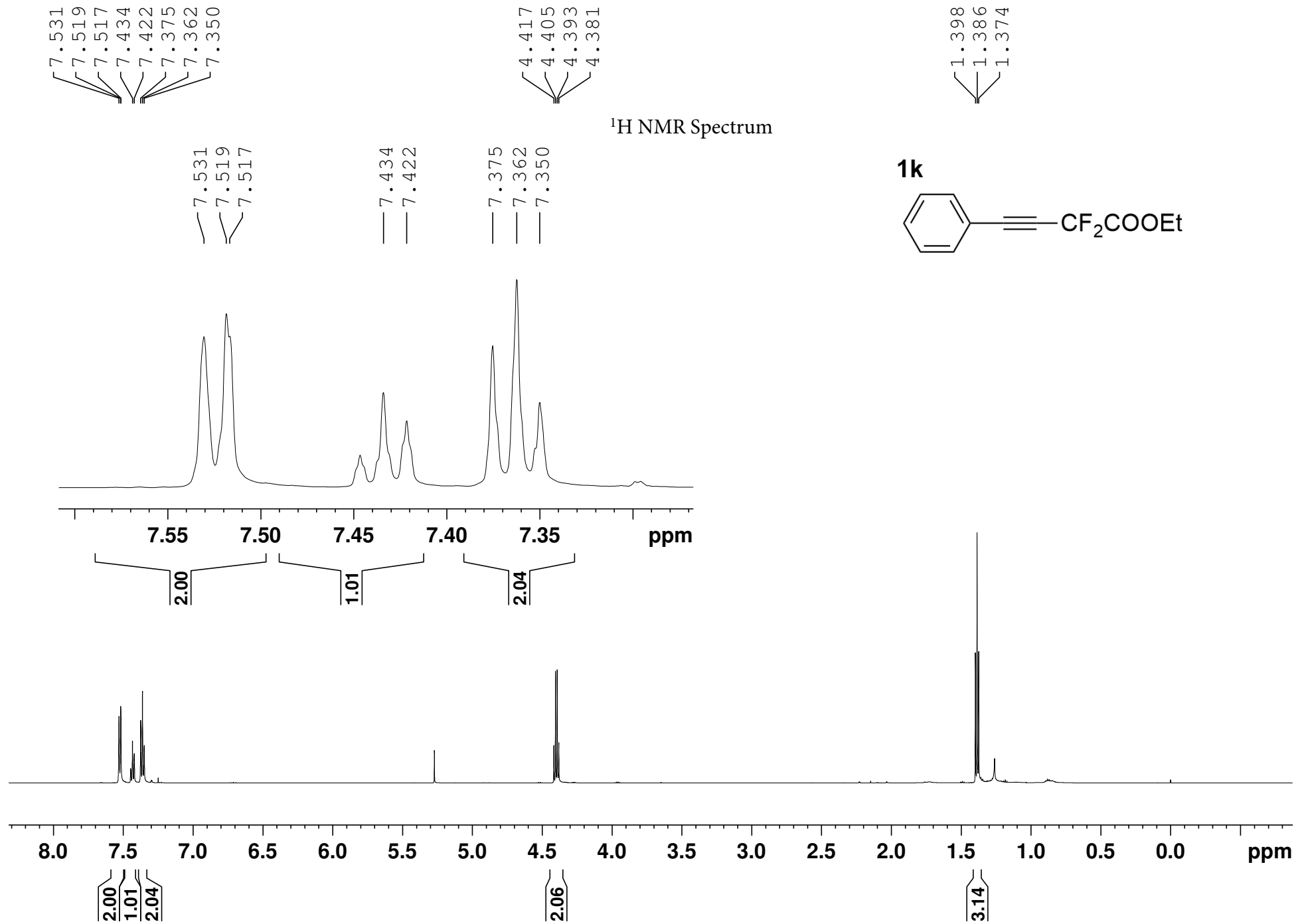


-97.63



1j





161.82
161.59
161.36

132.40
132.39
130.61
128.64
119.38
119.36
119.34

106.63
105.03
103.42

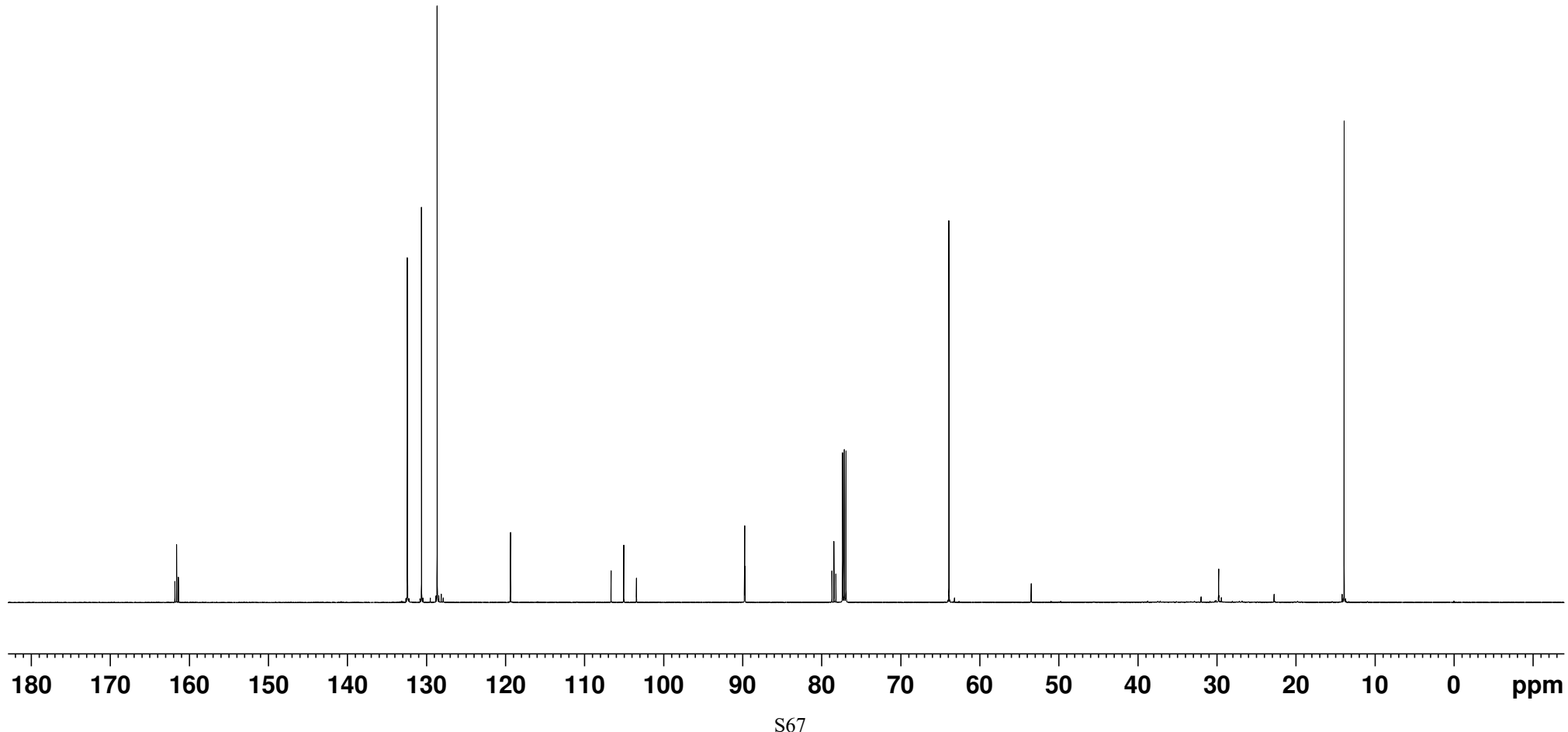
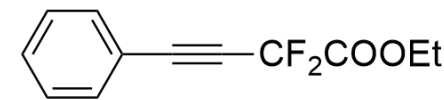
89.77
89.72
89.68
78.69
78.44
78.19

63.89

13.89

$^{13}\text{C} \{^1\text{H}\}$ NMR Spectrum

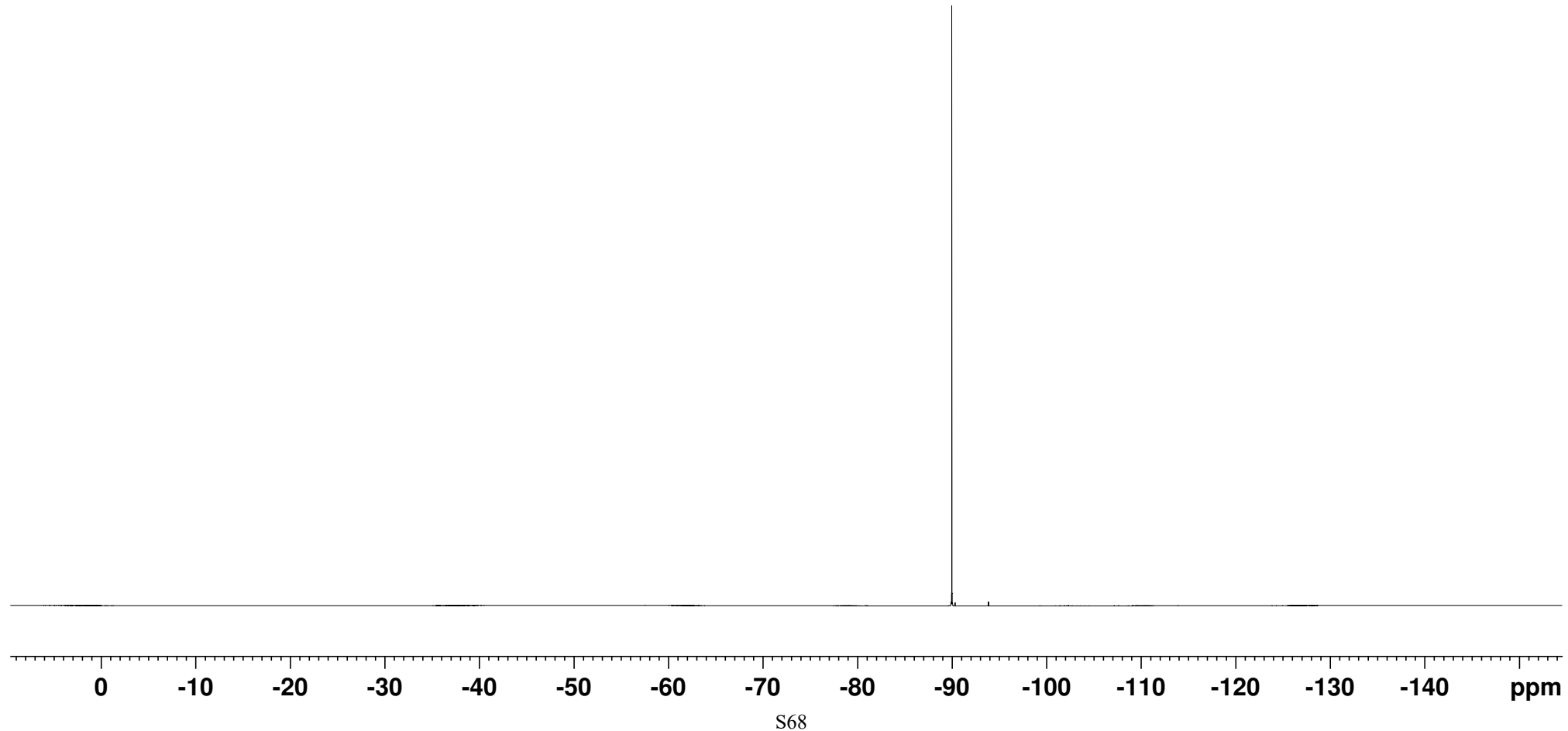
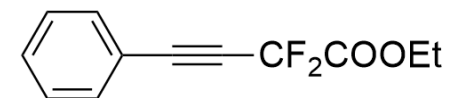
1k

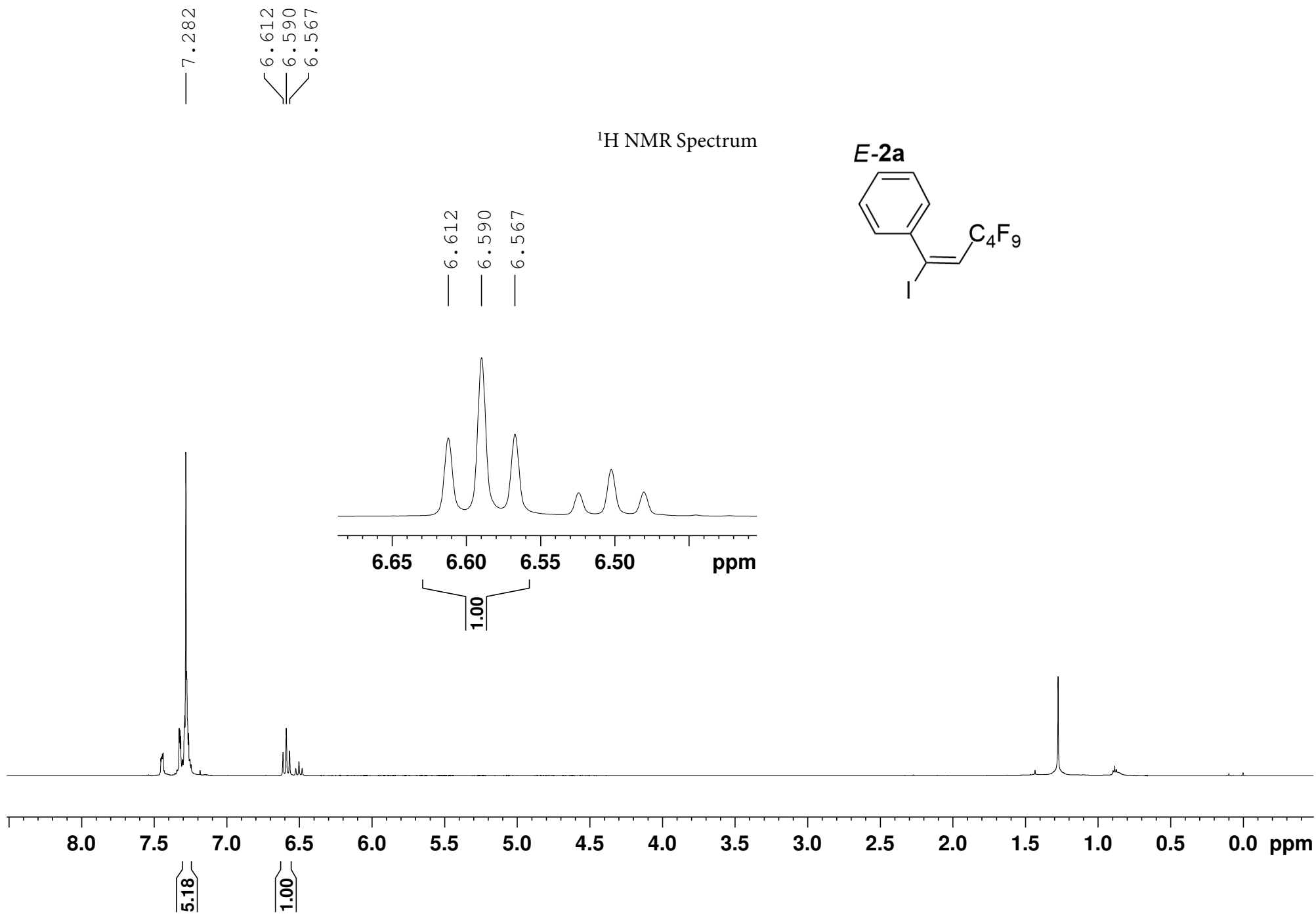




¹⁹F NMR Spectrum

1k

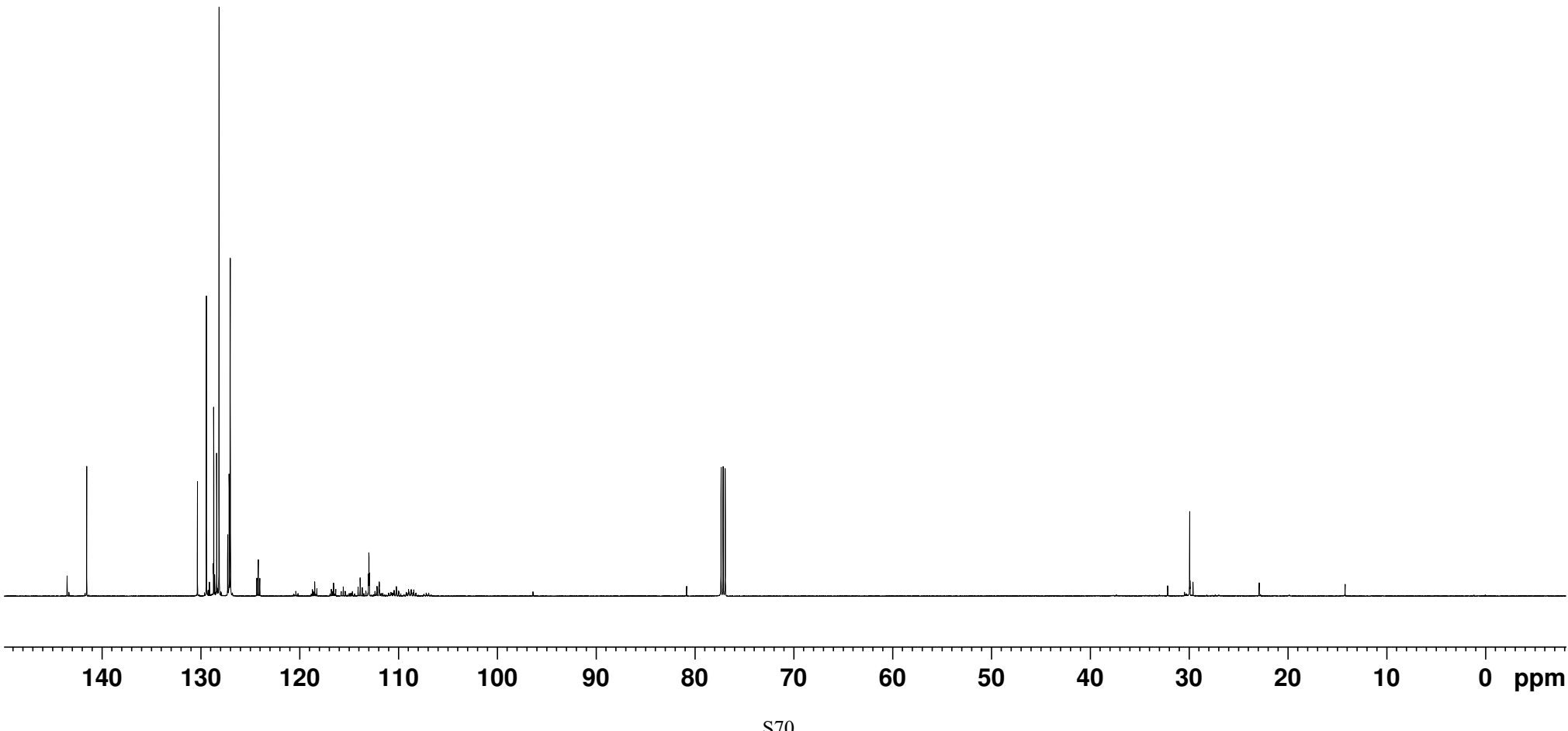
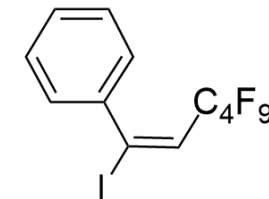


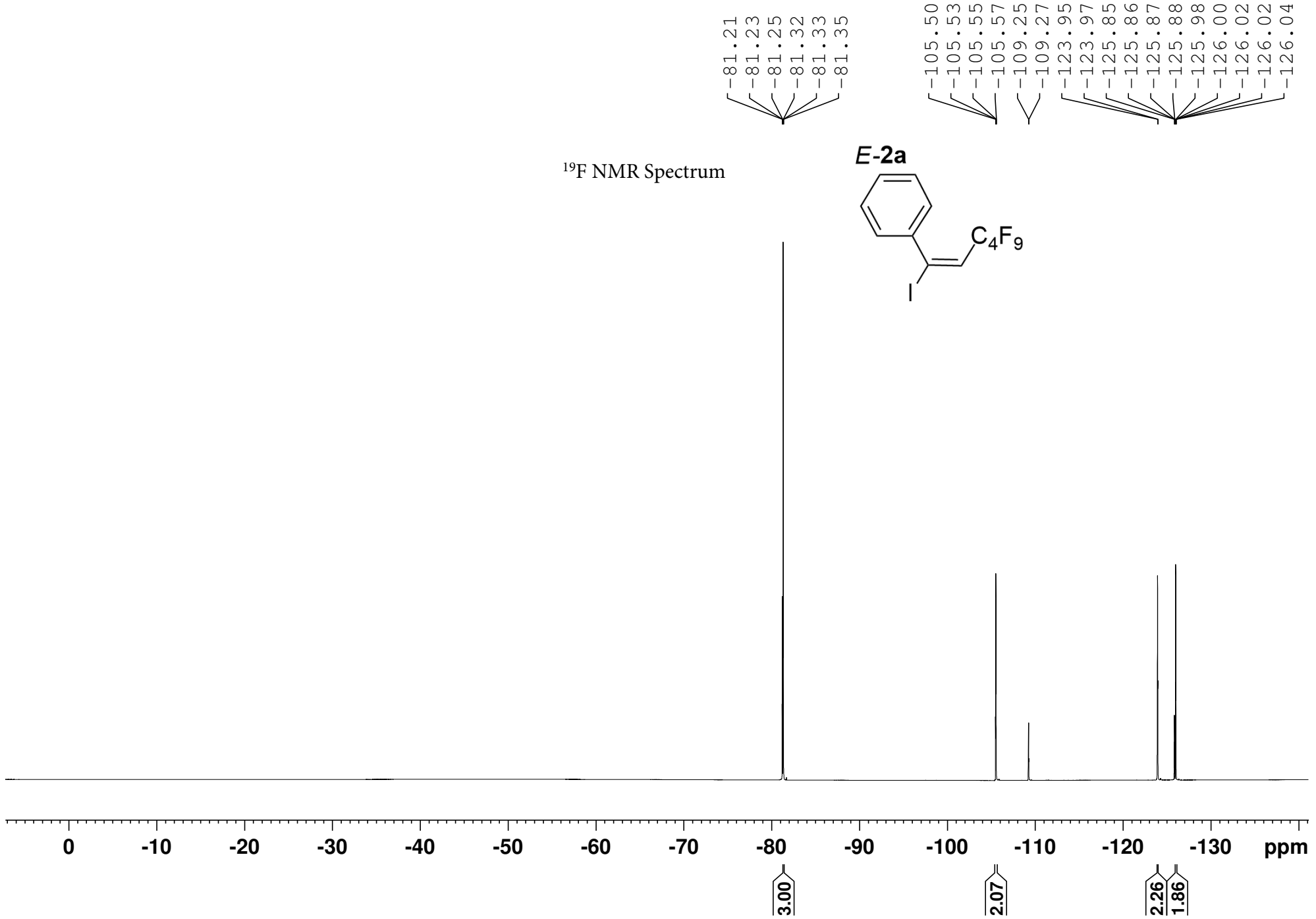


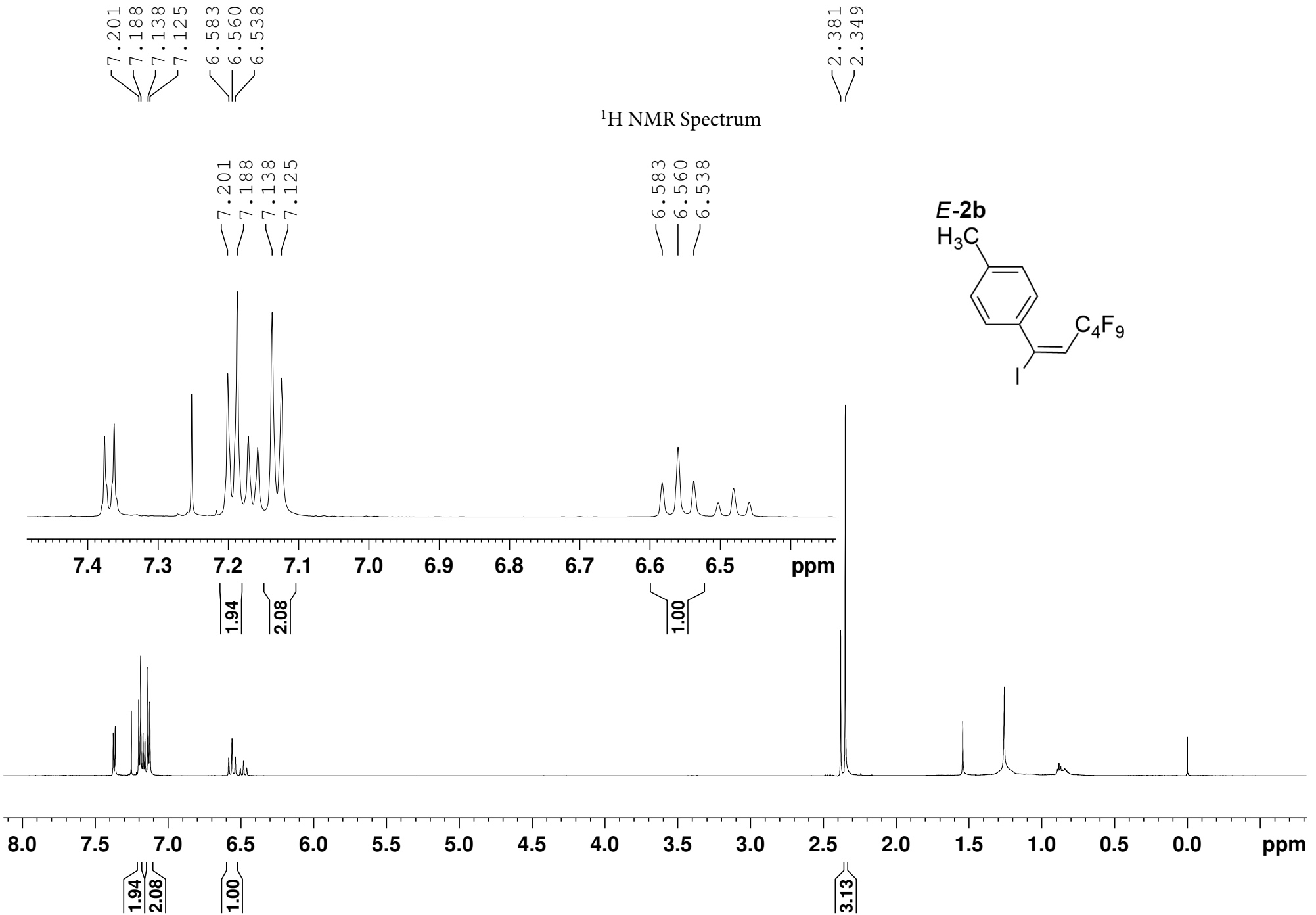
141.54
130.33
129.42
128.68
128.38
128.14
127.12
127.02
127.00
113.02
112.98
112.94

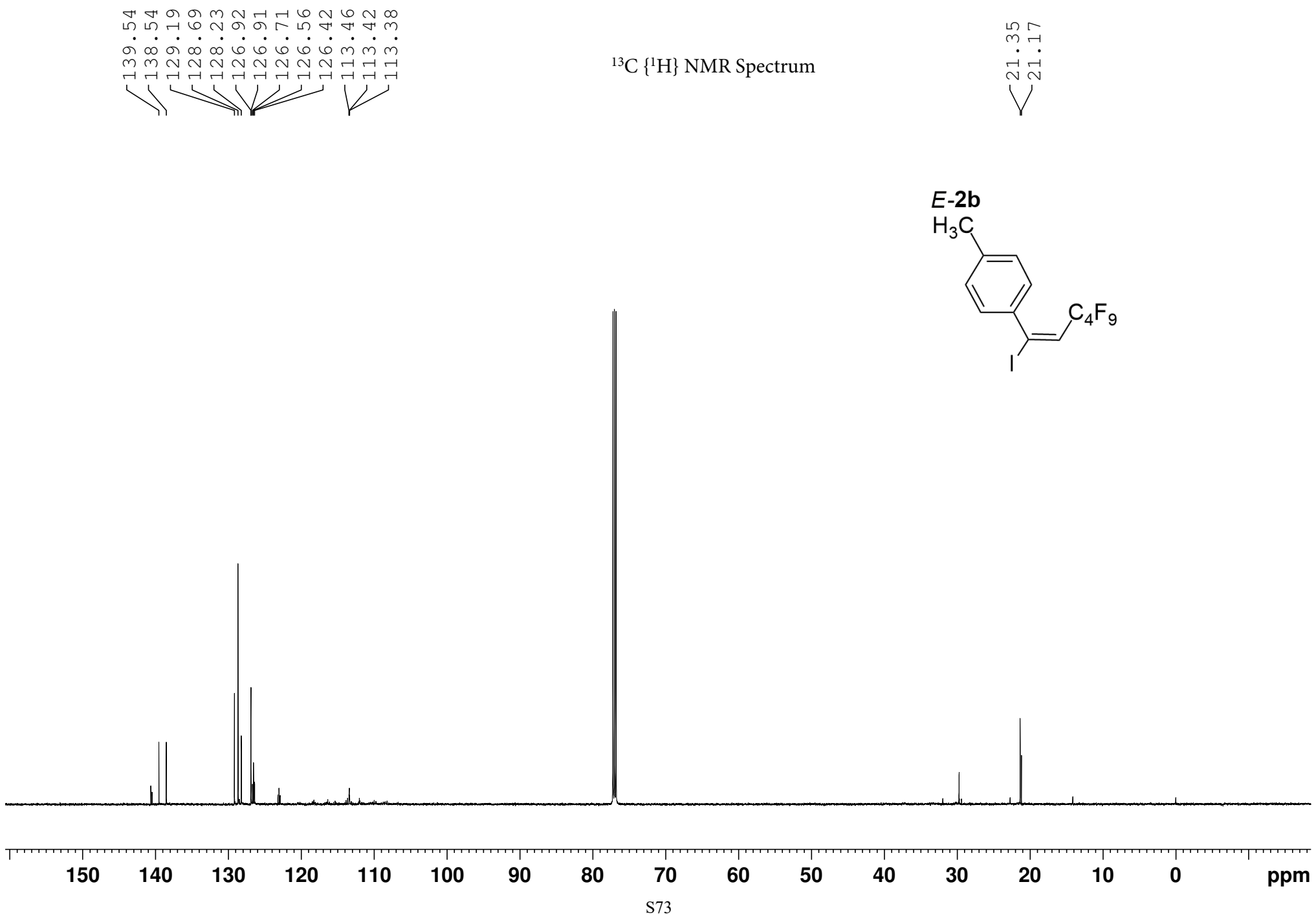
$^{13}\text{C} \{^1\text{H}\}$ NMR Spectrum

E-2a

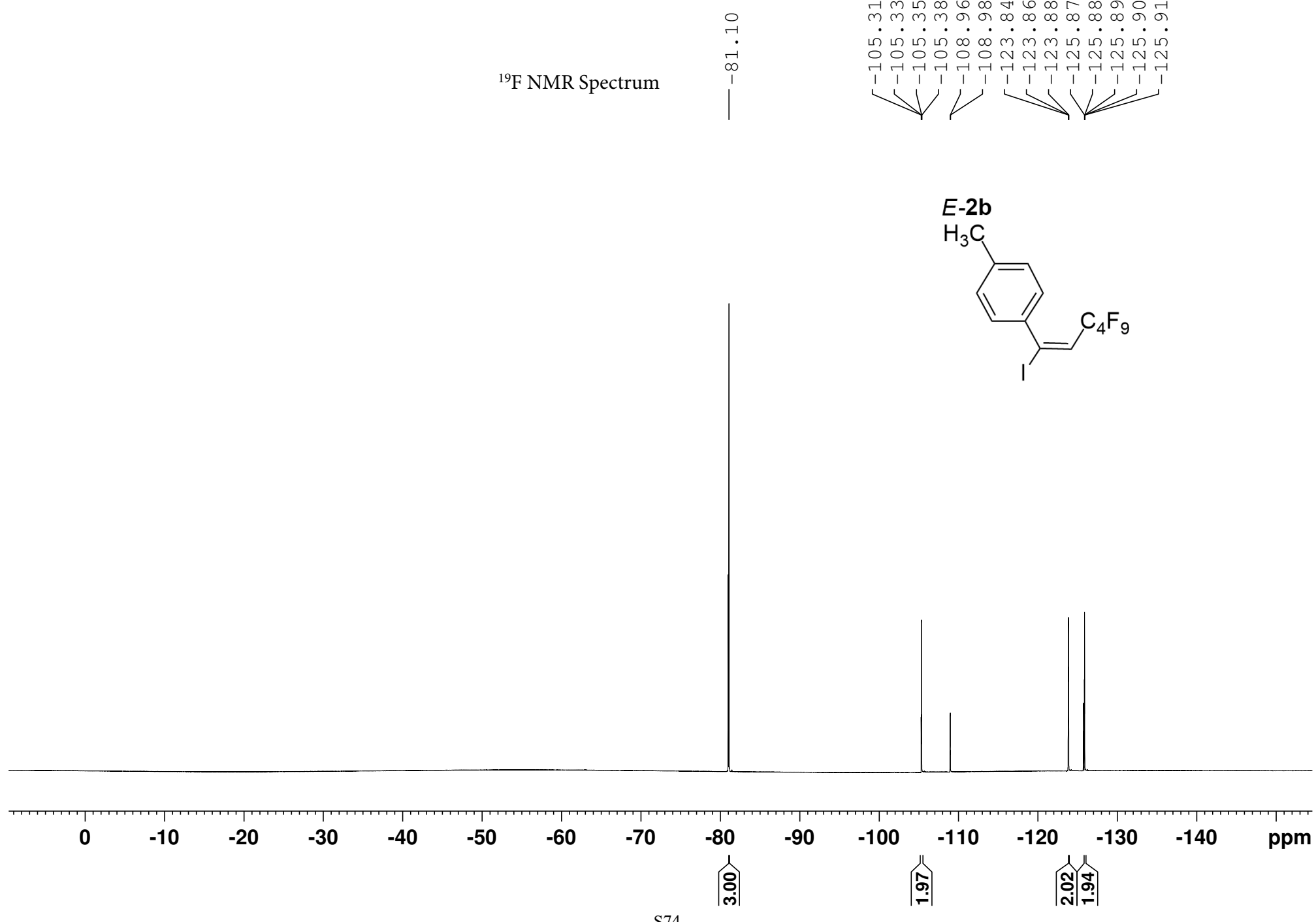






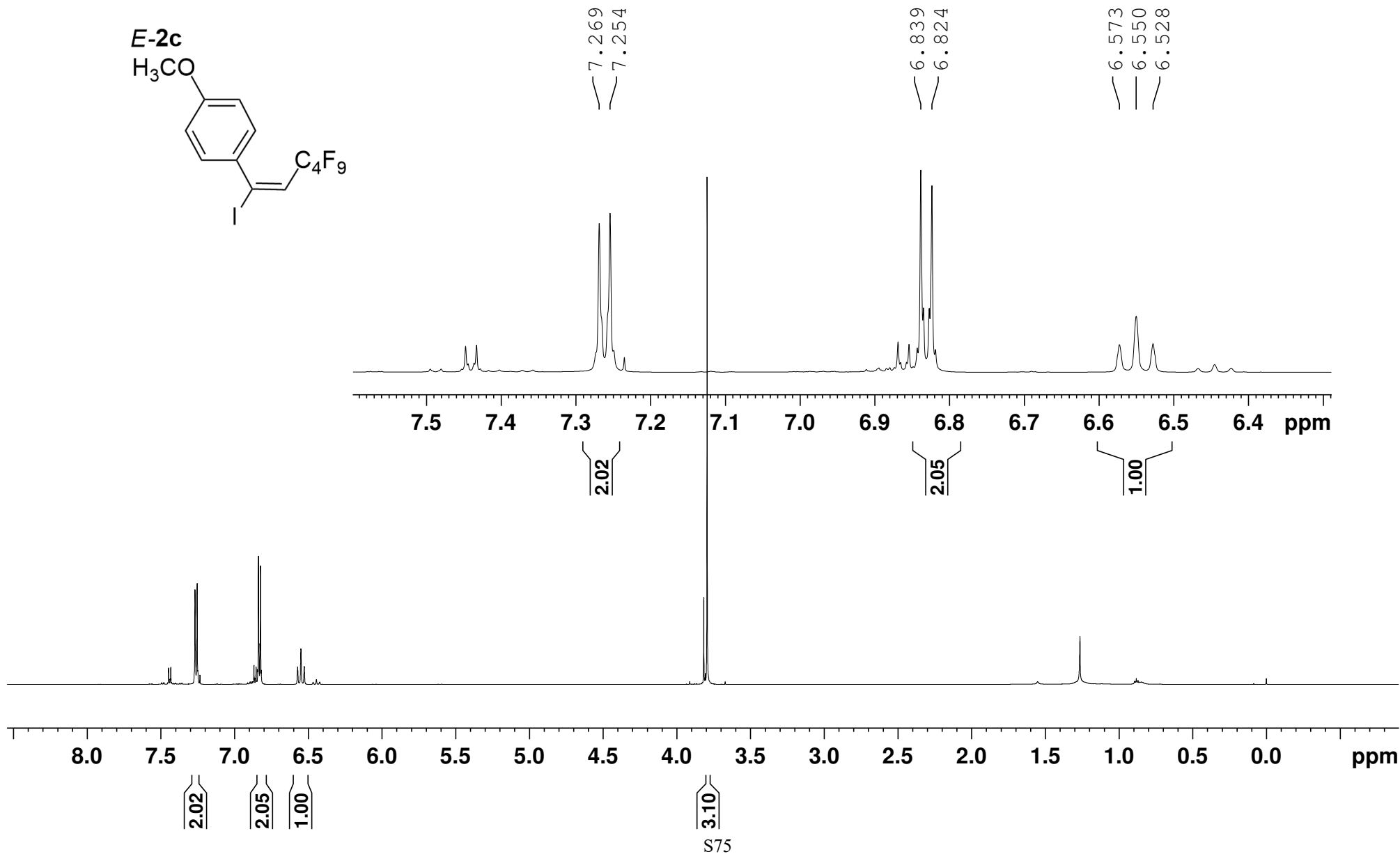
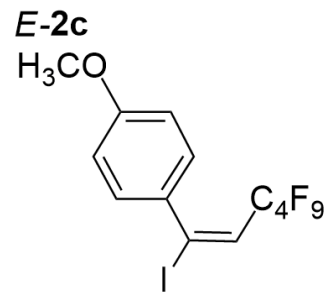


¹⁹F NMR Spectrum



7.269
7.254
6.839
6.824
6.573
6.550
6.528

3.794
¹H NMR Spectrum



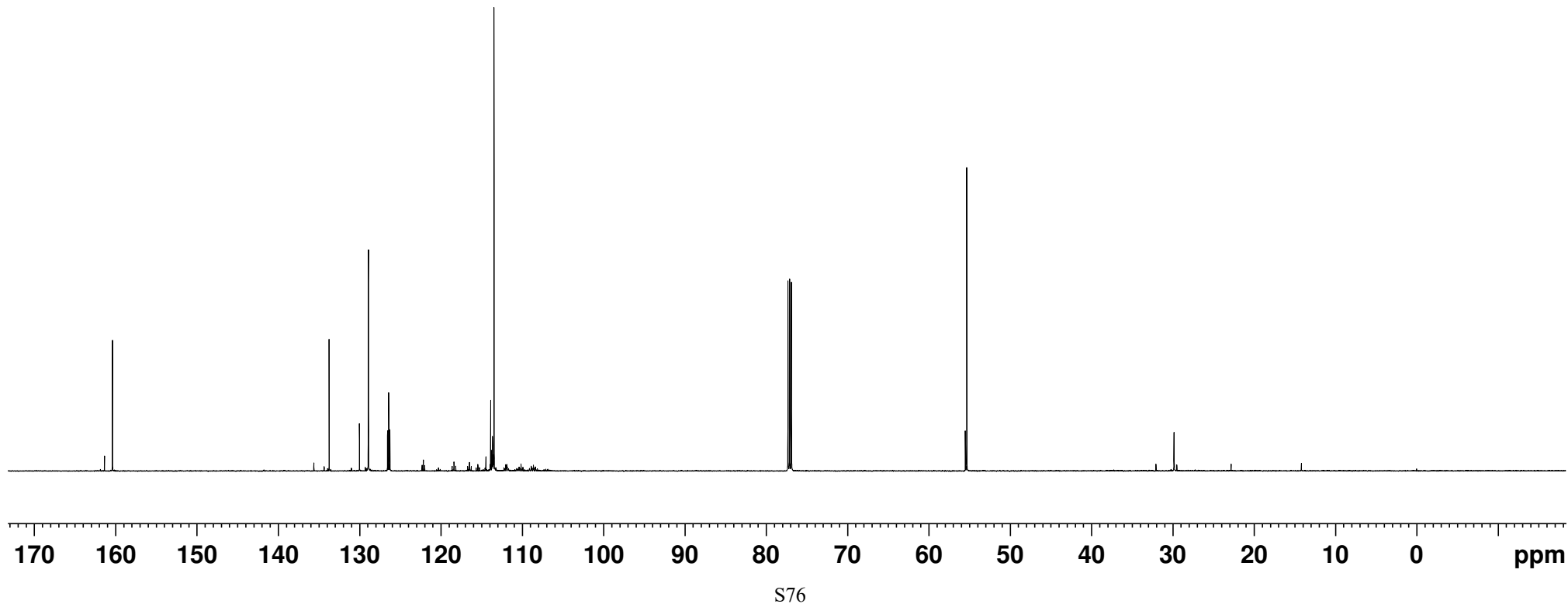
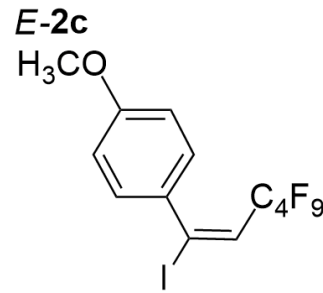
— 160.39

133.74
130.01
128.91
128.89
126.55
126.41
126.26

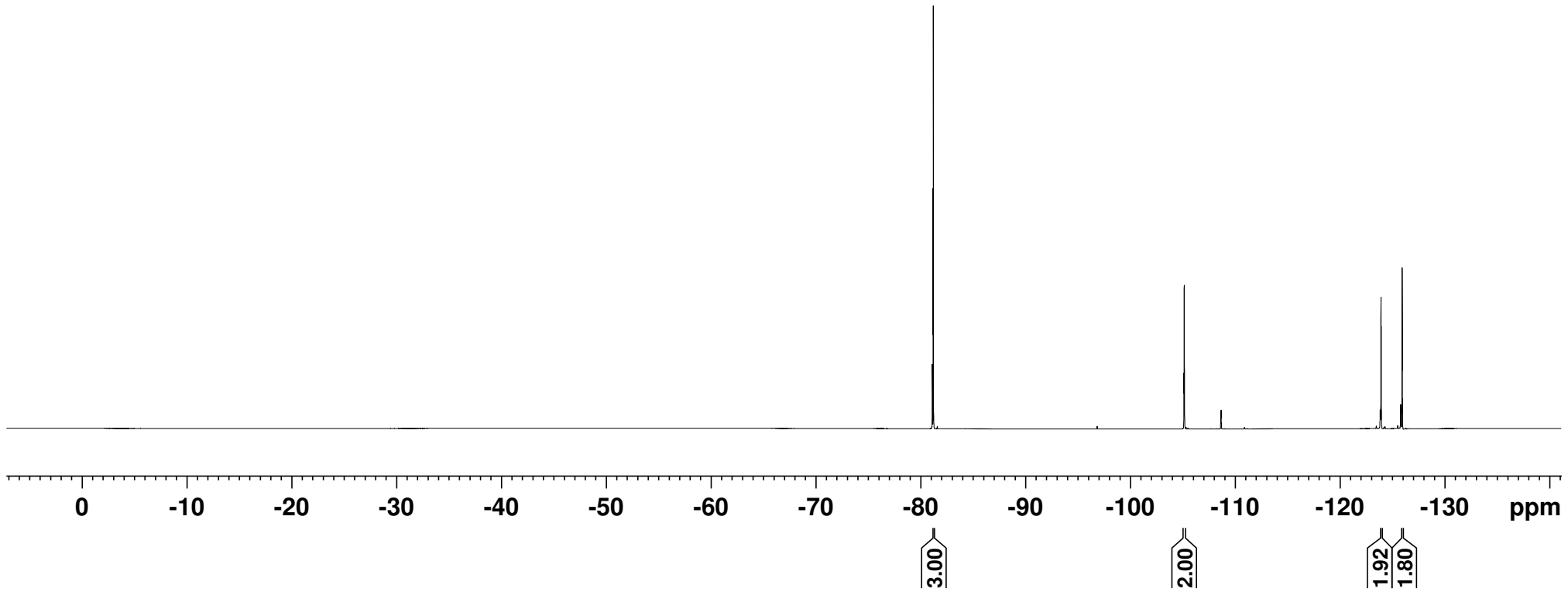
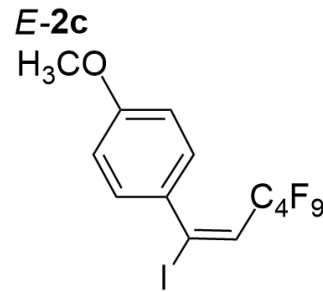
— 113.45

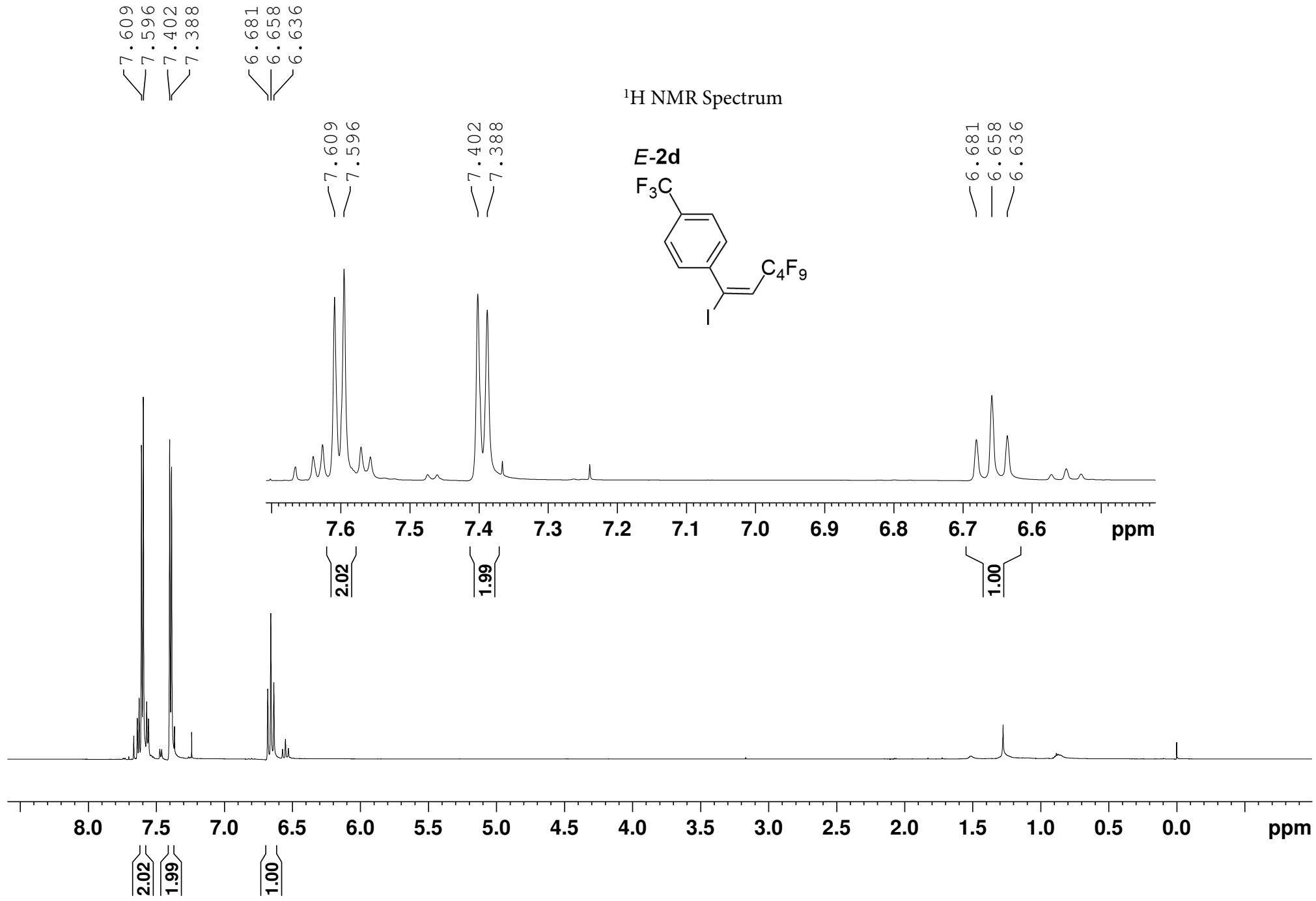
$^{13}\text{C} \{^1\text{H}\}$ NMR Spectrum

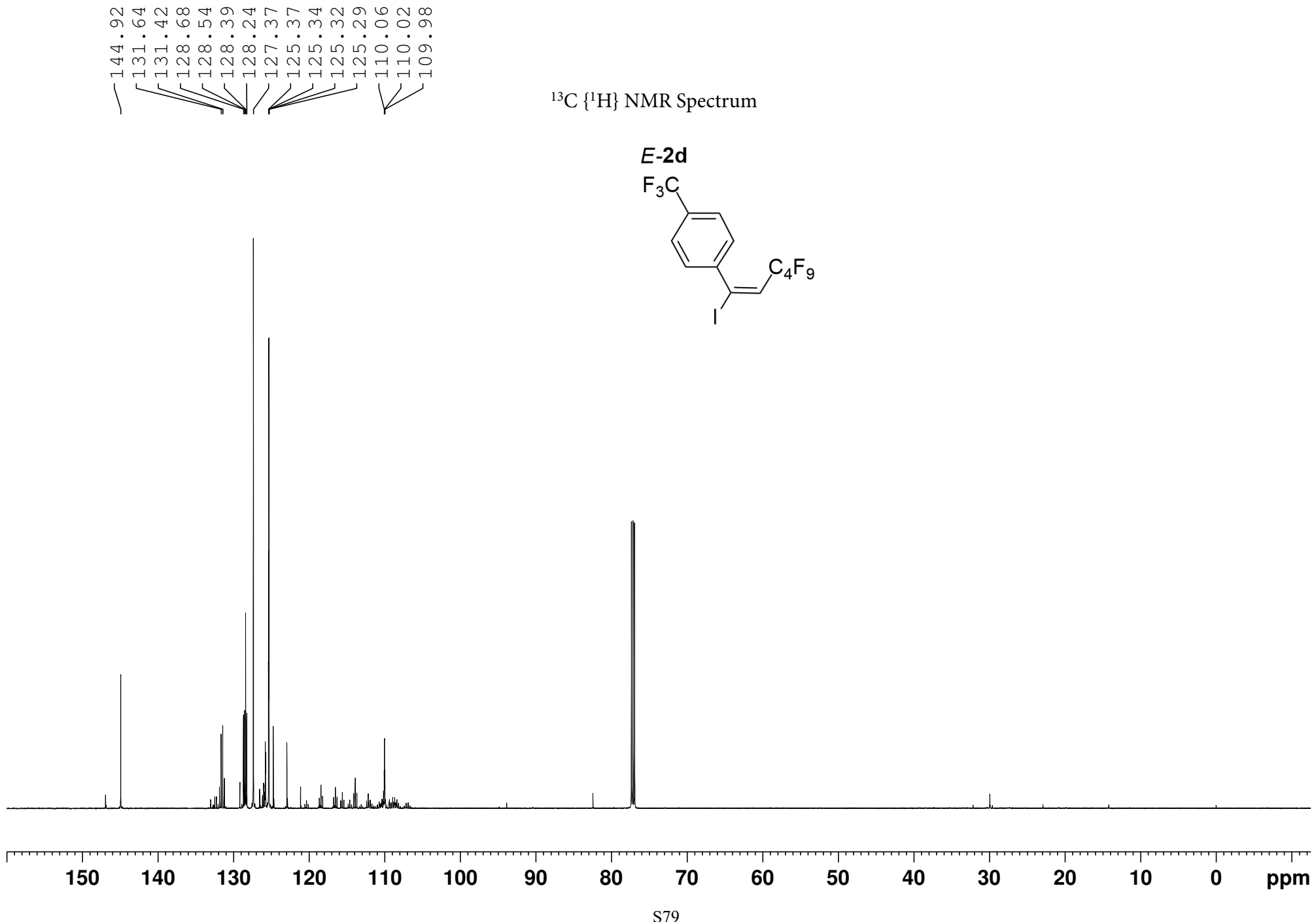
— 55.32



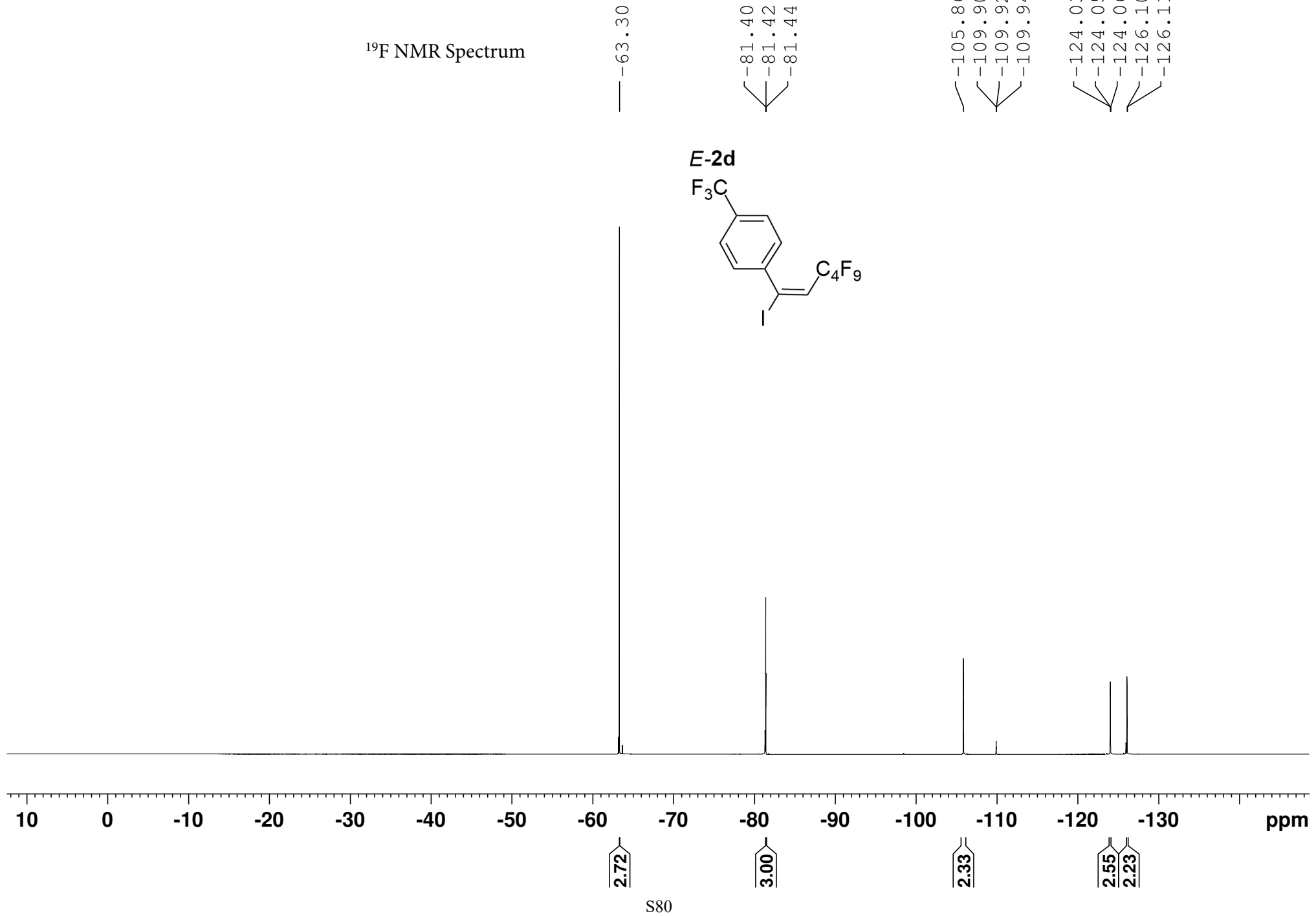
¹⁹F NMR Spectrum



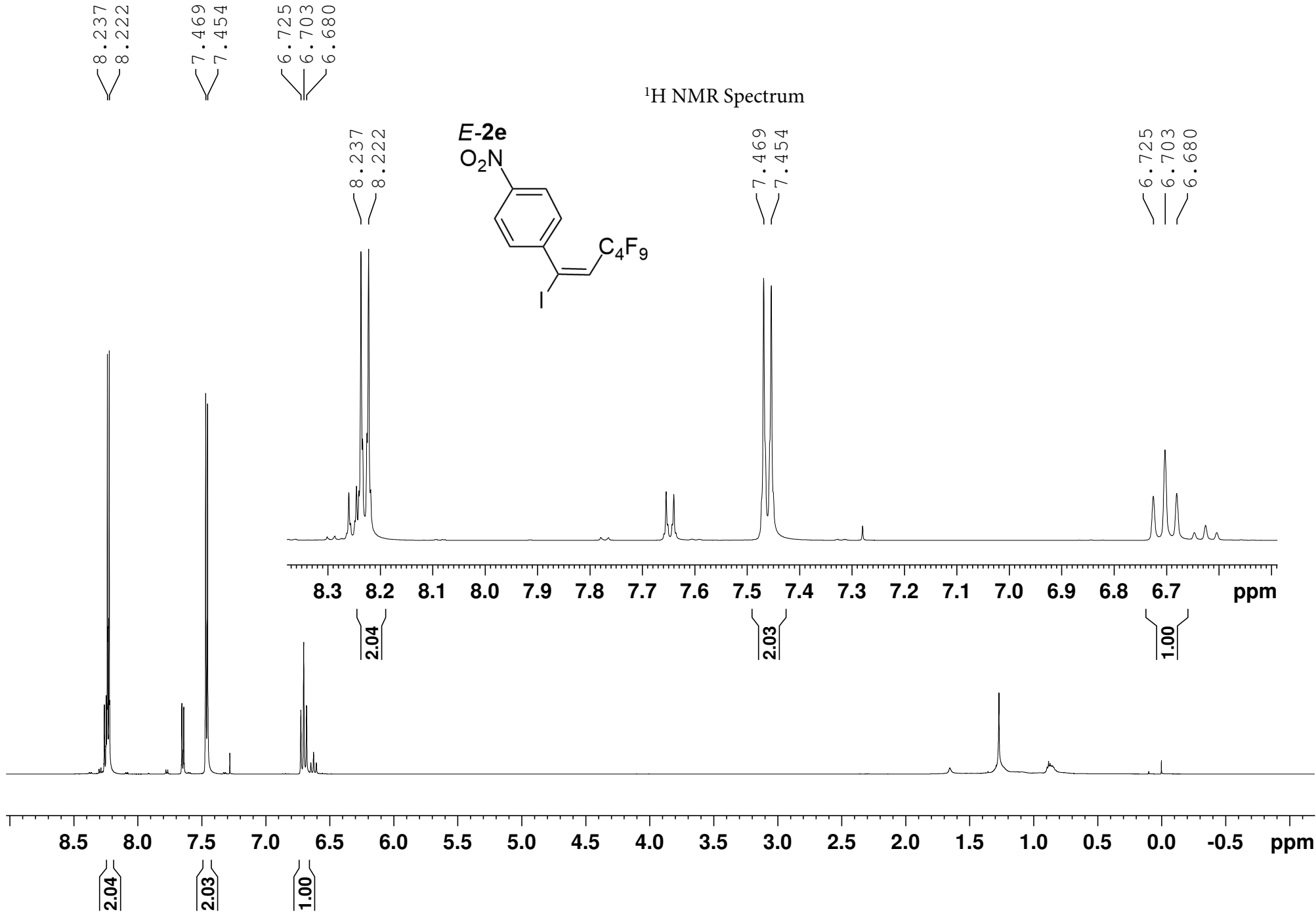


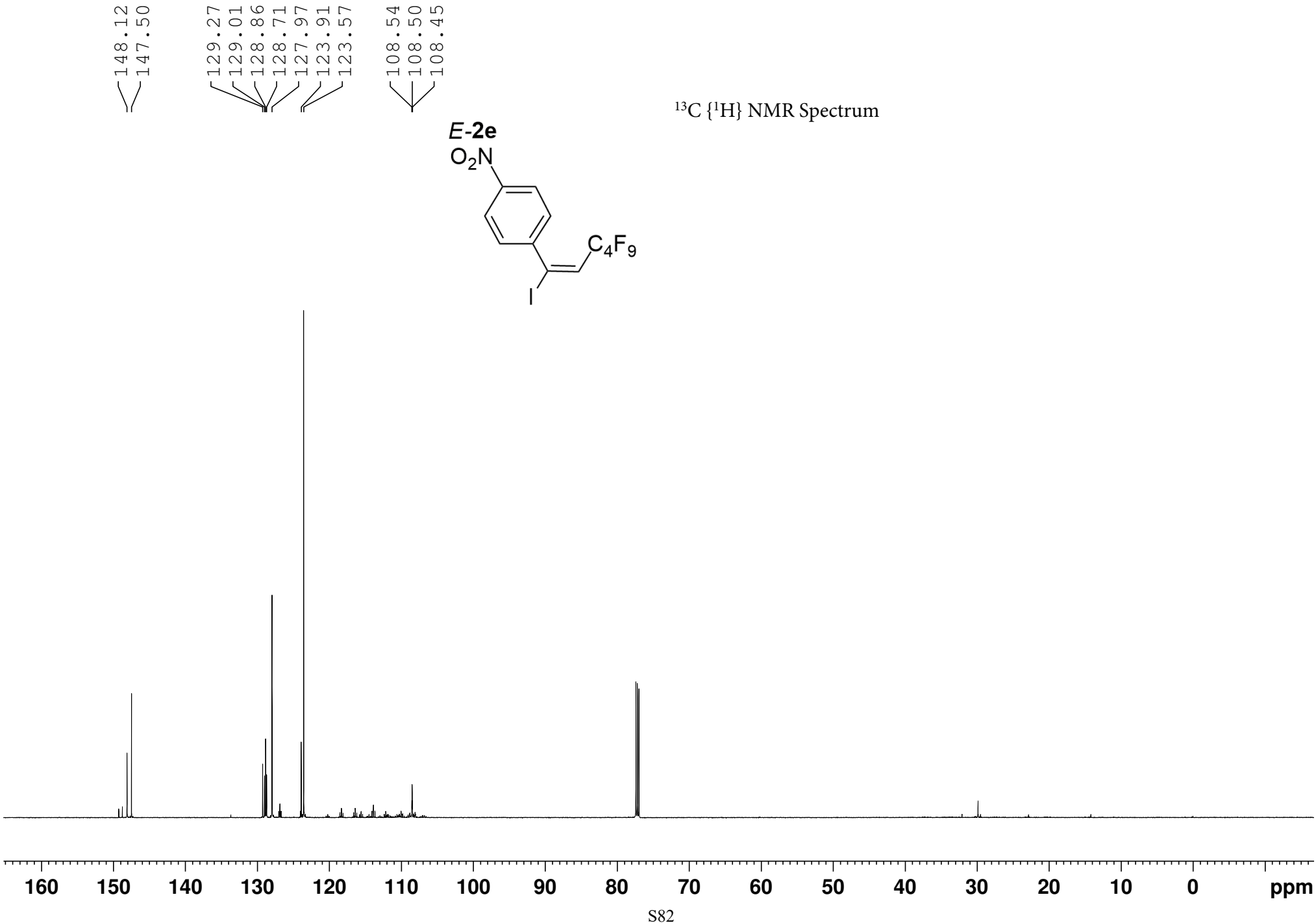


¹⁹F NMR Spectrum

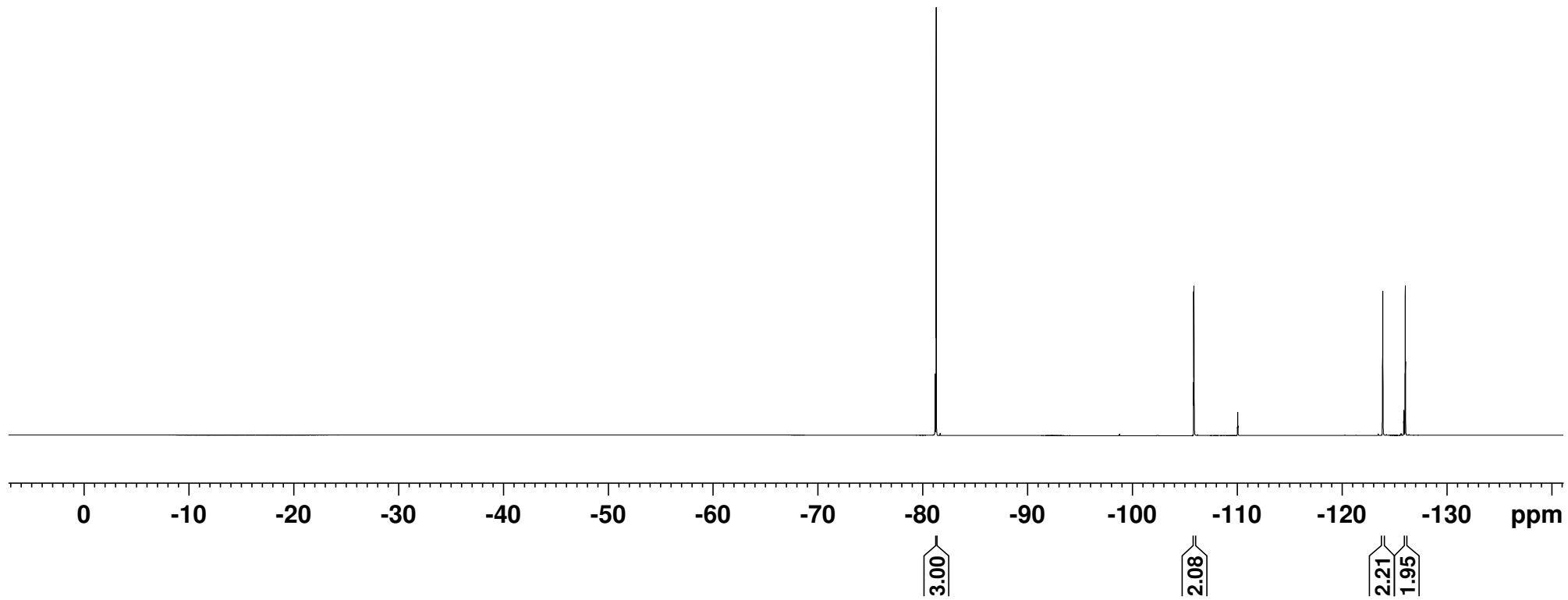
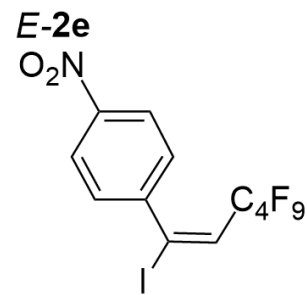


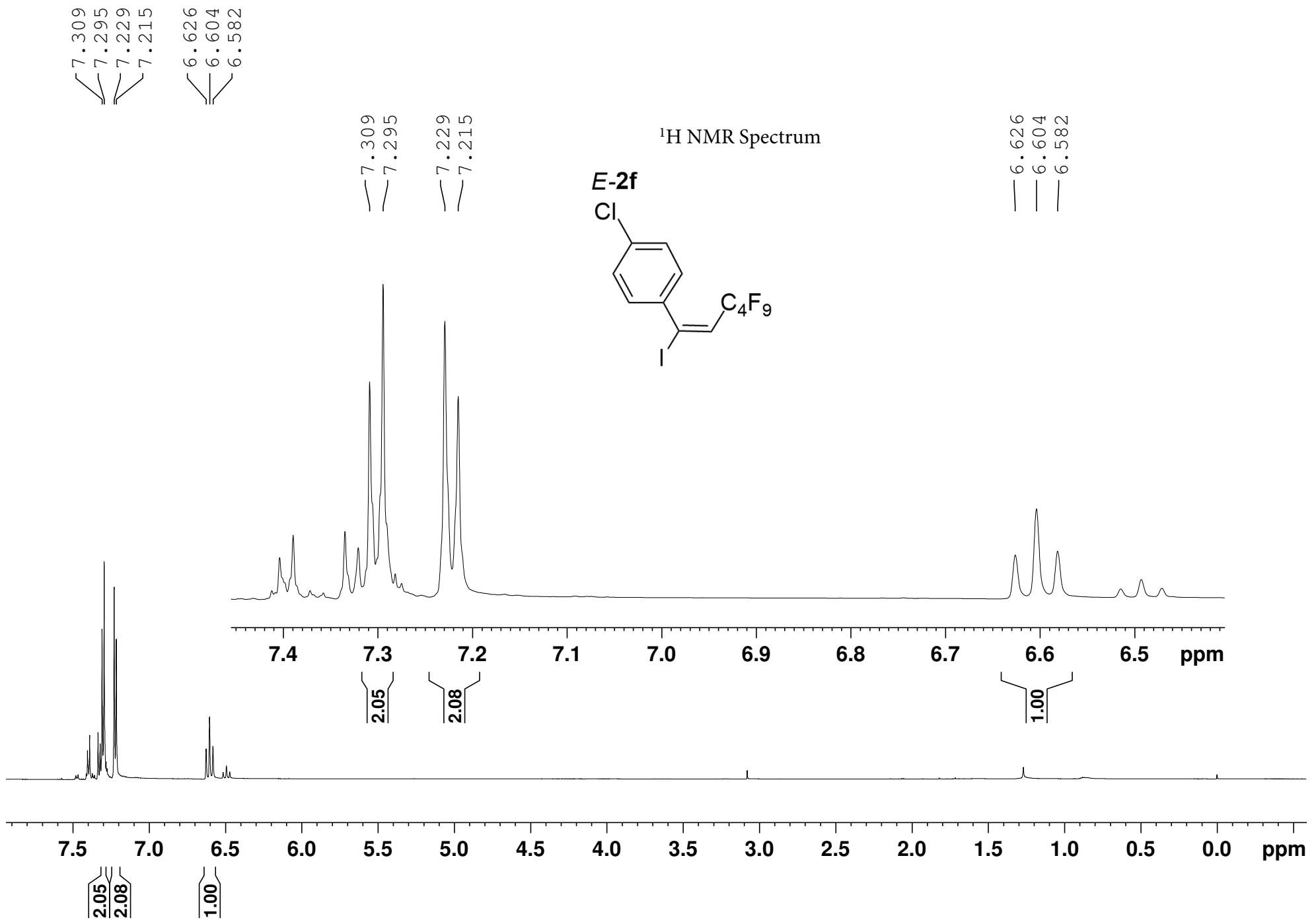
¹H NMR Spectrum





¹⁹F NMR Spectrum



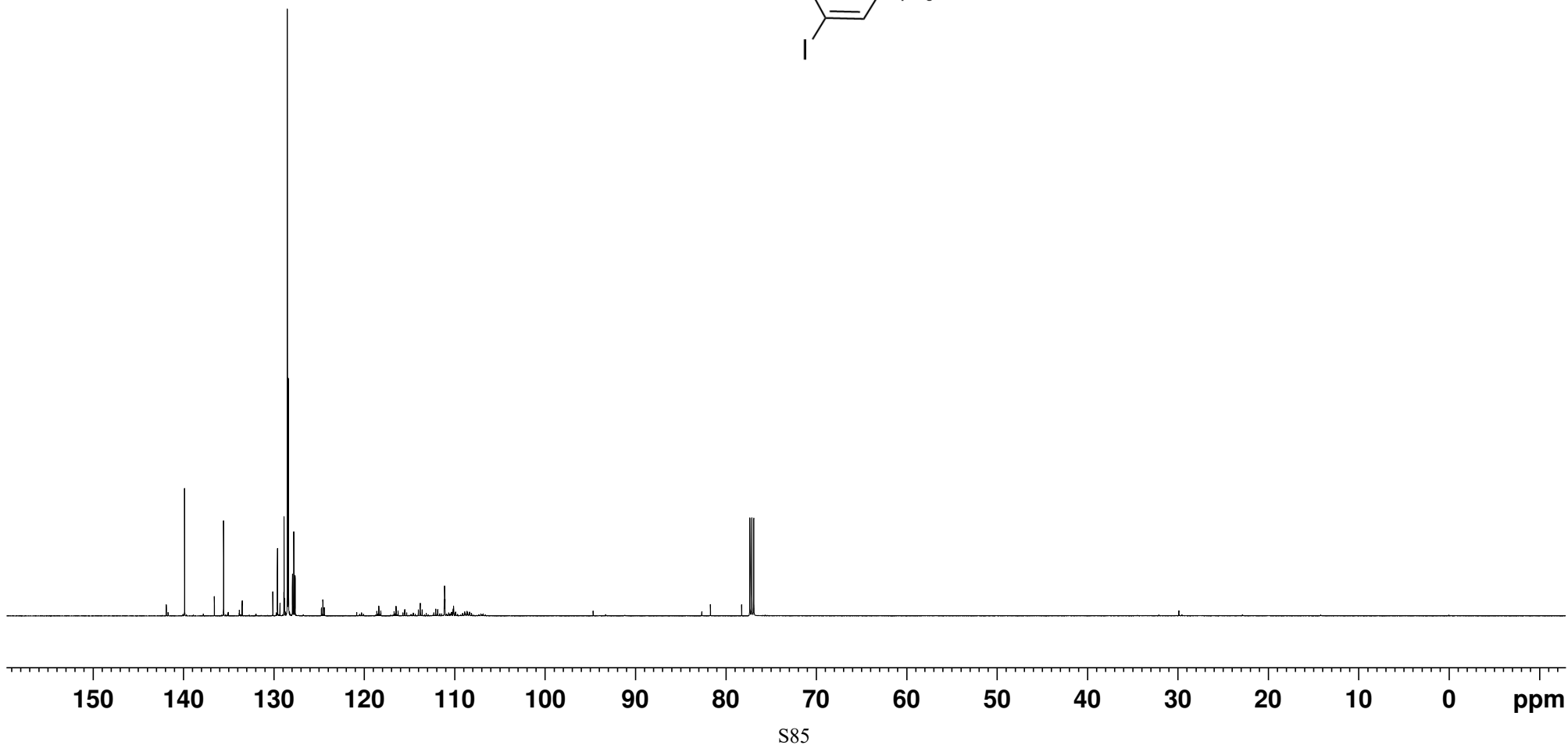
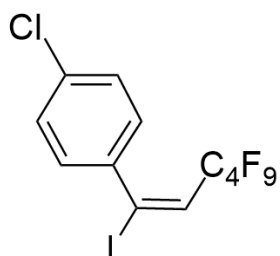


— 139.86
— 135.55
/ \ 129.60
/ \ 128.50
/ \ 128.39
— 127.79

— 111.14
— 111.10
— 111.06

¹³C {¹H} NMR Spectrum

E-2f

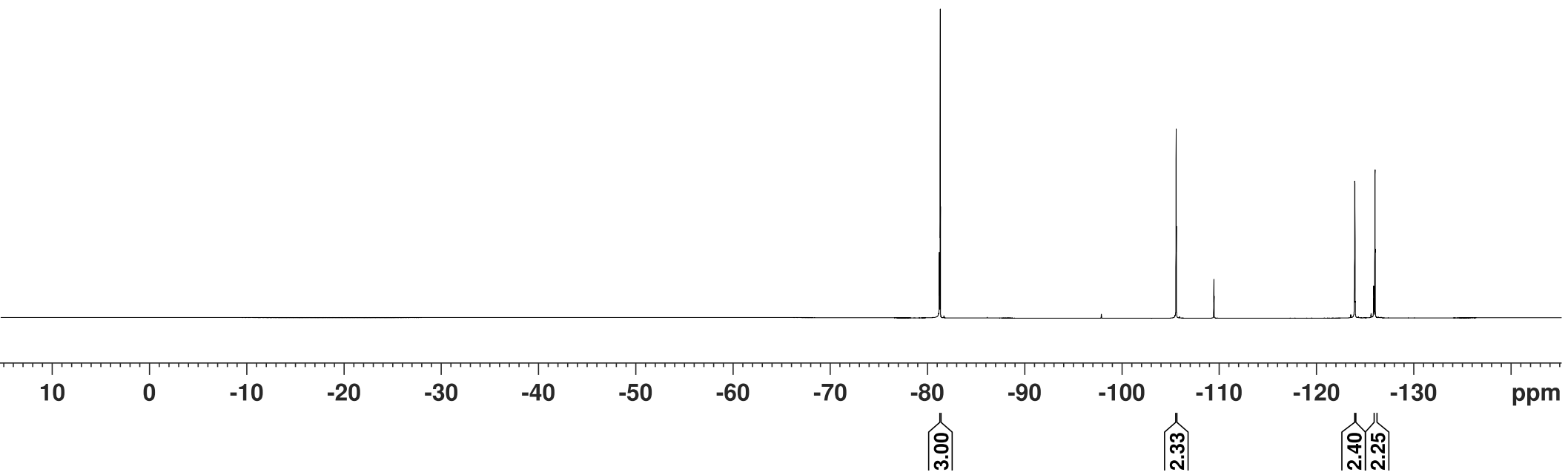
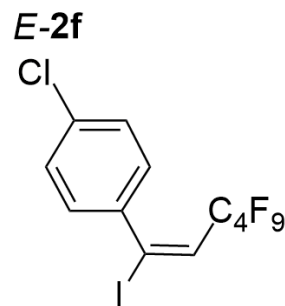


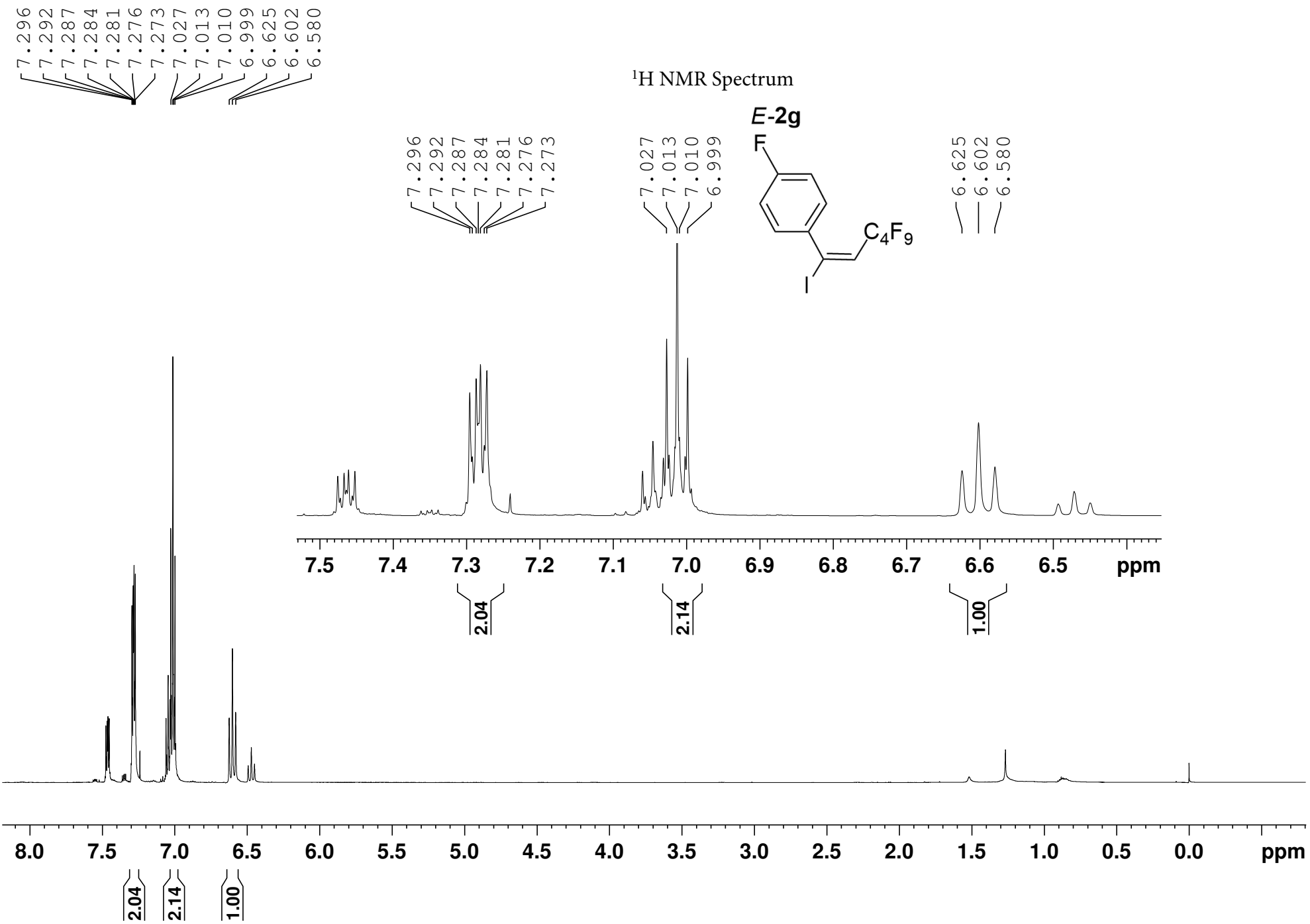
¹⁹F NMR Spectrum

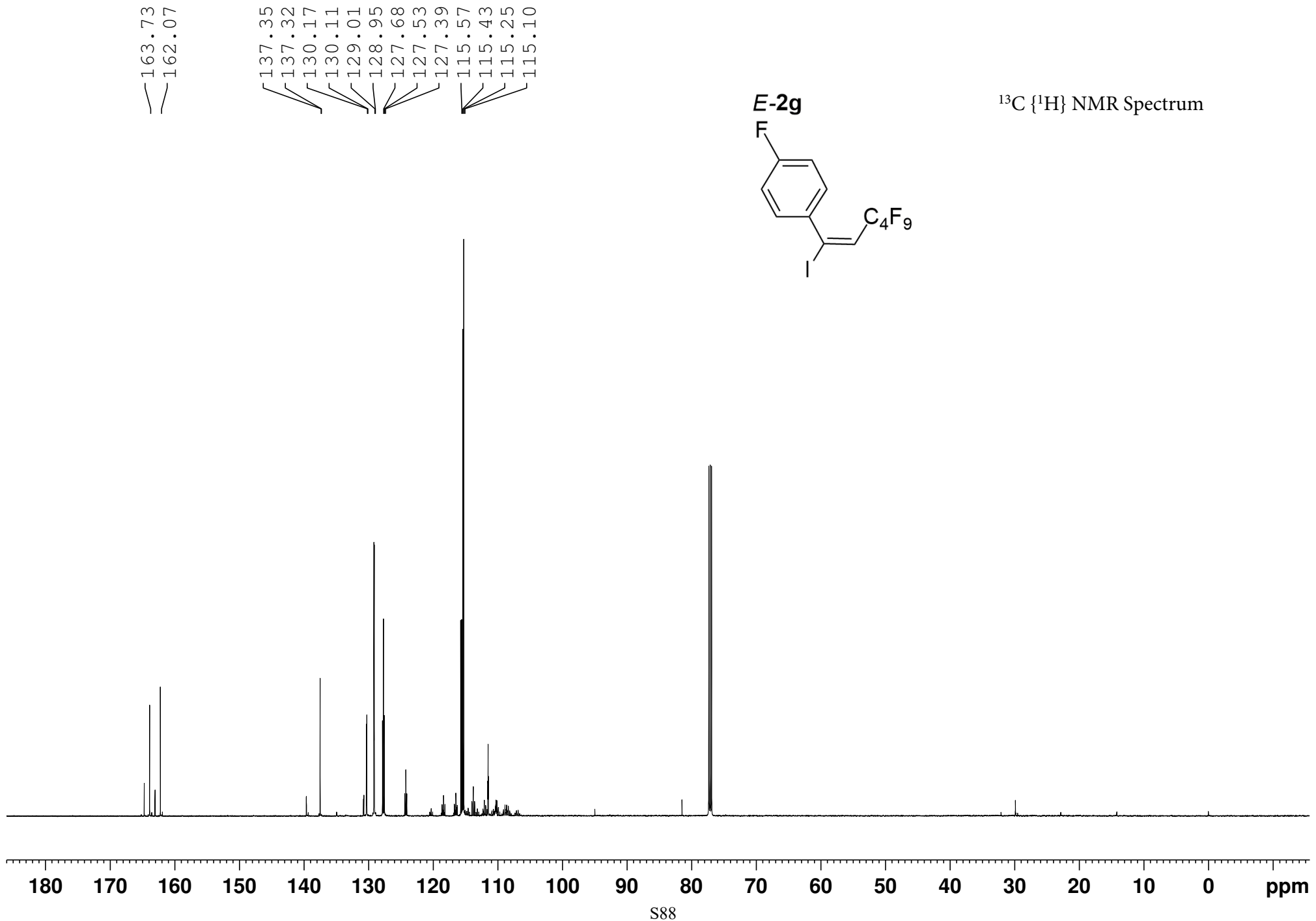
— -81.31

✓ -105.55
✓ -105.57
✓ -105.59
✓ -109.44
✓ -109.46
✓ -109.48

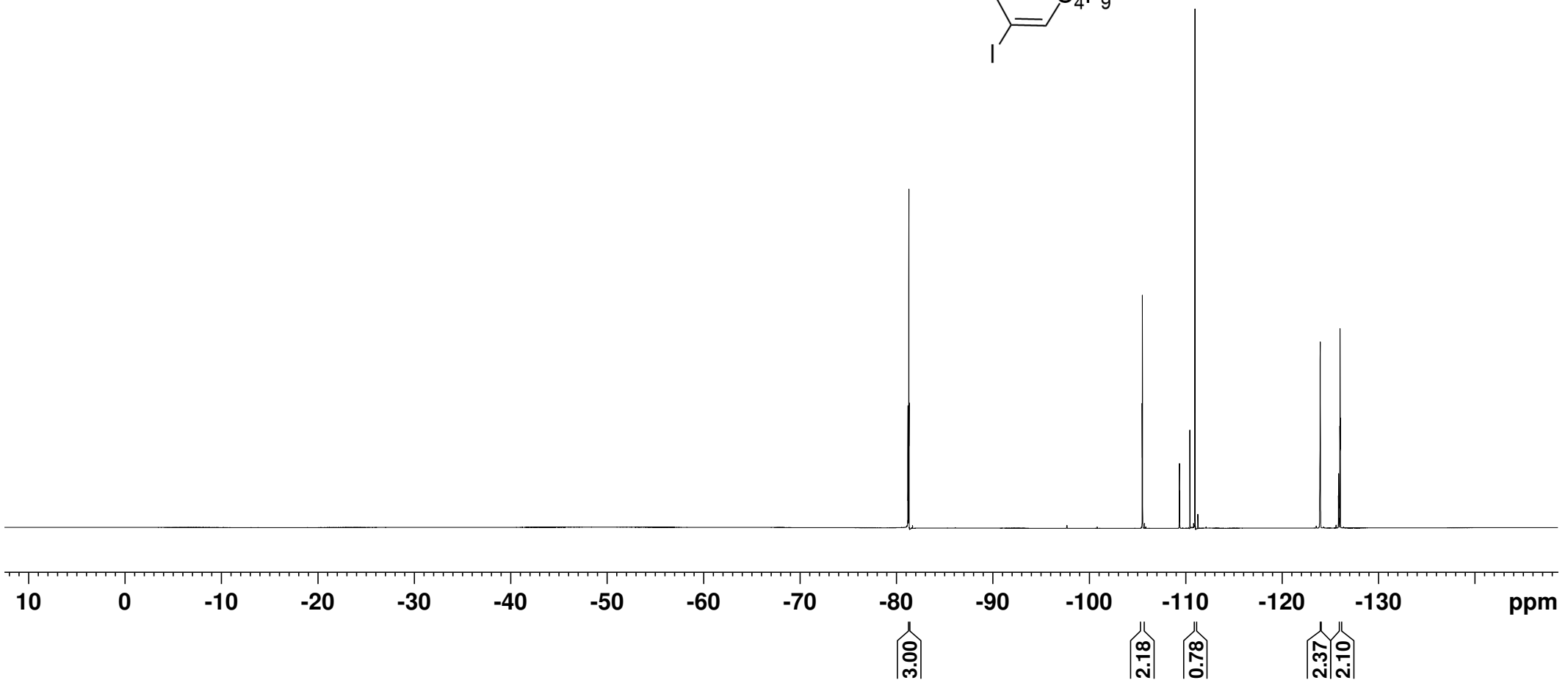
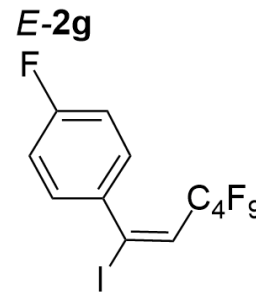
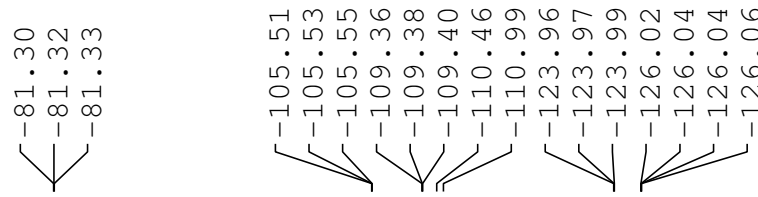
✓ -123.95
✓ -123.96
✓ -126.02
✓ -126.03







¹⁹F NMR Spectrum



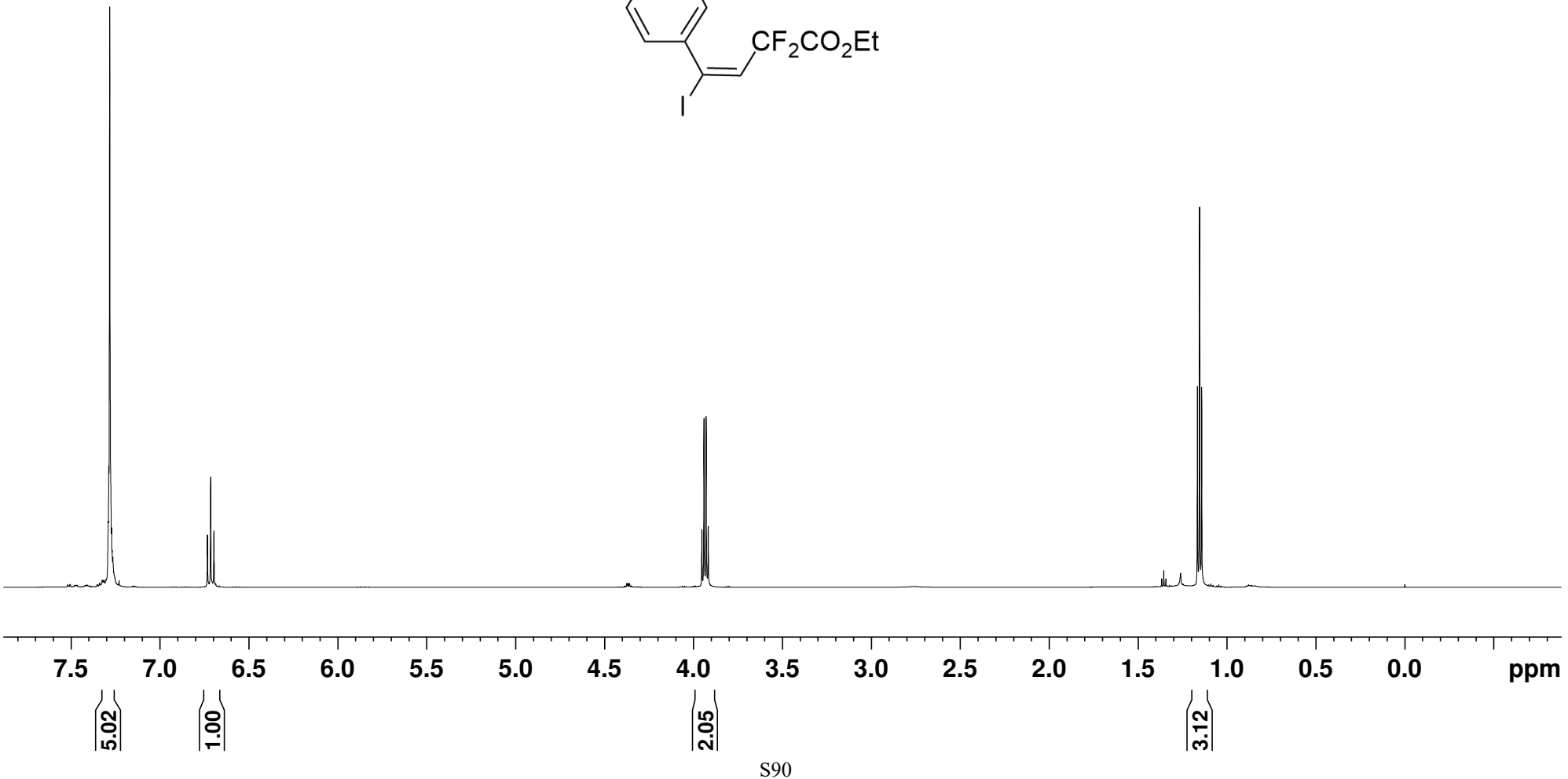
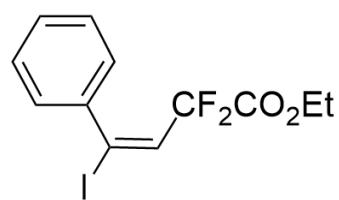
7.288
7.283
6.733
6.715
6.697

3.953
3.941
3.929
3.917

1.166
1.154
1.142

¹H NMR Spectrum

E-2h



162.64
162.42
162.20

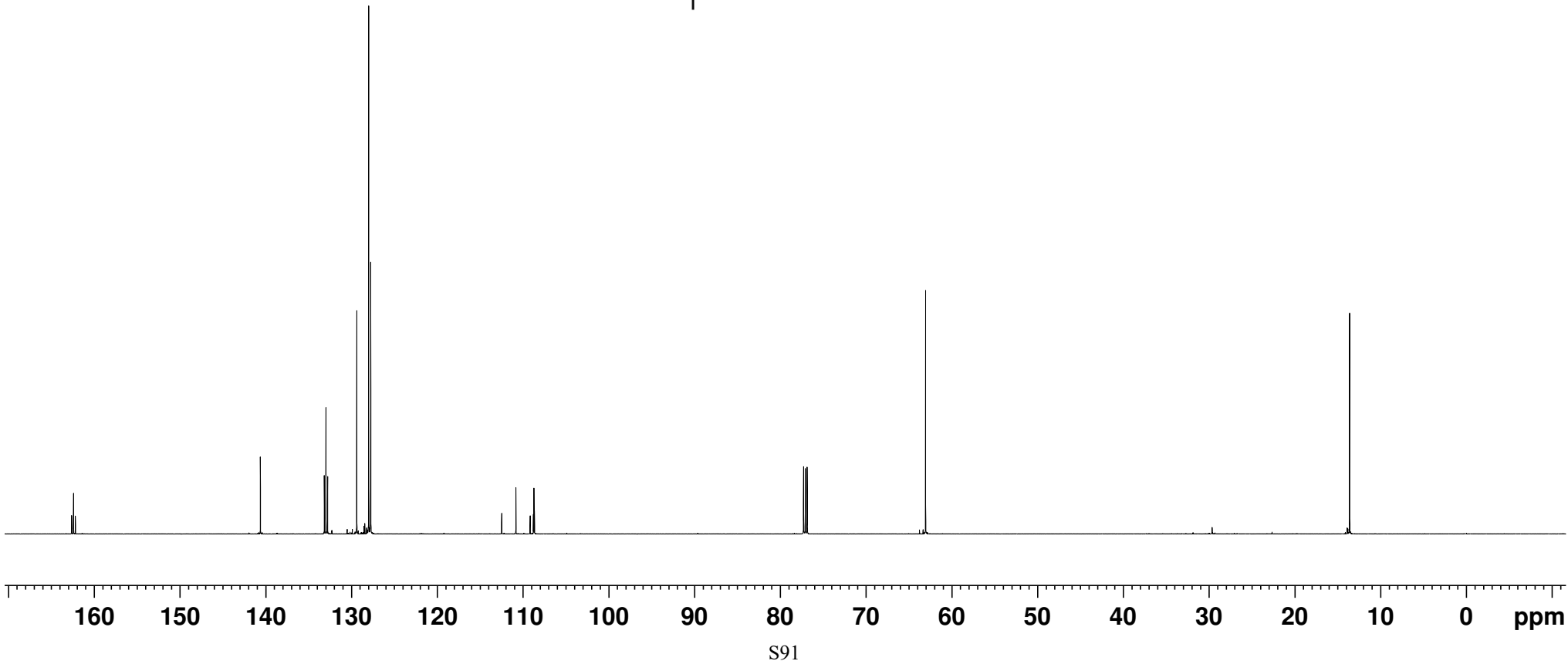
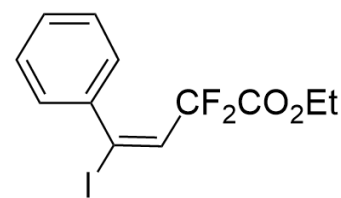
140.64
133.18
132.99
132.80
129.40
128.01
127.77
127.76
127.76
112.49
110.84
109.18
108.80
108.74
108.67

— 63.07

— 13.62

$^{13}\text{C} \{^1\text{H}\}$ NMR Spectrum

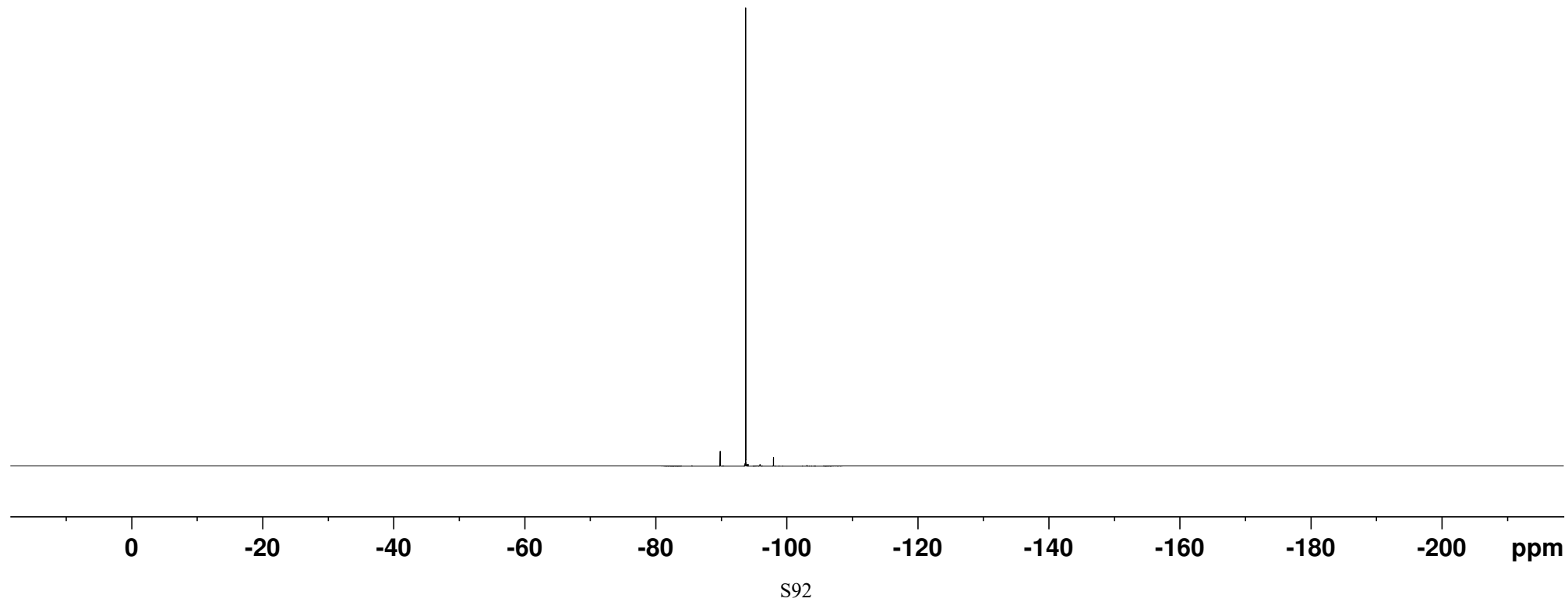
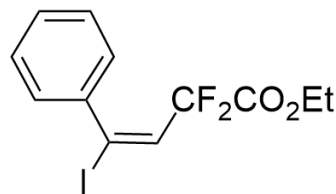
E-2h

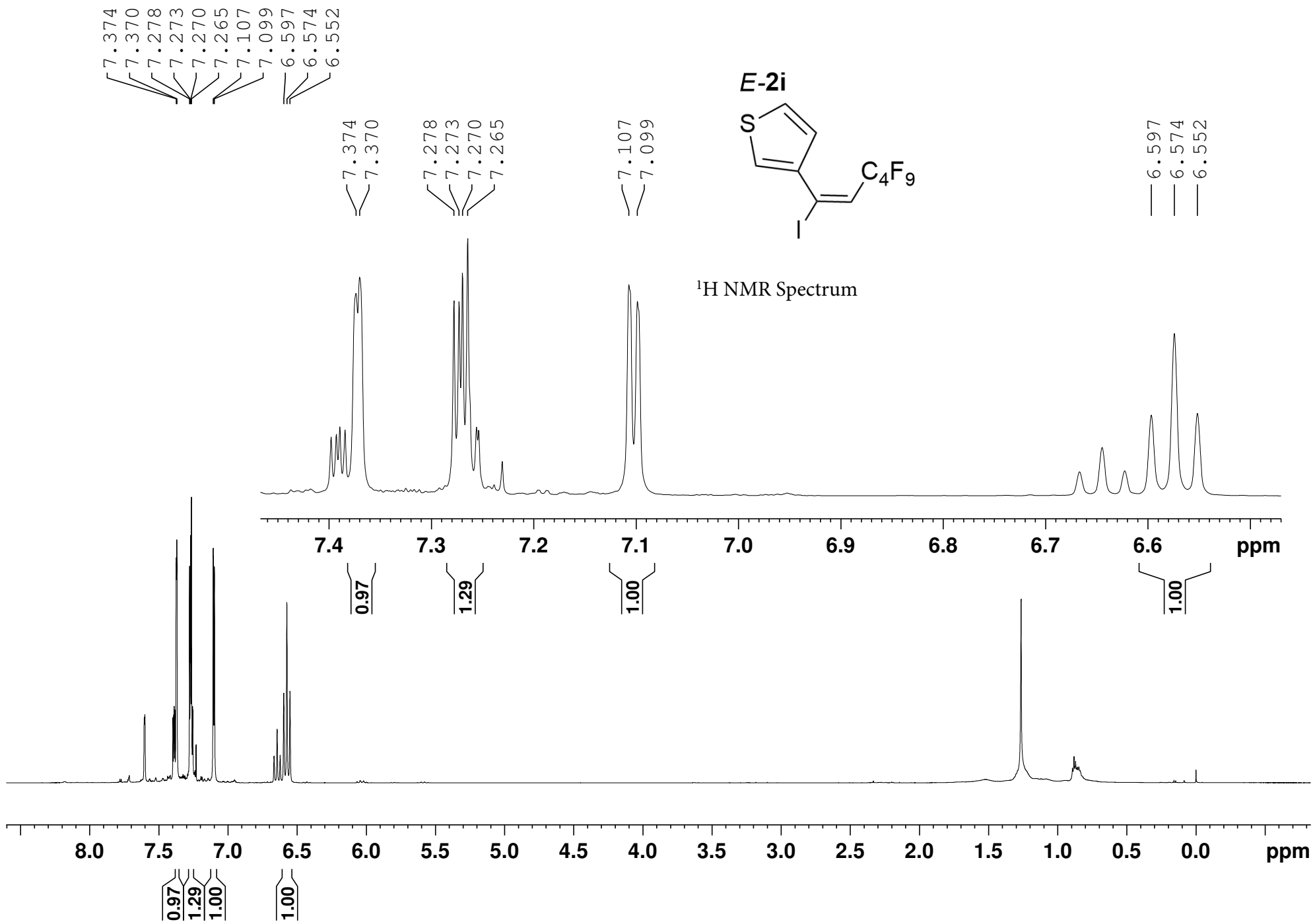


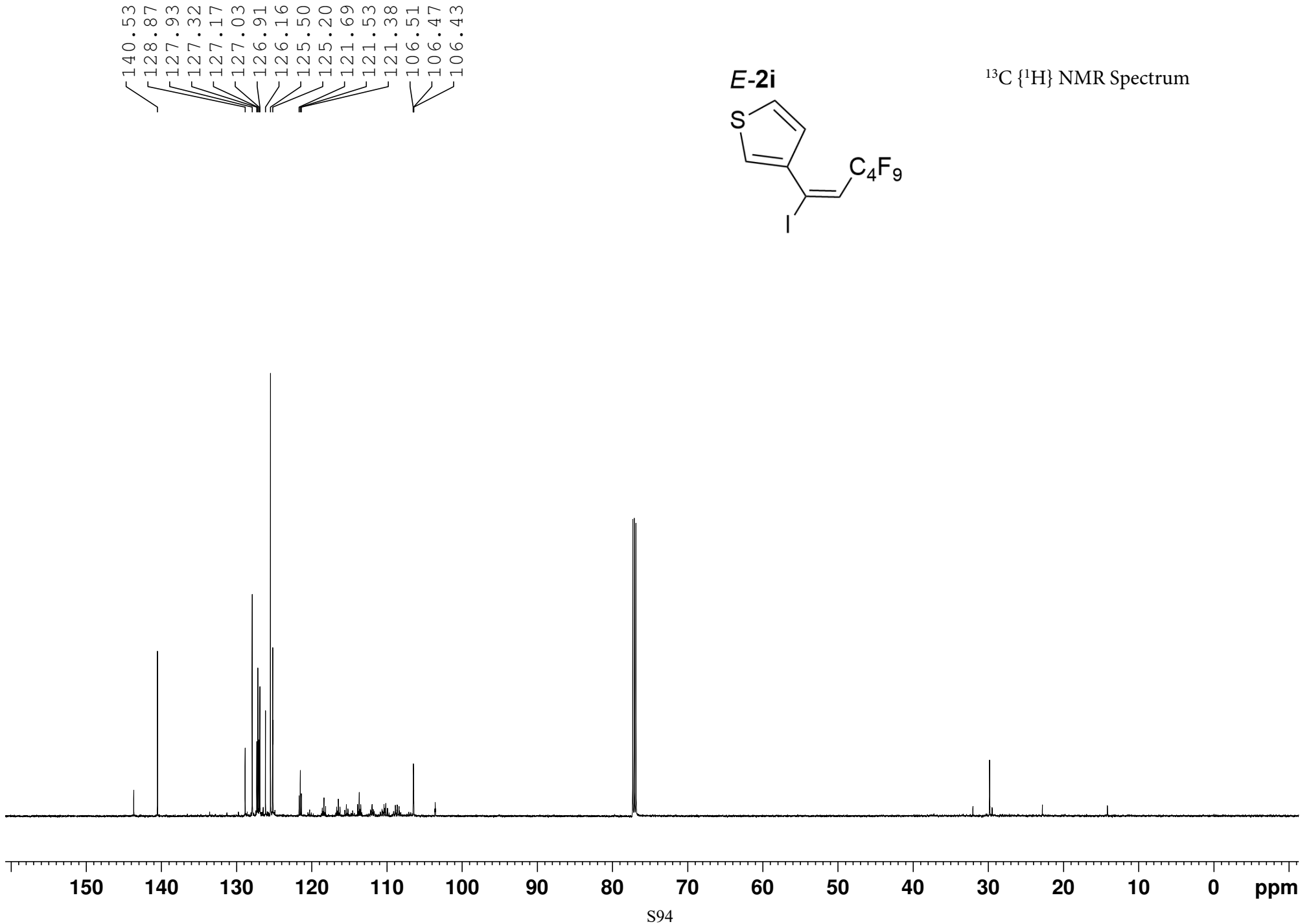
-93.73
-93.75

¹⁹F NMR Spectrum

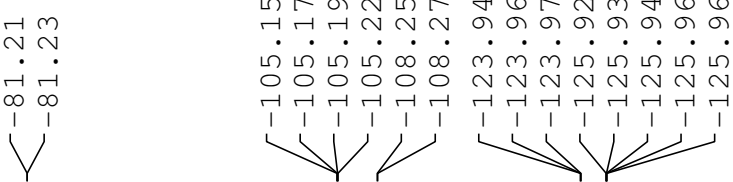
E-2h



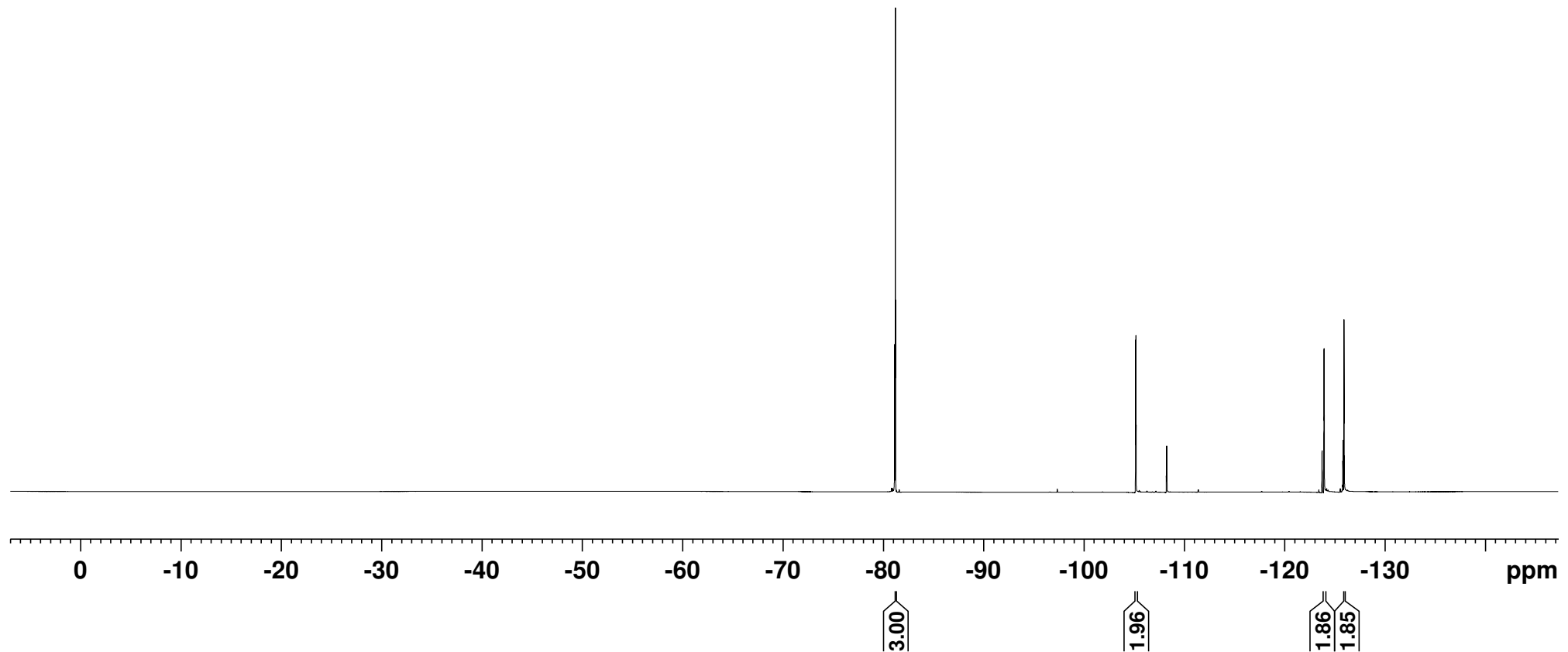
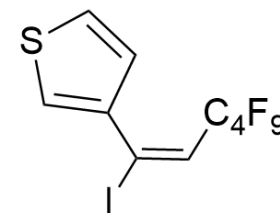


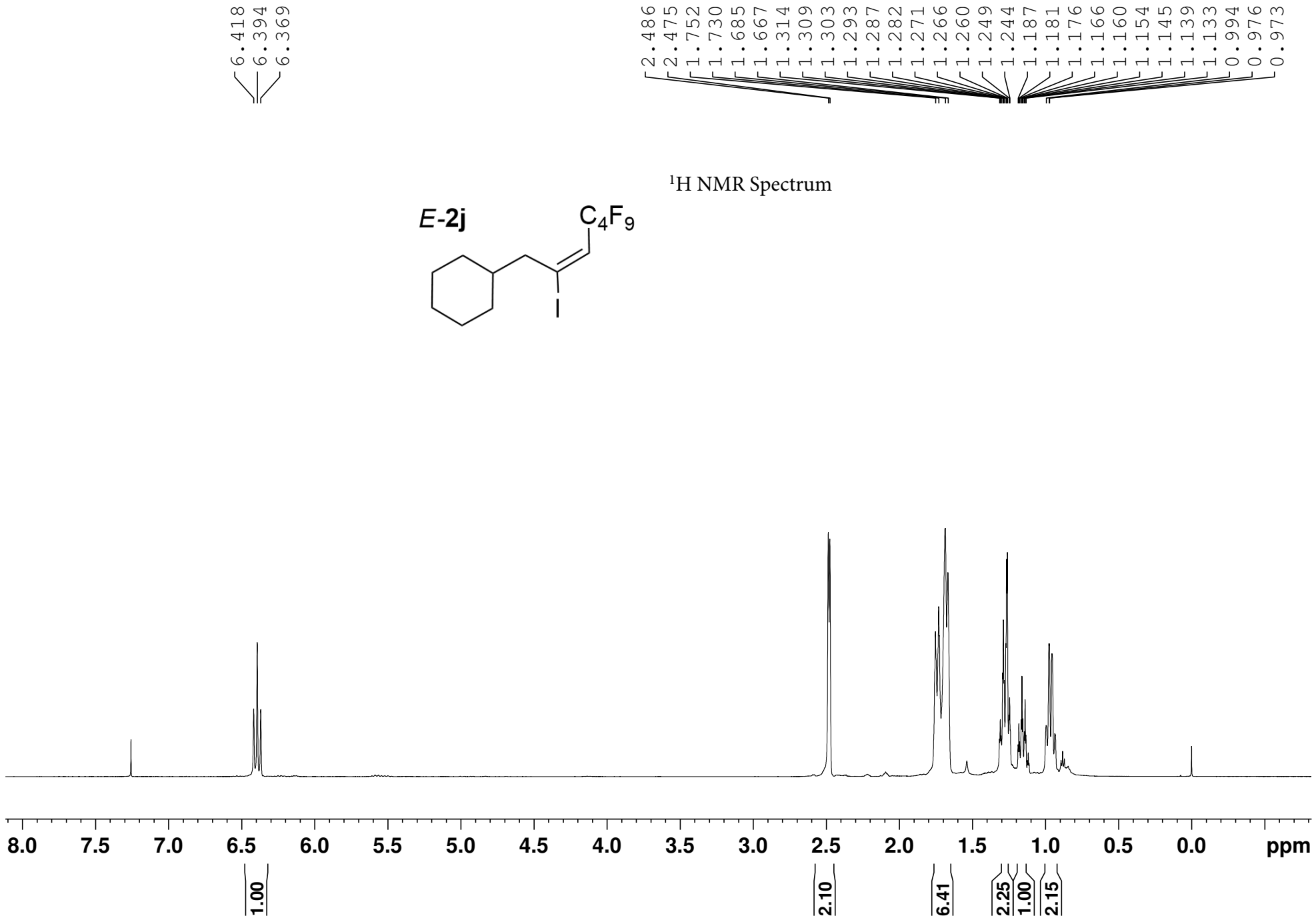


¹⁹F NMR Spectrum



E-2i

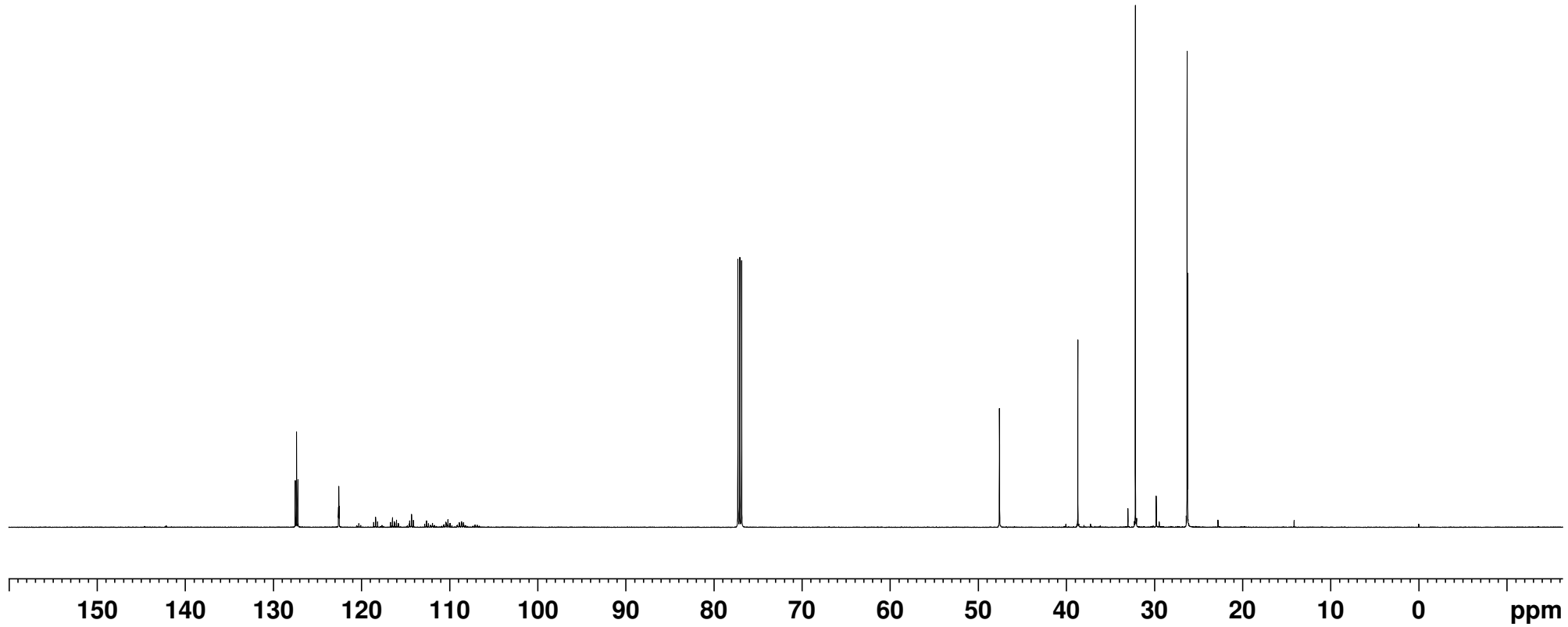
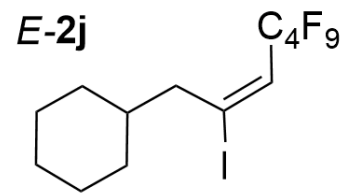




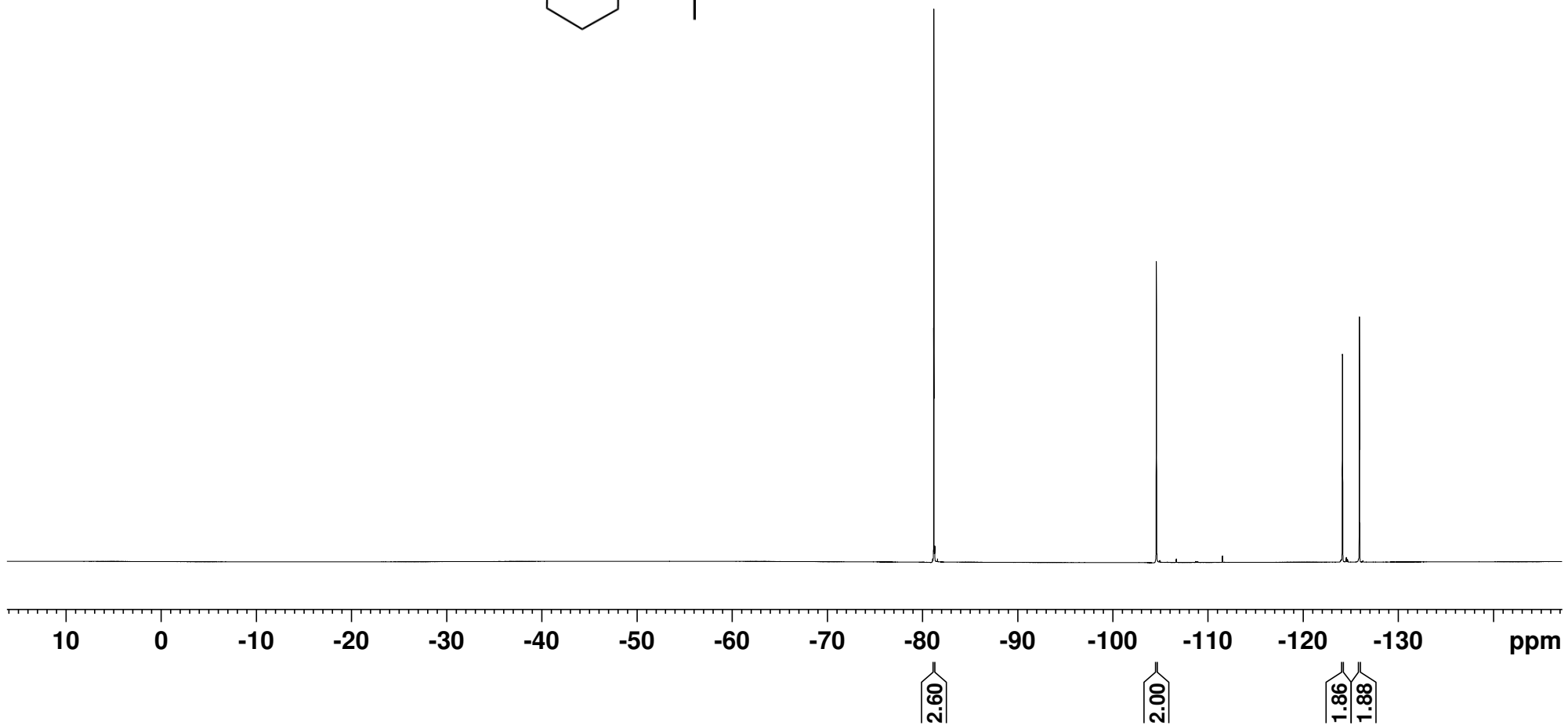
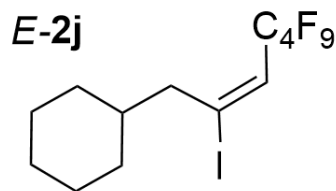
127.53
127.37
127.22
122.62
122.58
122.54

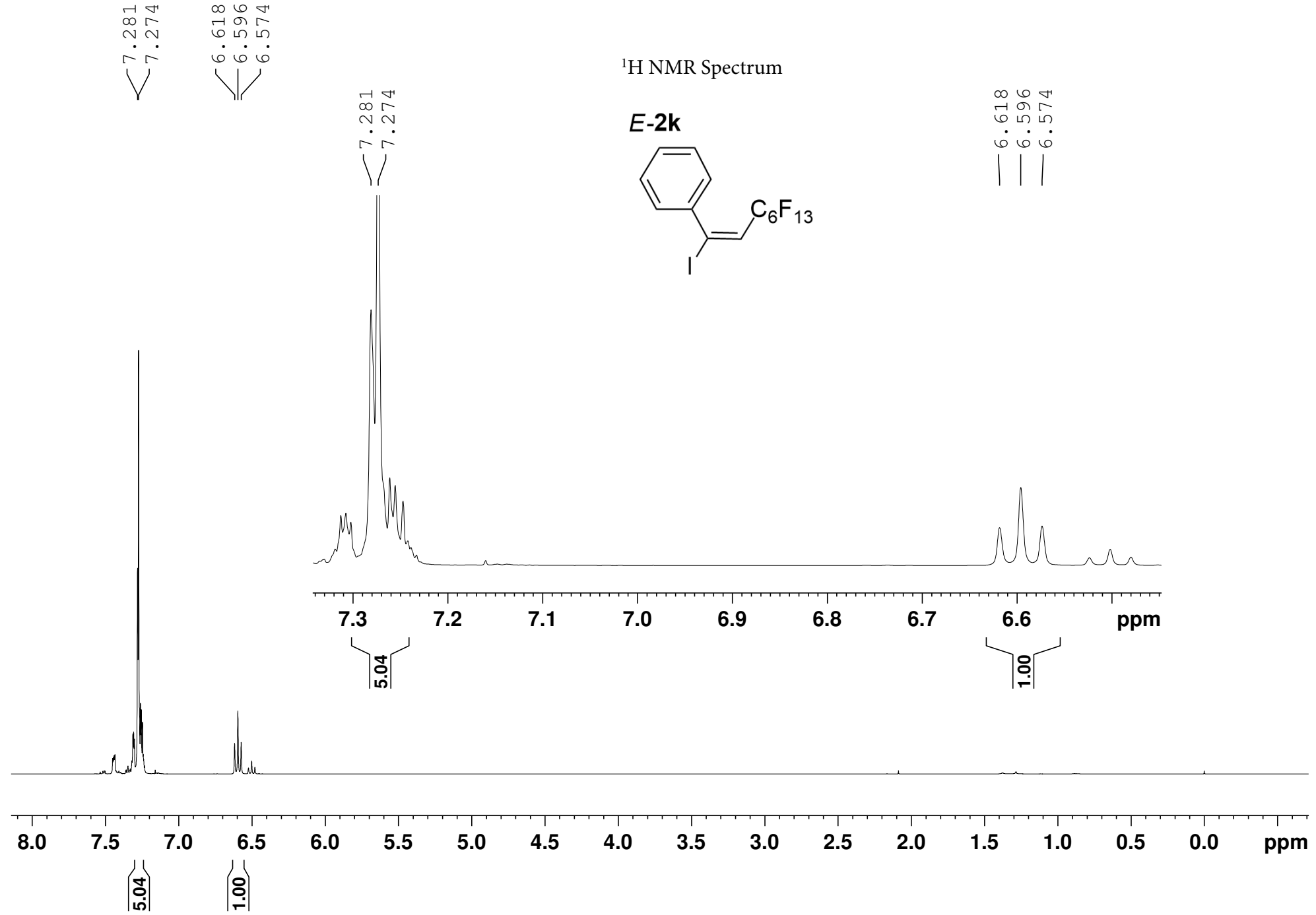
^{13}C { ^1H } NMR Spectrum

— 47.59
— 38.70
— 32.17
— 26.30
— 26.24



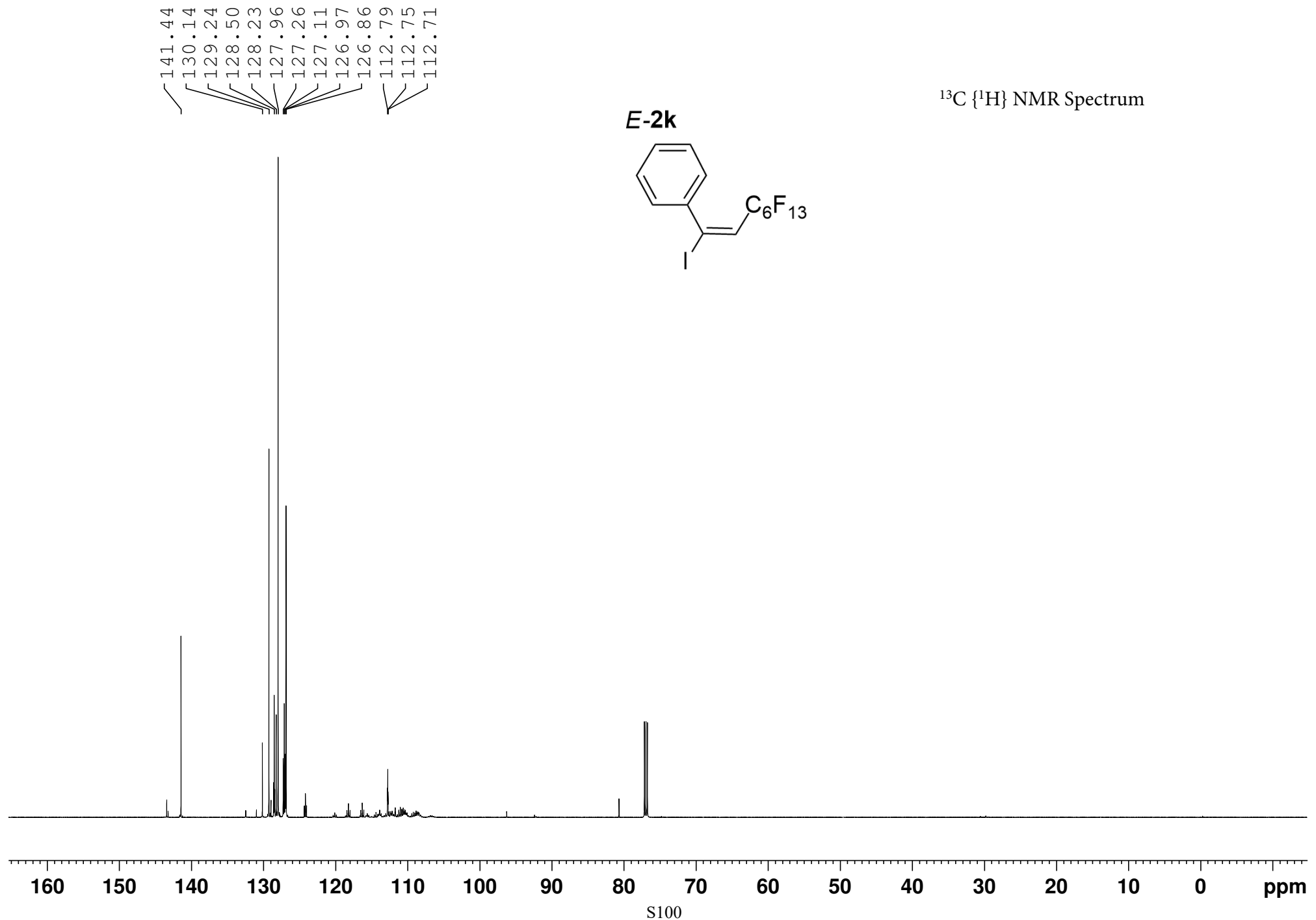
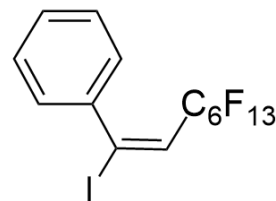
¹⁹F NMR Spectrum





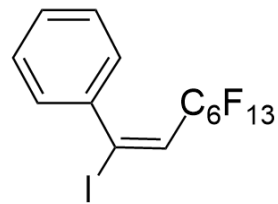
$^{13}\text{C} \{^1\text{H}\}$ NMR Spectrum

E-2k



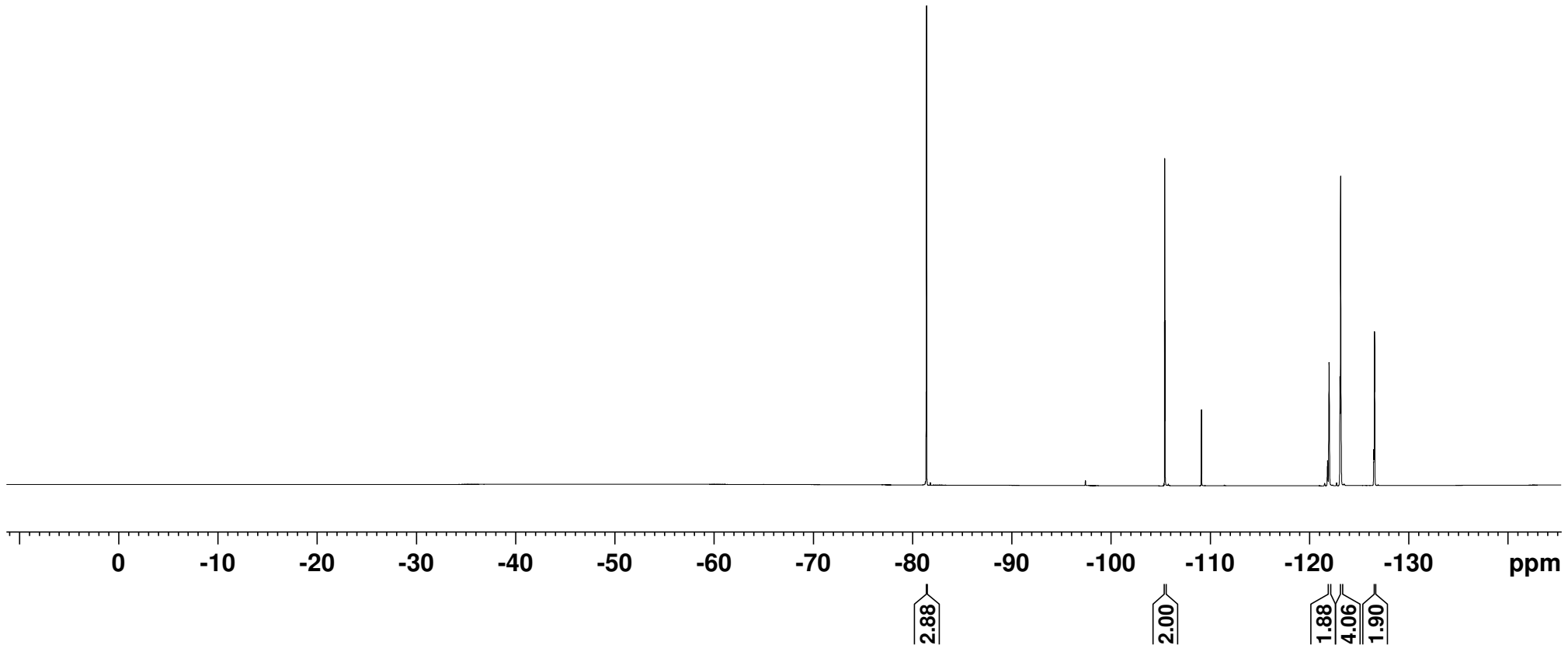
¹⁹F NMR Spectrum

E-2k

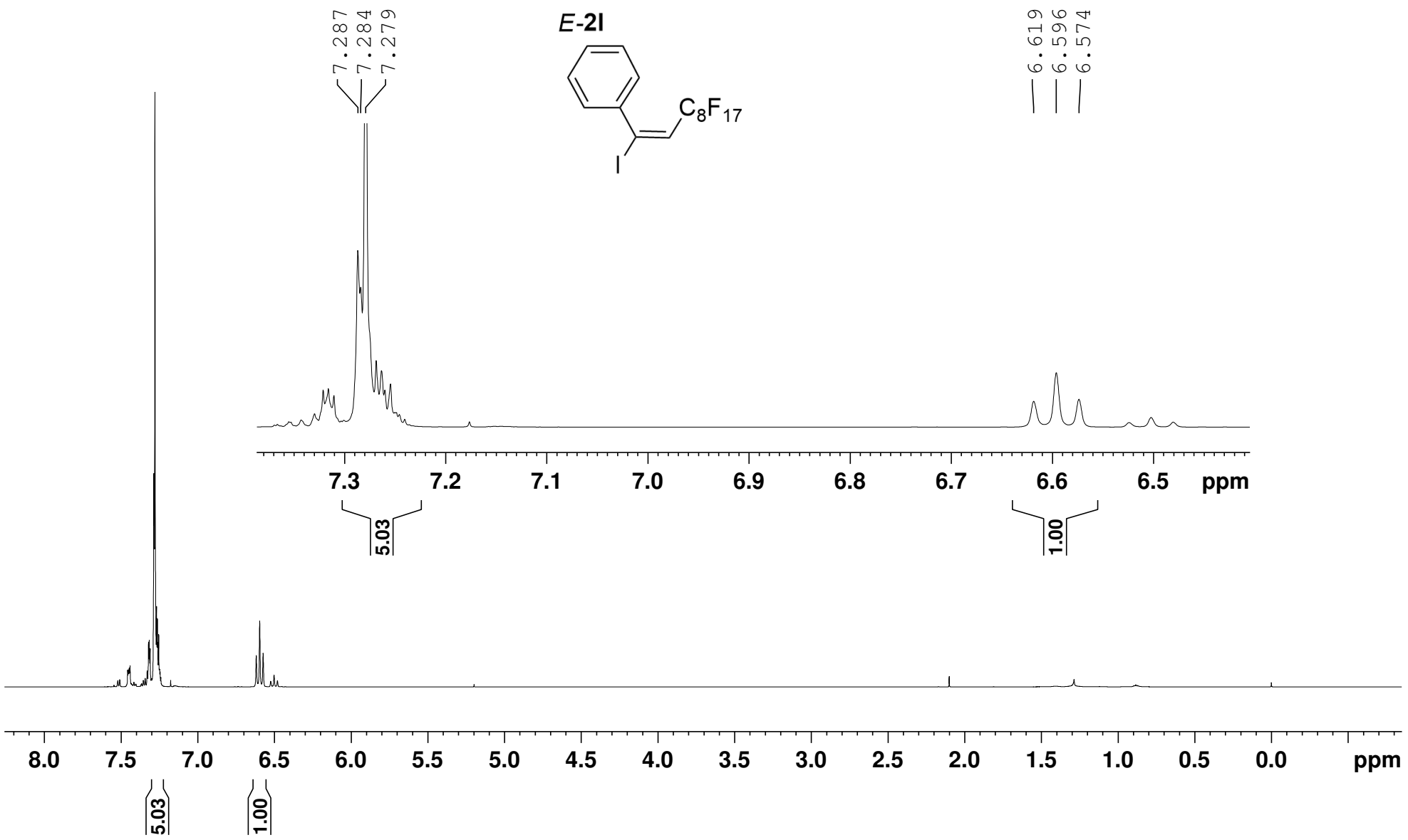


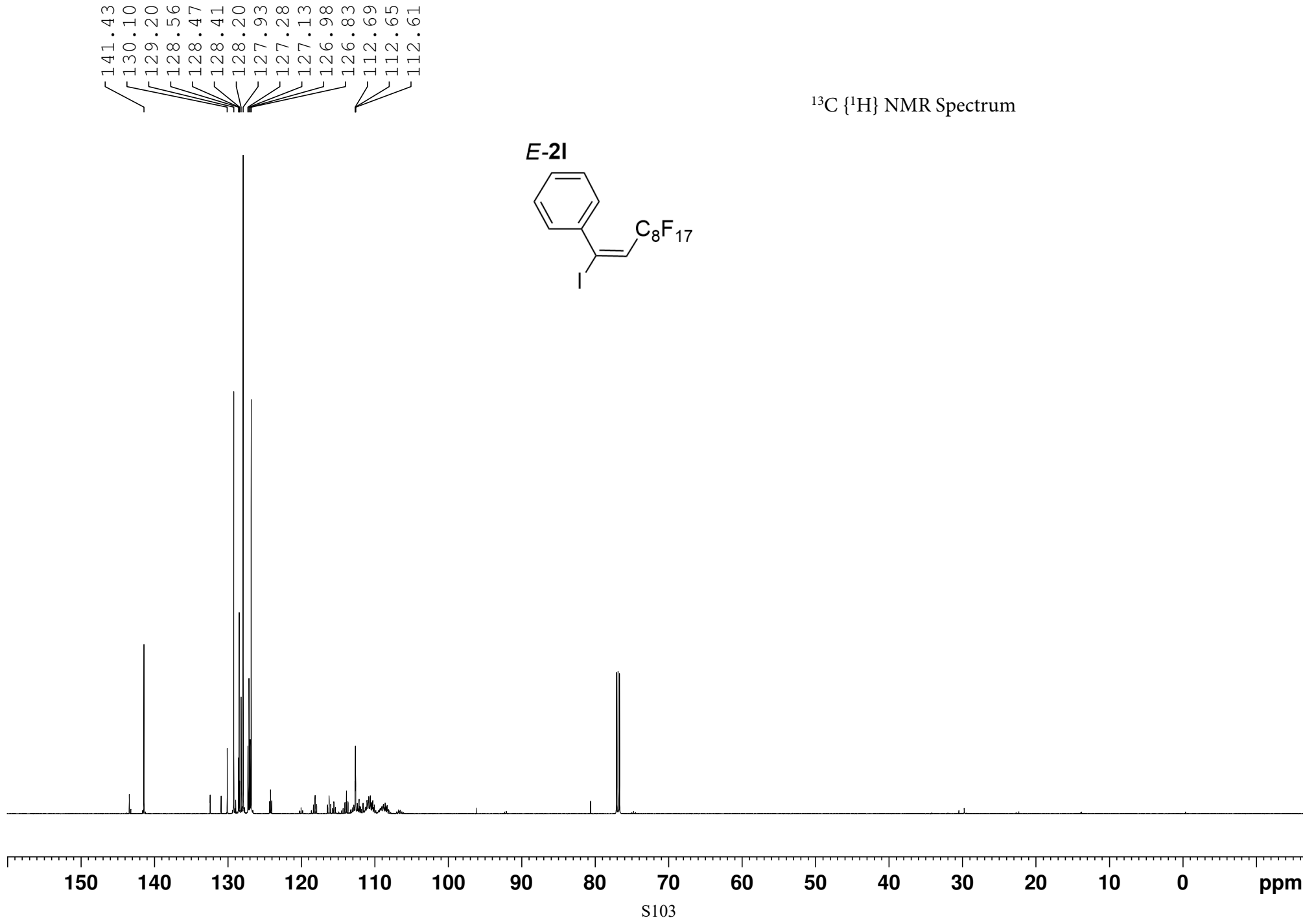
A list of chemical shifts (ppm) corresponding to the peaks in the spectrum:

- 81.38
- 81.39
- 81.41
- 81.43
- 81.44
- 105.42
- 105.44
- 105.46
- 109.11
- 109.13
- 109.15
- 122.00
- 123.10
- 123.16
- 126.51
- 126.55
- 126.56
- 126.58



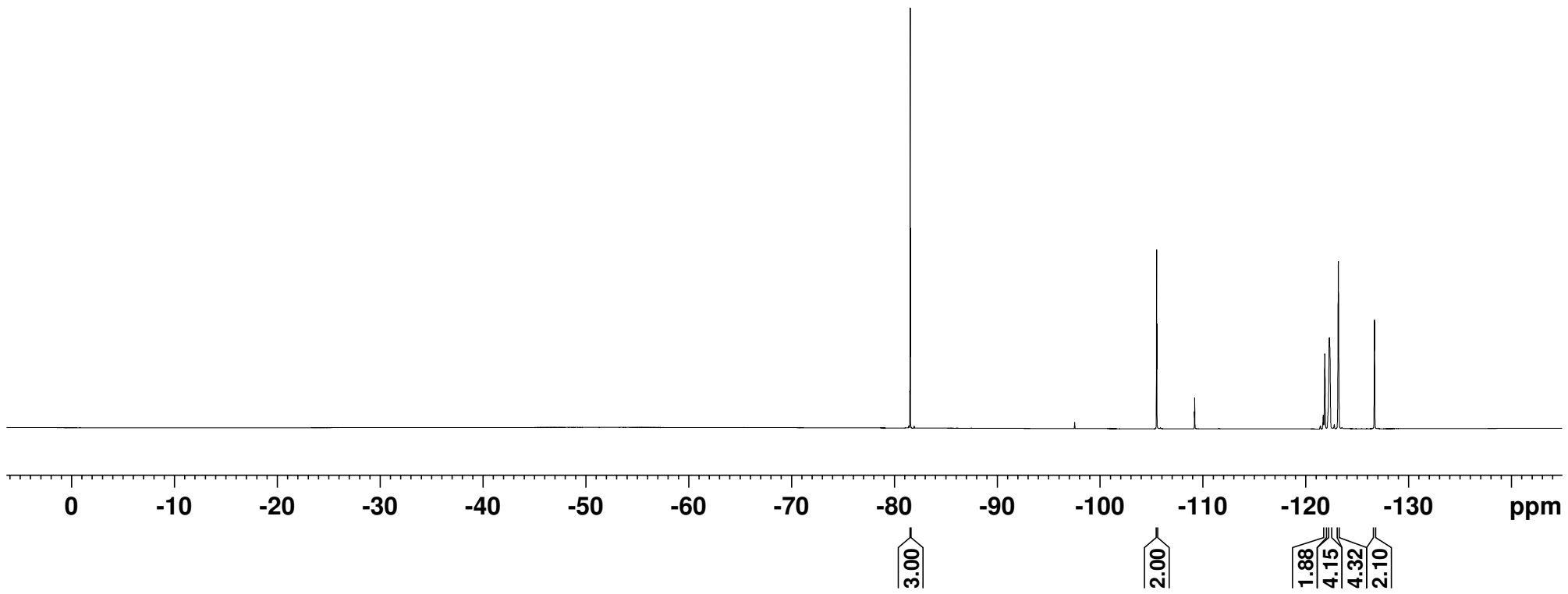
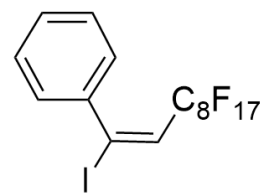
¹H NMR Spectrum





¹⁹F NMR Spectrum

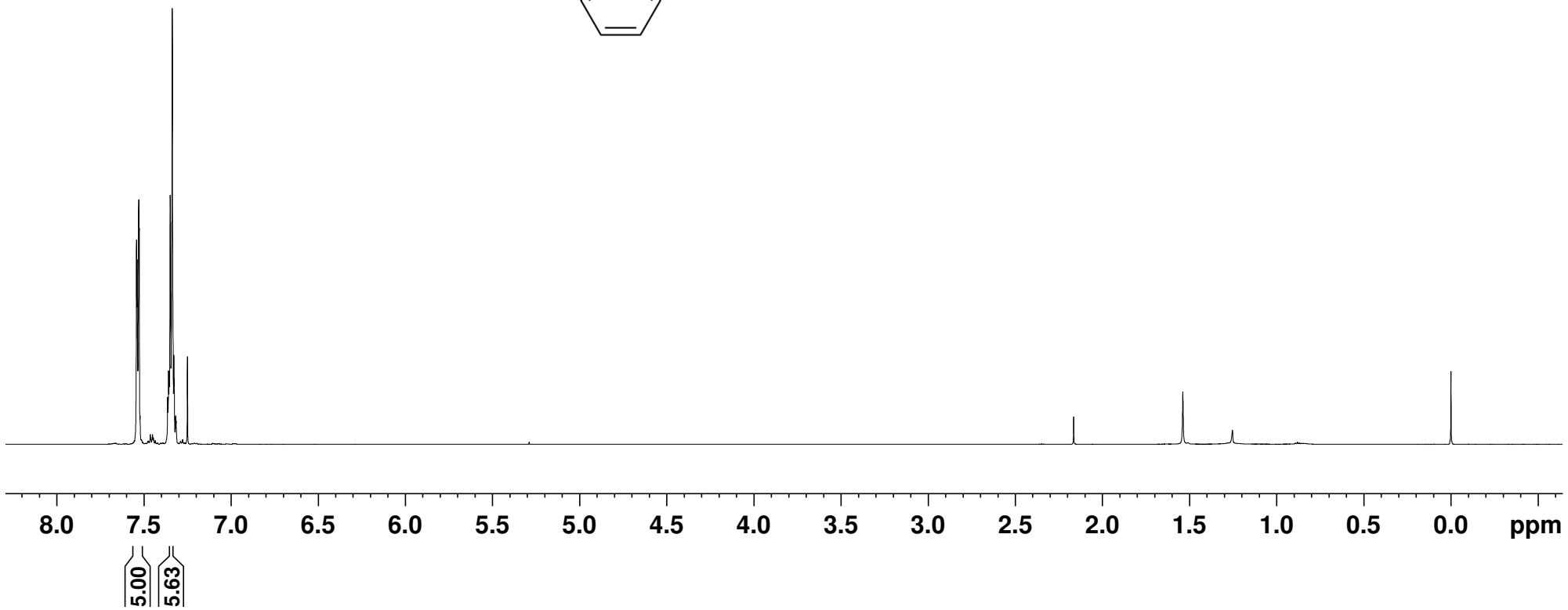
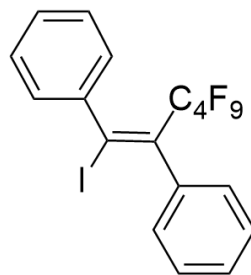
E-2I



7.543
7.539
7.530
7.527
7.359
7.354
7.349
7.340
7.338
7.329

¹H NMR Spectrum

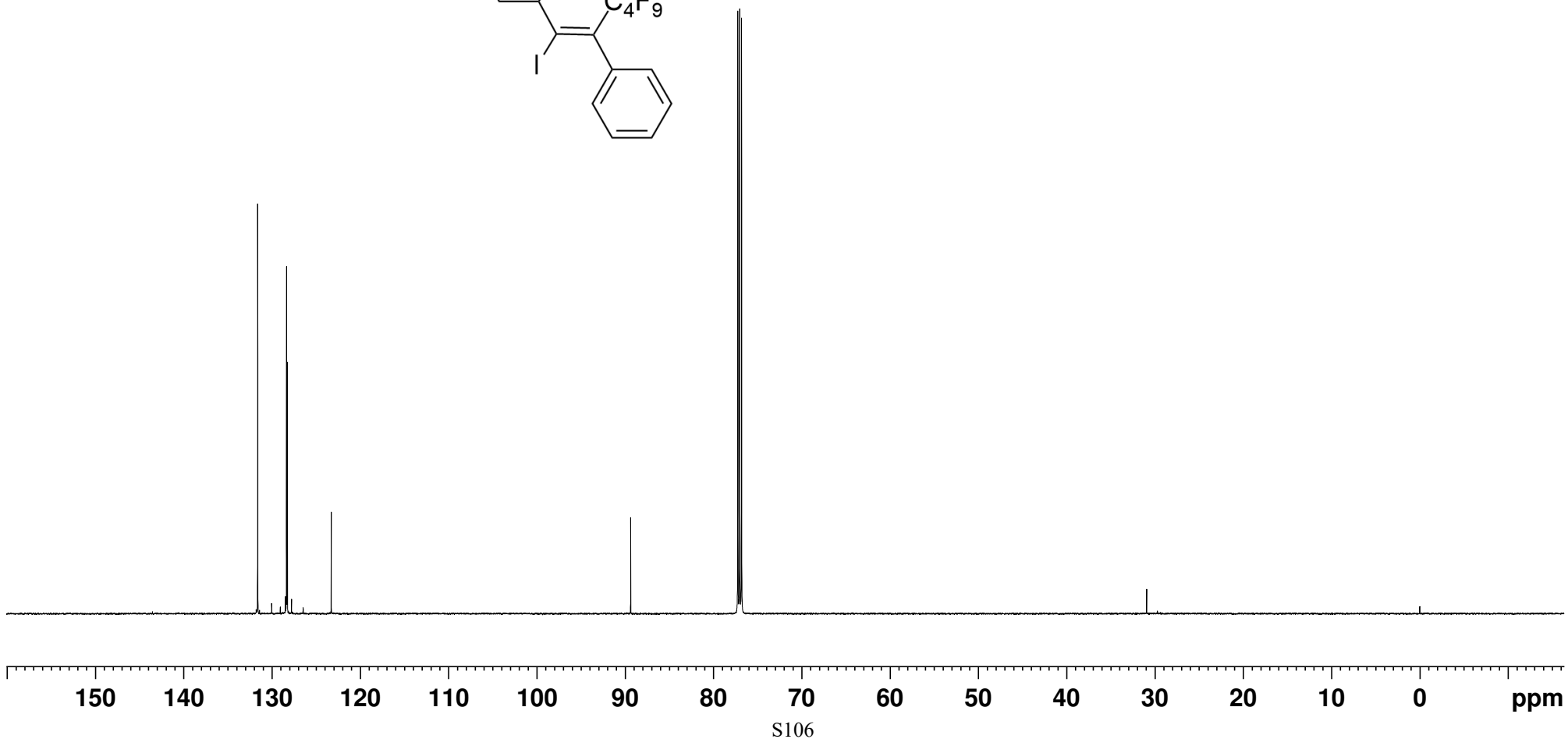
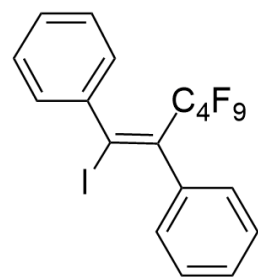
E-2m

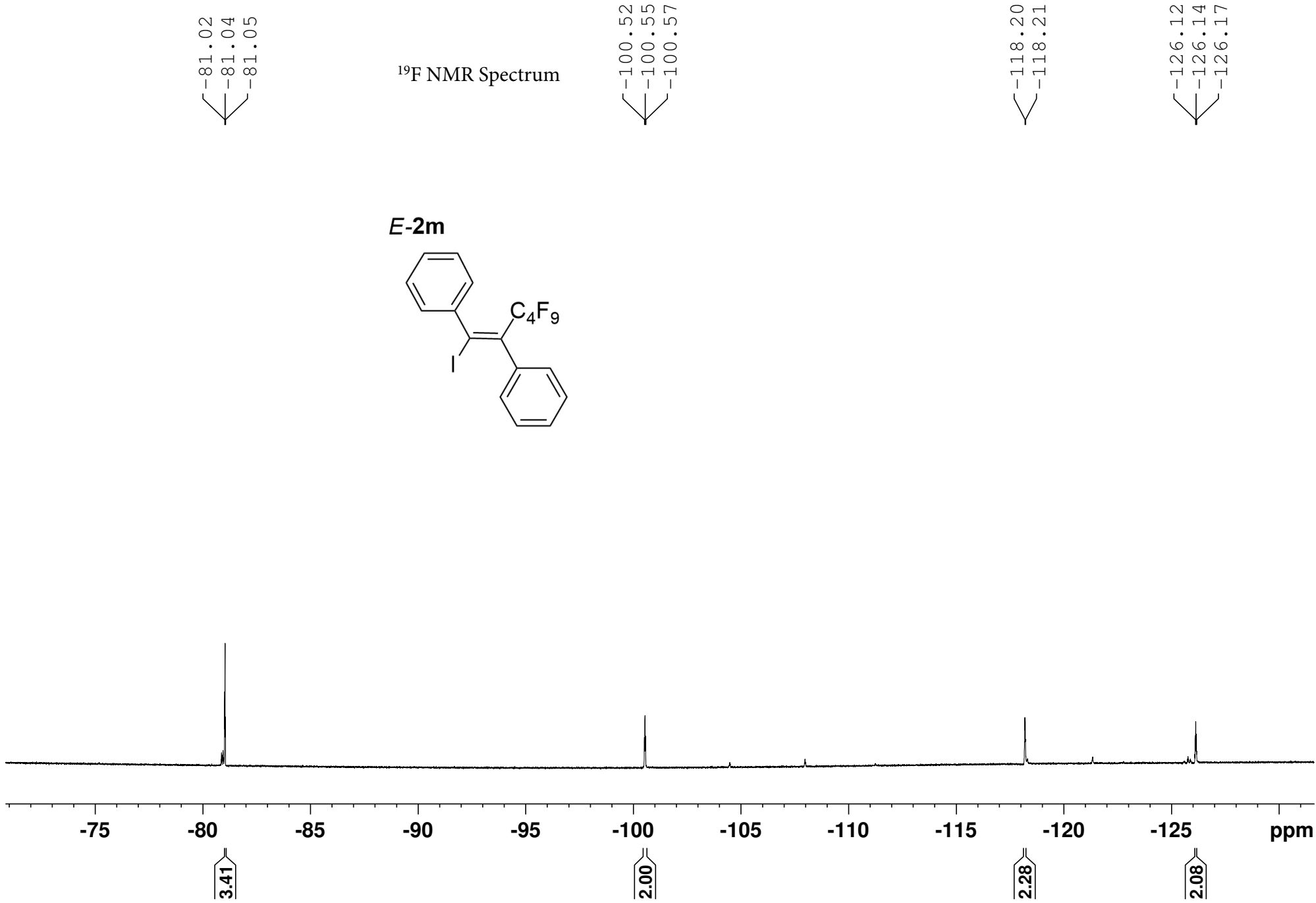


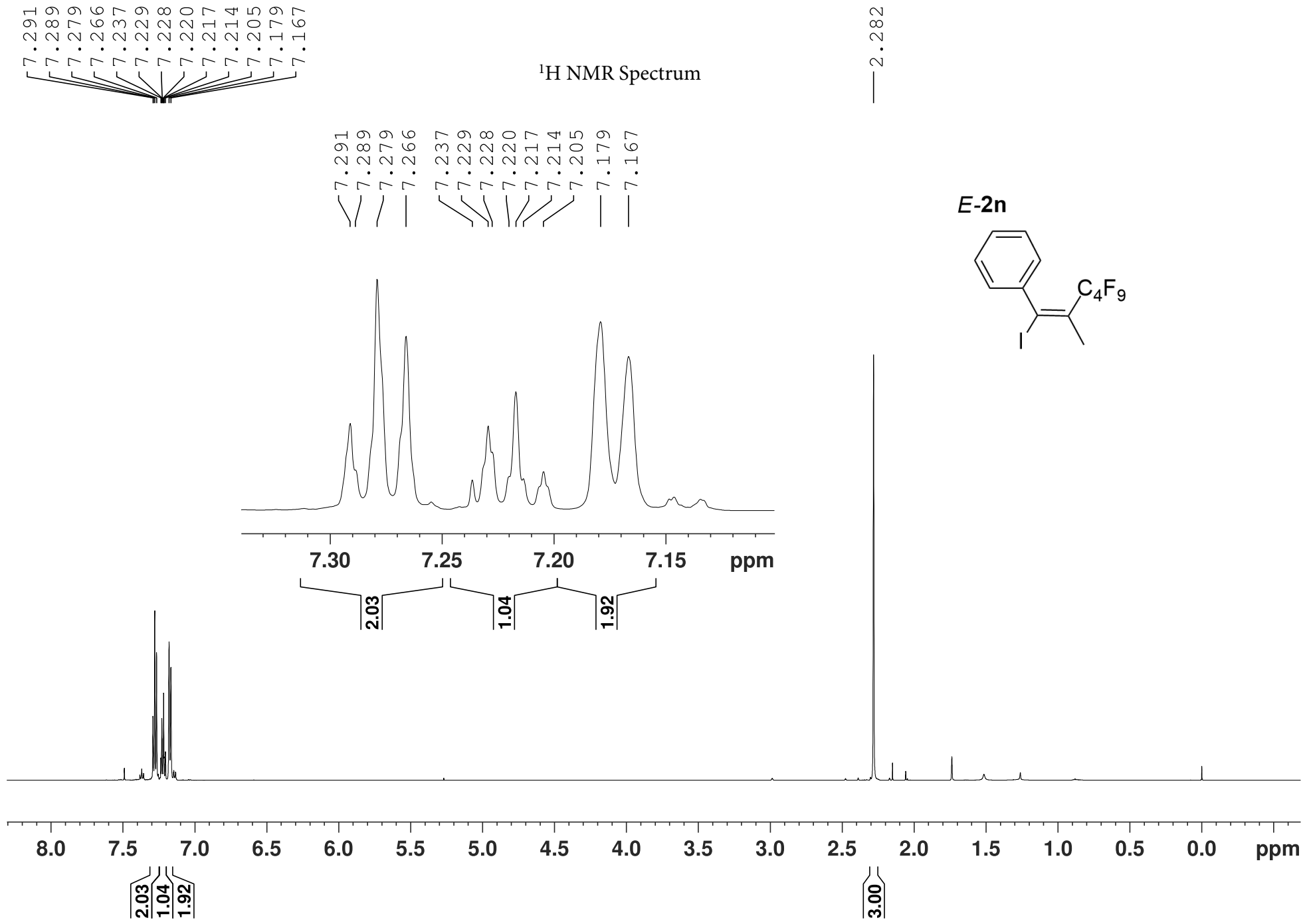
131.61
128.34
128.25
123.28

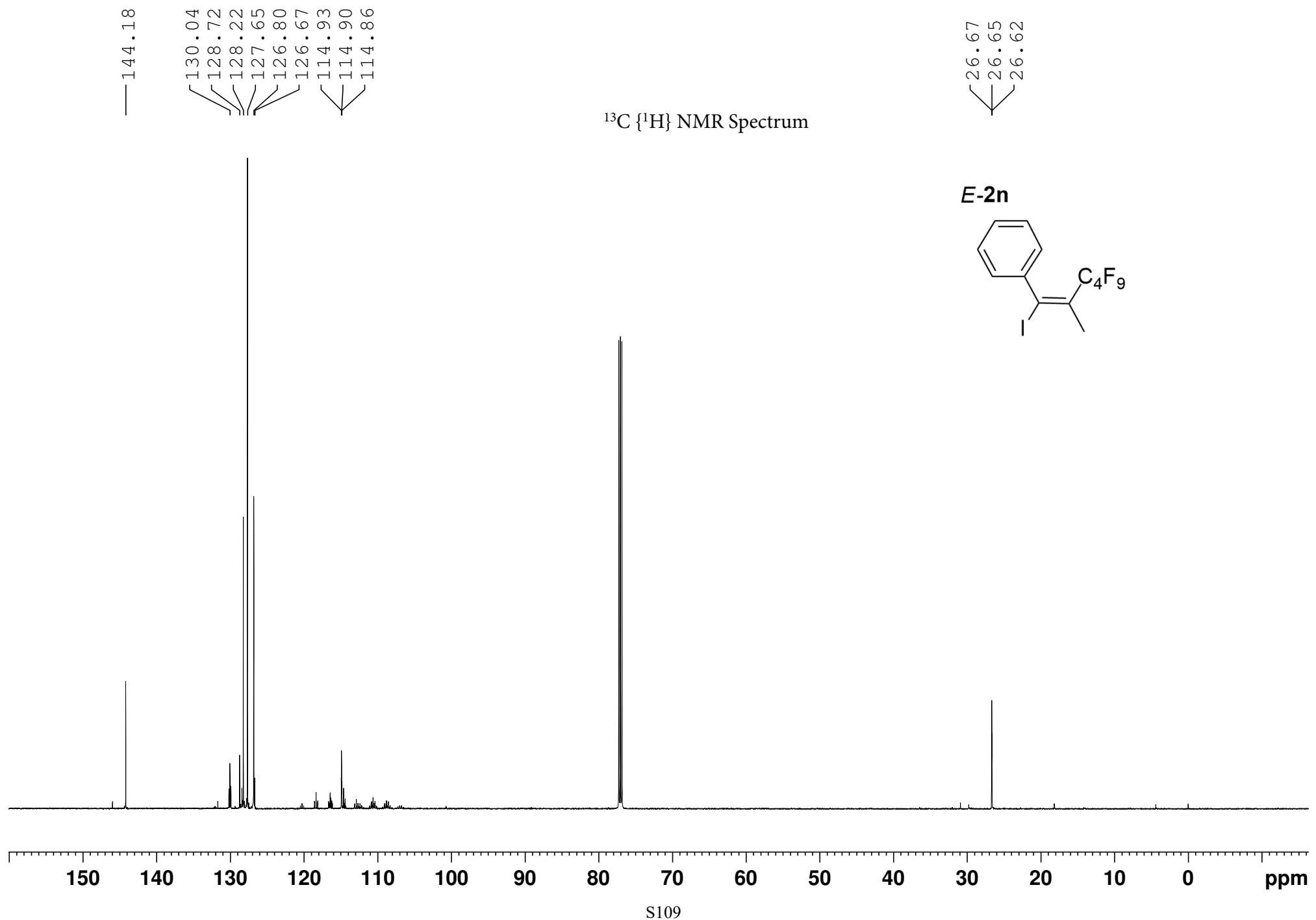
$^{13}\text{C} \{^1\text{H}\}$ NMR Spectrum

E-2m

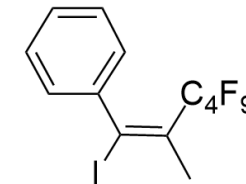




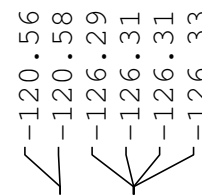
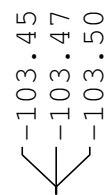
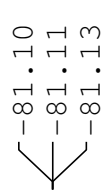




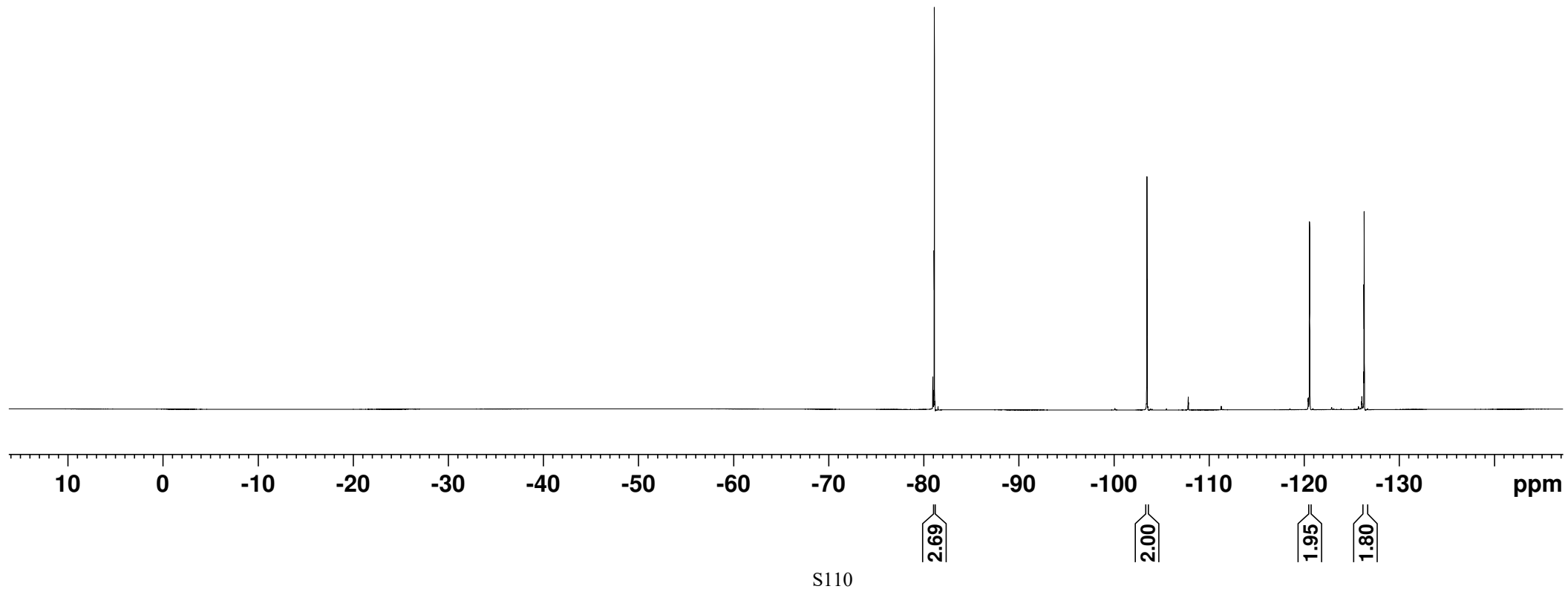
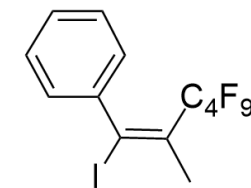
E-2n



¹⁹F NMR Spectrum



E-2n



10. References

- (1) S. Sprouse, K. A. King and P. J. Spellane, Watts, R. J. Photophysical Effects of Metal-Carbon σ Bonds in Ortho-Metalated Complexes of Ir(III) and Rh(III), *J. Am. Chem. Soc.*, 1984, **106**, 6647.
- (2) T. Sati, Y. Hamada, M. Sumikawa, S. Araki and H. Yamamoto, Solubility of Oxygen in Organic Solvents and Calculation of the Hansen Solubility Parameters of Oxygen, *Ind. Eng. Chen. Res.*, 2014, **53**, 19331.
- (3) Frisch, M. J.; Trucks, G.W.; Schlegel, H. B.; et al. Gaussian 09, Revision B.01; Gaussian, Inc.: Wallingford, CT, 2009.
- (4) (a) C. Lee, W. Yang and R. G. Parr, Development of the Colle-Salvetti Correlation-Energy Formula into a Functional of the Electron Density, *Phys. Rev. B: Condens. Matter Mater. Phys.*, 1988, **37**, 785; (b) A. D. Becke, Density-Functional Thermochemistry. III. The Role of Exact Exchange, *J. Chem. Phys.*, 1993, **98**, 5648.
- (5) A. Schäfer, H. Horn and R. Ahlrichs, Fully optimized contracted Gaussian basis sets for atoms Li to Kr, *J. Chem. Phys.*, 1992, **97**, 2571.
- (6) (a) P. J. Hay and W. R. Wadt, Ab Initio Effective Core Potentials for Molecular Calculations. Potentials for K to Au Including the Outermost Core Orbitals, *J. Chem. Phys.*, 1985, **82**, 299; (b) P. J. Hay and W. R. Wadt, Ab Initio Effective Core Potentials for Molecular Calculations. Potentials for the Transition Metal Atoms Sc to Hg, *J. Chem. Phys.*, 1985, **82**, 270.
- (7) G. Scalmani and M. J. Frisch, Continuous Surface Charge Polarizable Continuum Models of Solvation. I. General formalism, *J. Chem. Phys.*, 2010, **132**, 114110.
- (8) T. V. Jones, M. M. Slutsky, R. Laos, T. F. A. Greef and G. N. Tew, Solution ^1H NMR Confirmation of Folding in Short *o*-Phenylene Ethynylene Oligomers, *J. Am. Chem. Soc.*, 2005, **127**, 17235.
- (9) (a) M. P. Jennings, E. A. Cork and P. V. Ramachandran, A Facile Synthesis of Perfluoroalkyl Vinyl Iodides and Their Palladium-Mediated Cross-Coupling Reactions, *J. Org. Chem.*, 2000, **65**, 8763; (b) S. Domański and W. A Chaladaj, Broadly Applicable Method for Pd-Catalyzed Carboperfluoroalkylation of Terminal and Internal Alkynes: A Convenient Route to Tri- and Tetrasubstituted Olefins, *ACS Catal.*, 2016, **6**, 3452; (c) T. Rawner, E. Lutsker, C. A. Kaiser and O. Reiser, The Different Faces of Photoredox Catalysts: Visible-Light-Mediated Atom Transfer Radical Addition (ATRA) Reactions of Perfluoroalkyl Iodides with

- Styrenes and Phenylacetylenes, *ACS Catal.*, 2018, **8**, 3950; (d) S. Domański, B. Gatlik and W. Chaladaj, Pd-Catalyzed Boroperfluoroalkylation of Alkynes Opens a Route to One-Pot Reductive Carboperfluoroalkylation of Alkynes with Perfluoroalkyl and Aryl Iodides, *Org. Lett.*, 2019, **21**, 5021.
- (10) N. Iqbal, N. Iqbal, S. S. Han and E. J. Cho, Synthesis of Fluoroalkylated Alkynes via Visible-Light Photocatalysis, *Org. Biomol. Chem.*, 2019, **17**, 1758.
- (11) J. Li, L. Liu, K. Zheng, C. Zheng, H. Xiao and S. Fan, Silver-Mediated Perfluoroalkylation of Terminal Alkynes with Perfluoroalkyl Iodides, *J. Org. Chem.*, 2020, **85**, 8723;
- (12) T. Konno, J. Chae, M. Kanda, G. Nagai, K. Tamura, T. Ishihara and H. Yamanaka, Facile Syntheses of Various Per- or Polyfluoroalkylated Internal Acetylene Derivatives, *Tetrahedron*, 2003, **59**, 7571.
- (13) Q. Wang, Y.-T. He, J.-H. Zhao, Y.-F. Qiu, L. Zheng, J.-Y. Hu, Y.-C. Yang, X.-Y. Liu and Y.-M. Liang, Palladium-Catalyzed Regioselective Difluoroalkylation and Carbonylation of Alkynes, *Org. Lett.*, 2016, **18**, 2664.
- (14) (a) J.-J. Ma and W.-B. Yi, Copper-Catalyzed Fluoroalkylation of Alkynes, and Alkynyl & Vinyl Carboxylic Acids with Fluoroalkyl Halides, *Org. Biomol. Chem.*, 2017, **15**, 4295; (b) Yajima, T.; Ikegami, M. Metal-Free Visible-Light Radical Iodoperfluoroalkylation of Terminal Alkenes and Alkynes, *Eur. J. Org. Chem.*, 2017, 2126; (c) T. Xu, C. W. Cheung and X. Hu, Iron-Catalyzed 1,2-Addition of Perfluoroalkyl Iodides to Alkynes and Alkenes, *Angew. Chem. Int. Ed.*, 2014, **53**, 4910.